

# UC Davis

## Research Reports

### Title

Reflective Cracking Study: Initial Construction, Phase 1 HVS Testing, and Overlay Construction

### Permalink

<https://escholarship.org/uc/item/21b4m2zp>

### Authors

Bejarano, Manuel O.

Jones, David

Morton, Bruce S.

et al.

### Publication Date

2008-10-01

Peer reviewed

# Reflective Cracking Study: Initial Construction, Phase 1 HVS Testing, and Overlay Construction

**Authors:**

M. Bejarano, D. Jones, B. Morton, and C. Scheffy

Partnered Pavement Research Program (PPRC) Contract Strategic Plan Element 4.10:  
Development of Improved Rehabilitation Designs for Reflective Cracking

---

**PREPARED FOR:**

California Department of Transportation  
Division of Research and Innovation  
Office of Roadway Research

**PREPARED BY:**

University of California  
Pavement Research Center  
UC Davis, UC Berkeley

---





**Title:** Reflective Cracking Study: Initial Construction, Phase 1 HVS Testing, and Overlay Construction

**Authors:** M. Bejarano, D. Jones, B. Morton, and C Scheffy

**Prepared for:**  
Caltrans

**FHWA No:**  
CA091073A

**Date:**  
October 2005

**Contract No:**  
65A0172

**Client Reference No:**  
SPE 4.10

**Status:**  
Stage 6, Approved Version

**Abstract:**

This first-level report describes the design and construction of a Heavy Vehicle Simulator (HVS) test track that will be used to validate Caltrans overlay strategies for the rehabilitation of cracked asphalt concrete. The report also summarizes the first phase of HVS testing, carried out on six separate sections to crack the pavement, as well as design and construction of the overlays for the reflective cracking HVS experiments. The construction, preliminary field and laboratory data, and accelerated pavement tests reveal several issues regarding the performance of the asphalt concrete pavement cross section tested under the Heavy Vehicle Simulator.

The test track was constructed in September 2001. HVS testing took place between December 21, 2001, and March 25, 2003. Each section was trafficked with a 60 kN (13,500 lb) load using a bi-directional loading pattern with wander. Pavement temperature at 50 mm depth was maintained at 20°C (68°F) using a temperature control chamber. Findings from the HVS testing include:

- Analysis of deflection measurements revealed that the modulus of the asphalt concrete was significantly affected by the asphalt concrete temperature.
- The performance of the HVS test sections appeared to be significantly influenced by the behavior of the aggregate base. Sections that were tested during the dry months lasted longer both in fatigue and surface rutting than the sections tested during the wet months.
- Air-void contents and thicknesses were similar for the test sections; therefore, the effect of these variables could not be addressed.
- Deflection results could not be satisfactorily used as an indicator of aggregate base performance. Aggregate base moduli were higher during the cold/wet months but decreased rapidly when tested under the HVS. The aggregate base moduli of the sections during the dry/warm months were lower than those during the cold/wet months, but the sections tested during the dry period had longer pavement lives.

Deflections determined with the RSD during HVS testing and an FWD after testing were used to determine overlay thicknesses. A full-thickness design of 90 mm (3.5 in) was selected for the AR4000-D control section and one of the modified binder mixes (MB-G). The remaining sections were designed as half-thickness (45 mm) (1.7 in). The overlays were placed on June 14, 2003.

**Keywords:**

Reflective cracking, overlay, modified binder, HVS test, MB Road

**Related documents:**

None

**Signatures:**

D. Jones  
2nd Author

J. Harvey  
Technical Review

D. Spinner  
Editor

J. Harvey  
Principal Investigator

M. Samadien  
Caltrans Contract Manager

## **DISCLAIMER**

---

The contents of this report reflect the views of the authors who are responsible for the facts and accuracy of the data presented herein. The contents do not necessarily reflect the official views or policies of the State of California or the Federal Highway Administration. This report does not constitute a standard, specification, or regulation.

## **PROJECT OBJECTIVES**

---

The objective of this project is to develop improved rehabilitation designs for reflective cracking for California.

This objective will be met after completion of four tasks identified by the Caltrans/Industry Rubber Asphalt Concrete Task Group (RACTG):

1. Develop improved mechanistic models of reflective cracking in California
2. Calibrate and verify these models using laboratory and HVS testing
3. Evaluate the most effective strategies for reflective cracking
4. Provide recommendations for reflective cracking strategies

This document addresses Tasks 2 and 3.

## **ACKNOWLEDGEMENTS**

---

The University of California Pavement Research Center acknowledges the assistance of the Rubber Pavements Association, Valero Energy Corporation, and Paramount Petroleum which contributed funds and asphalt binders for the construction of the Heavy Vehicle Simulator test track discussed in this study.

## **REFLECTIVE CRACKING STUDY REPORTS**

---

The reports prepared during the reflective cracking study document data from construction, Heavy Vehicle Simulator (HVS) tests, laboratory tests, and subsequent analyses. These include a series of first- and second-level analysis reports and two summary reports. On completion of the study this suite of documents will include:

1. Reflective Cracking Study: Initial Construction, Phase 1 HVS testing and Overlay Construction (UCPRC-RR-2005-03).
2. Reflective Cracking Study: First-level Report on the HVS Rutting Experiment (UCPRC-RR-2007-06).
3. Reflective Cracking Study: First-level Report on HVS Testing on Section 590RF — 90 mm MB4-G Overlay (UCPRC-RR-2006-04).
4. Reflective Cracking Study: First-level Report on HVS Testing on Section 589RF — 45 mm MB4-G Overlay (UCPRC-RR-2006-05).
5. Reflective Cracking Study: First-level Report on HVS Testing on Section 587RF — 45 mm RAC-G Overlay (UCPRC-RR-2006-06).
6. Reflective Cracking Study: First-level Report on HVS Testing on Section 588RF — 90 mm AR4000-D Overlay (UCPRC-RR-2006-07).
7. Reflective Cracking Study: First-level Report on HVS Testing on Section 586RF — 45 mm MB15-G Overlay (UCPRC-RR-2006-12).
8. Reflective Cracking Study: First-level Report on HVS Testing on Section 591RF — 45 mm MAC15-G Overlay (UCPRC-RR-2007-04).
9. Reflective Cracking Study: HVS Test Section Forensic Report (UCPRC-RR-2007-05).
10. Reflective Cracking Study: First-level Report on Laboratory Fatigue Testing (UCPRC-RR-2006-08).
11. Reflective Cracking Study: First-level Report on Laboratory Shear Testing (UCPRC-RR-2006-11).
12. Reflective Cracking Study: Back Calculation of FWD Data from HVS Test Sections (UCPRC-RR-2007-08).
13. Reflective Cracking Study: Second-level Report on the MB Road Experiment (UCPRC-RR-2007-09).
14. Reflective Cracking Study: Summary Report (UCPRC-SR-2007-01). Detailed summary report.
15. Reflective Cracking Study: Summary Report (UCPRC-SR-2007-03). Four page summary report.

# CONVERSION FACTORS

<b>SI* (MODERN METRIC) CONVERSION FACTORS</b>				
<b>APPROXIMATE CONVERSIONS TO SI UNITS</b>				
Symbol	Convert From	Multiply By	Convert To	Symbol
<b>LENGTH</b>				
in	inches	25.4	millimeters	mm
ft	feet	0.305	meters	m
<b>AREA</b>				
in <sup>2</sup>	square inches	645.2	square millimeters	mm <sup>2</sup>
ft <sup>2</sup>	square feet	0.093	square meters	m <sup>2</sup>
<b>VOLUME</b>				
ft <sup>3</sup>	cubic feet	0.028	cubic meters	m <sup>3</sup>
<b>MASS</b>				
lb	pounds	0.454	kilograms	kg
<b>TEMPERATURE (exact degrees)</b>				
°F	Fahrenheit	5 (F-32)/9 or (F-32)/1.8	Celsius	C
<b>FORCE and PRESSURE or STRESS</b>				
lbf	poundforce	4.45	newtons	N
lbf/in <sup>2</sup>	poundforce/square inch	6.89	kilopascals	kPa
<b>APPROXIMATE CONVERSIONS FROM SI UNITS</b>				
Symbol	Convert From	Multiply By	Convert To	Symbol
<b>LENGTH</b>				
mm	millimeters	0.039	inches	in
m	meters	3.28	feet	ft
<b>AREA</b>				
mm <sup>2</sup>	square millimeters	0.0016	square inches	in <sup>2</sup>
m <sup>2</sup>	square meters	10.764	square feet	ft <sup>2</sup>
<b>VOLUME</b>				
m <sup>3</sup>	cubic meters	35.314	cubic feet	ft <sup>3</sup>
<b>MASS</b>				
kg	kilograms	2.202	pounds	lb
<b>TEMPERATURE (exact degrees)</b>				
C	Celsius	1.8C+32	Fahrenheit	F
<b>FORCE and PRESSURE or STRESS</b>				
N	newtons	0.225	poundforce	lbf
kPa	kilopascals	0.145	poundforce/square inch	lbf/in <sup>2</sup>

\*SI is the symbol for the International System of Units. Appropriate rounding should be made to comply with Section 4 of ASTM E380.

(Revised March 2003)

## EXECUTIVE SUMMARY

---

This first-level report describes the design and construction of a Heavy Vehicle Simulator (HVS) test track that will be used to validate Caltrans overlay strategies for the rehabilitation of cracked asphalt concrete. The report also summarizes the first phase of HVS testing, carried out on six separate sections to crack the pavement, as well as design and construction of the overlays for the reflective cracking HVS experiments. The construction, preliminary field and laboratory data, and accelerated pavement tests reveal several issues regarding the performance of the asphalt concrete pavement cross section tested under the Heavy Vehicle Simulator.

The pavement was designed according to the Caltrans Highway Design Manual Chapter 600 using the computer program *NEWCON90*. Design thickness was based on a subgrade R-value of 5 and a Traffic Index of 7 (~121,000 ESALs).

The test track was constructed in September 2001 according to Caltrans practice. During construction, the existing aggregate base and asphalt concrete layer were first milled to a depth of 250 mm (10 in), which removed all material to the surface of the subgrade. The subgrade was then scarified to a depth of 150 mm (6 in), watered, remixed, and then graded to uniform cross-slope of two percent. The prepared surface was compacted with a sheepsfoot roller, and finished with a 20-ton steel-wheel roller to remove the surface irregularities formed by the sheepsfoot roller. Compaction was monitored with a nuclear gauge. Drainage ditches were constructed along each edge of the pavement. Seven Time Domain Reflectometers (TDRs) and five pressure cells were installed in the subgrade. The aggregate base was constructed in a uniform thickness of 410 mm (16 in) along the 80-m (262 ft) length of the test sections. The material was placed in three lifts of 150 mm (6 in), 150 mm, and 110 mm (4.3 in) to achieve a relatively uniform material and then compacted using a steel drum vibratory roller. Compaction was monitored with a nuclear gauge. Seven TDRs were positioned at elevations corresponding to the lifts of the aggregate base. Six TDRs were installed after the first lift and one was installed after the second lift. The aggregate base was primed two days prior to paving using a CS-70 binder.

The mix design was a 19 mm (0.75 in) maximum, medium coarse type A dense-graded asphalt concrete with an AR-4000 binder and asphalt content of 5.0 percent (aggregate basis). The aggregate was sourced from the Dutra San Rafael Quarry with a blend of sand from Tidewater. The asphalt concrete was placed in two lifts of 45 mm (1.8 in) each with a paving width of 3.7 m (12 ft). A tack coat was applied between lifts. Each lift was compacted using a steel drum roller. Compaction was controlled with a nuclear density testing gauge, based on the maximum theoretical density of the mix. Average thickness of the asphalt



concrete layer was 79 mm. Asphalt extractions from two samples indicated a binder content by weight of aggregate of between 4.3 and 5.7 percent (target binder content was 5.0 percent). Average air-void contents in the asphalt concrete were 9.7 and 10.3 percent for the first and second lifts, respectively.

A full suite of laboratory tests, together with Falling Weight Deflectometer tests on the test track, were carried out to characterize the materials. The findings of these tests are summarized as follows:

- Proper compaction of the subgrade and aggregate base layers was primarily affected by the water content in these layers. Current Caltrans specifications for subgrade and aggregate base compaction do not explicitly address this issue, and water content during compaction is left for the field engineer to decide. Water content based on optimum moisture content to reach the maximum wet density according to Caltrans specifications would produce a base/soil too wet to compact. Performance of unbound layers could be negatively affected if this issue is not addressed.
- The compaction of the aggregate base layer was significantly affected by the support provided by the subgrade. Data indicated that low aggregate base moduli were obtained in locations where low subgrade moduli were observed.
- The asphalt concrete layer had a significant effect on the behavior of the aggregate base and subgrade. In general, the asphalt concrete provided a confining pressure that increased the modulus of the aggregate base. In addition, it provided additional cover to the subgrade by reducing the subgrade vertical stresses, which in turn increased the subgrade modulus.

Six sections were demarcated onto the test track for HVS testing, which took place between December 21, 2001, and March 25, 2003. Each section was trafficked with a 60 kN (13,500 lb) load using a bi-directional loading pattern with wander. Pavement temperature at 50 mm depth was maintained at 20°C (68°F) using a temperature control chamber. A summary of the repetitions applied, and the average maximum rut depth and crack density measured on each section on completion of testing is provided in Table 1.

**Table 1: Summary of HVS Testing on the DGAC Layer**

Section	Repetitions	Rut Depth (mm [in])	Crack Density (m/m <sup>2</sup> [ft/ft <sup>2</sup> ])
567RF	78,500	13.7 (0.54)	8.1 (2.5)
568RF	377,556	14.2 (0.56)	5.5 (1.7)
573RF	983,982	3.8 (0.15)	5.9 (1.8)
571RF	1,101,553	14.1 (0.56)	6.2 (1.9)
572RF	537,074	8.8 (0.35)	8.1 (2.5)
569RF	217,116	15.3 (0.60)	4.1 (1.3)

Findings from the HVS testing include:

- Analysis of FWD measurements during the course of the study revealed that the modulus of the asphalt concrete was significantly affected by the asphalt concrete temperature. In general lower moduli were obtained during the hot summer months, and higher moduli during the cold winter months, as expected.
- The performance of the HVS test sections appeared to be significantly influenced by the behavior of the aggregate base. Sections that were tested during the dry months lasted longer both in fatigue and surface rutting than the sections tested during the wet months.
- Air-void contents and thicknesses were similar for the test sections; therefore, the effect of these variables could not be addressed.
- Analysis of FWD and Road Surface Deflectometer test results indicated that the modulus of the aggregate base can not be used as an indicator of aggregate base performance. Aggregate base moduli were higher during the cold/wet months but decreased rapidly when tested under the HVS. The aggregate base moduli of the sections during the dry/warm months were lower than those during the cold/wet months, but the sections tested during the dry period had longer pavement lives.

Deflections determined with the RSD during HVS testing and an FWD after testing were used to determine overlay thicknesses. A full-thickness design of 90 mm (3.5 in) was selected for the AR4000-D control section and one of the modified binder mixes (MB-G). The remaining sections were designed as half-thickness (45 mm) (1.7 in). The six different overlay treatments on the test track included:

- Full-thickness (90 mm) AR4000-D included for control purposes.
- Half-thickness (45 mm) RAC-G included for control purposes.
- Full-thickness (90 mm) MB4-G.
- Half-thickness (45 mm) MB4-G.
- Half-thickness (45 mm) MB4-G with 15 percent tire rubber.
- Half-thickness (45 mm) MAC15TR.

The overlays were placed on June 14, 2003. The test track was first broomed, after which a tack coat was applied. The half-thickness overlays were placed in a single lift and compacted with a steel drum roller. The full-thickness overlays were placed in two lifts, with a tack coat applied between lifts.



# TABLE OF CONTENTS

---

<b>EXECUTIVE SUMMARY</b> .....	<b>v</b>
<b>LIST OF TABLES</b> .....	<b>xi</b>
<b>LIST OF FIGURES</b> .....	<b>xii</b>
<b>1. INTRODUCTION</b> .....	<b>1</b>
1.1. Objectives .....	1
1.2. Overall Project Organization .....	1
1.3. Structure and Content of this Report .....	4
1.4. Measurement Units.....	4
<b>2. TEST TRACK LAYOUT AND CONSTRUCTION</b> .....	<b>5</b>
2.1. Test Track Location.....	5
2.2. Test Track Design.....	7
2.3. Staking of the Test Pavement .....	7
2.4. Milling of Existing Aggregate Base and Asphalt Concrete.....	8
2.5. Subgrade Compaction.....	8
2.6. Drainage Construction .....	9
2.7. Subgrade Instrumentation .....	9
2.8. Aggregate Base Construction .....	10
2.9. Aggregate Base Instrumentation.....	11
2.10. Priming of the Aggregate Base and Installation of Strain Gages .....	11
2.11. Asphalt Concrete Mix Design .....	12
2.12. Paving Operation .....	12
2.13. Full Depth Patching .....	13
2.14. Shoulder Backing and Completion of Instrumentation .....	13
<b>3. MATERIAL TESTING</b> .....	<b>15</b>
3.1. Air-Void Content and Thickness of Asphalt Concrete Layer.....	15
3.2. Asphalt Extraction and Gradations.....	18
3.3. Dynamic Cone Penetrometer Testing of Unbound Materials.....	18
3.4. Unbound Materials Classification .....	20
3.5. Falling Weight Deflectometer Tests.....	21
3.5.1 FWD Testing on the Subgrade during Construction .....	21
3.5.2 FWD Testing on the Aggregate Base.....	21
3.5.3 FWD Testing on the Asphalt Concrete .....	23
3.5.4 Phase 1 FWD Testing.....	28

<b>4.</b>	<b>PHASE 1 HVS TESTING .....</b>	<b>35</b>
4.1.	Test Section Layout.....	35
4.2.	Pavement Instrumentation and Monitoring Methods .....	35
4.3.	Test Section Design .....	35
4.4.	Test Summary.....	38
4.4.1	Test Section Failure Criteria.....	38
4.4.2	Environmental Conditions.....	38
4.4.3	Test Duration and Configuration.....	38
4.5.	HVS Test Data Summary .....	39
4.5.1	Climate Conditions.....	39
4.5.2	Elastic Deflection .....	39
4.5.3	Permanent Deformation .....	42
4.5.4	Visual Inspection.....	44
4.5.5	Test Summary .....	46
<b>5.</b>	<b>OVERLAY DESIGN AND CONSTRUCTION .....</b>	<b>47</b>
5.1.	Overlay Design.....	47
5.2.	Overlay Construction.....	47
5.2.1	Surface Preparation .....	48
5.2.2	Overlay Placement .....	48
5.2.3	Density Measurements .....	48
5.3.	Materials Testing .....	49
<b>6.</b>	<b>CONCLUSIONS .....</b>	<b>51</b>
<b>7.</b>	<b>REFERENCES.....</b>	<b>55</b>
	<b>APPENDIX A: INITIAL CONSTRUCTION BID DOCUMENTATION.....</b>	<b>56</b>
	<b>APPENDIX B: INSTRUMENTATION TYPES AND LOCATIONS ON TEST SECTIONS .....</b>	<b>65</b>
	<b>APPENDIX C: INFORMATION FOR OVERLAY CONSTRUCTION .....</b>	<b>68</b>

## LIST OF TABLES

---

Table 3.1: FWD Test Location.....	21
Table 3.2: Summary of Moduli of Pavement Layers and the Subgrade.....	23
Table 3.3: Summary of Average Asphalt Concrete Modulus along the Pavement Section.....	23
Table 3.4: Summary of Aggregate Base Moduli along Pavement Section.....	27
Table 3.5: Average FWD Deflections by Date.....	29
Table 4.1: Asphalt Concrete Thickness and Air-Void Content of HVS Test Sections.....	38
Table 4.2: Summary of Testing on the DGAC Layer.....	39
Table 4.3: Summary of Surface Rutting Performance.....	43
Table 5.1: Summary of Surface Rutting Performance.....	47
Table 5.2: Overlay Descriptions.....	47
Table 5.3: Design versus Actual Binder Contents.....	49
Table 5.4: Air-Void Contents.....	50
Table 6.1: Summary of HVS Testing on the DGAC Layer.....	52

## LIST OF FIGURES

---

Figure 1.1: Timeline for the Reflective Cracking Study.....	3
Figure 2.1: Location of HVS test track at Richmond Field Station (1).....	5
Figure 2.2: Location of HVS test track at Richmond Field Station (2).....	5
Figure 2.3: Layout of Reflective Cracking Study project.....	6
Figure 2.4: Test track pavement design.....	7
Figure 2.5: Milling of existing roadway.....	8
Figure 2.6: Exposed subgrade.....	8
Figure 2.7: Subgrade preparation.....	9
Figure 2.8: Installation of Time Domain Reflectometer.....	10
Figure 2.9: Installation of pressure cell.....	10
Figure 2.10: Base construction.....	11
Figure 2.11: Base priming.....	12
Figure 2.12: Installation of strain gauges.....	12
Figure 2.13: Asphalt concrete placement.....	13
Figure 2.14: Nuclear density testing.....	13
Figure 3.1: Relationship between air-void content measurements.....	15
Figure 3.2: Air-void content relative frequency and cumulative histogram.....	16
Figure 3.3: Air-void distribution in asphalt concrete layer along the project.....	17
Figure 3.4: Relative frequency and cumulative histogram for asphalt concrete thickness.....	17
Figure 3.5: Distribution of asphalt concrete thickness across pavement section.....	18
Figure 3.6: Asphalt concrete mix gradations.....	19
Figure 3.7: DCP data for unbound materials.....	20
Figure 3.8: Thickness of aggregate base estimated from DCP measurements.....	20
Figure 3.9: FWD determined aggregate base modulus (tested on base).....	22
Figure 3.10: FWD determined subgrade modulus (tested on base).....	22
Figure 3.11: Relative frequency and cumulative histogram for base modulus.....	22
Figure 3.12: Relative frequency and cumulative histogram for subgrade modulus.....	22
Figure 3.13: Back-calculated modulus of asphalt concrete (tested on AC).....	24
Figure 3.14: Back-calculated modulus of aggregate base (tested on AC).....	24
Figure 3.15: Back-calculated modulus of subgrade (tested on AC).....	24
Figure 3.16: Relative frequency of asphalt concrete modulus.....	24
Figure 3.17: Cumulative histogram of asphalt concrete modulus.....	25
Figure 3.18: Distribution of asphalt concrete moduli along the pavement section.....	25

Figure 3.19: Relative frequency of base layer modulus. ....	26
Figure 3.20: Cumulative histogram of base layer modulus. ....	26
Figure 3.21: Distribution of aggregate base moduli along pavement section. ....	26
Figure 3.22: Relative frequency and cumulative histogram of subgrade modulus. ....	27
Figure 3.23: Distribution of subgrade moduli along pavement section. ....	28
Figure 3.24: Comparison of aggregate base and subgrade moduli. ....	28
Figure 3.25: FWD deflections at the load plate ( $D_0$ ) along the pavement section. ....	29
Figure 3.26: Summary of back-calculated moduli for pavement section. ....	30
Figure 3.27: Effect of temperature on modulus of the asphalt concrete layer. ....	32
Figure 3.28: Variation of asphalt concrete moduli along the pavement section. ....	32
Figure 3.29: Variation of aggregate base modulus with asphalt concrete modulus. ....	32
Figure 3.30: Variation of aggregate base modulus with subgrade modulus. ....	32
Figure 3.31: Average aggregate base modulus along the pavement test section. ....	33
Figure 3.32: Average subgrade modulus along the pavement test section. ....	33
Figure 3.33: Variation of moisture content with precipitation over time. ....	33
Figure 3.34: Variation of modulus with time as a function of moisture content for aggregate base. ....	33
Figure 3.35: Variation of modulus with time as a function of moisture content for subgrade. ....	34
Figure 4.1: Test section layout and location of instruments. ....	36
Figure 4.2: Pavement layer thicknesses for Phase 1 HVS test sections (design and actual). ....	37
Figure 4.3: Sequence climatic conditions during Phase 1 HVS testing. ....	40
Figure 4.4: RSD surface deflections. ....	40
Figure 4.5: Backcalculated asphalt concrete moduli for HVS sections. ....	41
Figure 4.6: Backcalculated aggregate base and subgrade moduli for HVS sections. ....	42
Figure 4.7: Summary of surface rutting performance. ....	43
Figure 4.8: Cracking patterns and rut depths on Sections 567RF through 573RF after HVS testing. ....	45
Figure 4.9: Summary of surface cracking performance. ....	46
Figure 5.1: Overlay placement (RAC-G). ....	48
Figure 5.2: Overlay compaction (AR4000-D). ....	48
Figure 5.3: Overlay placement (MB4-G). ....	48
Figure 5.4: Gradation for AR4000-D overlay. ....	50
Figure 5.5: Gradation for modified binder overlays. ....	50





# 1. INTRODUCTION

---

## 1.1. Objectives

The first-level analysis presented in this report is part of Partnered Pavement Research Center Strategic Plan Element 4.10 (PPRC SPE 4.10) being undertaken for the California Department of Transportation (Caltrans) by the University of California Pavement Research Center (UCPRC). The objective of the study is to evaluate the reflective cracking performance of asphalt binder mixes used in overlays for rehabilitating cracked asphalt concrete pavements in California. The study includes mixes modified with rubber and polymers, and it will develop tests, analysis methods, and design procedures for mitigating reflective cracking in overlays. This work is part of a larger study on modified binder (MB) mixes being carried out under the guidance of the Caltrans Pavement Standards Team (PST) (1), which includes laboratory and accelerated pavement testing using the Heavy Vehicle Simulator (carried out by the UCPRC), and the construction and monitoring of field test sections (carried out by Caltrans).

## 1.2. Overall Project Organization

This UCPRC project is a comprehensive study, carried out in three phases, involving the following primary elements (2):

- Phase 1
  - The construction of a test pavement and subsequent overlays;
  - Six separate Heavy Vehicle Simulator (HVS) tests to crack the pavement structure;
  - Placing of six different overlays on the cracked pavement;
- Phase 2
  - Six HVS tests that assessed the susceptibility of the overlays to high-temperature rutting (Phase 2a);
  - Six HVS tests to determine the low-temperature reflective cracking performance of the overlays (Phase 2b);
  - Laboratory shear and fatigue testing of the various hot-mix asphalts (Phase 2c);
  - Falling Weight Deflectometer (FWD) testing of the test pavement before and after construction and before and after each HVS test;
  - Forensic evaluation of each HVS test section;
- Phase 3
  - Performance modeling and simulation of the various mixes using models calibrated with data from the primary elements listed above.

## Phase 1

In this phase, a conventional dense-graded asphalt concrete (DGAC) test pavement was constructed at the Richmond Field Station (RFS) in the summer of 2001. The pavement was divided into six cells, and within each cell a section of the pavement was trafficked with the HVS until the pavement failed by either fatigue ( $2.5 \text{ m/m}^2$  [0.76 ft/ft<sup>2</sup>]) or rutting (12.5 mm [0.5 in]). This period of testing began in the summer of 2001 and was concluded in the spring of 2003. In June 2003 each test cell was overlaid with either conventional DGAC or asphalt concrete with modified binders as follows:

- Full-thickness (90 mm) AR4000-D dense graded asphalt concrete overlay, included as a control for performance comparison purposes (AR-4000 is approximately equivalent to a PG64-16 performance grade binder);
- Full-thickness (90 mm) MB4-G gap-graded overlay;
- Half-thickness (45 mm) rubberized asphalt concrete gap-graded overlay (RAC-G), included as a control for performance comparison purposes;
- Half-thickness (45 mm) MB4-G gap-graded overlay;
- Half-thickness (45 mm) MB4-G gap-graded overlay with minimum 15 percent recycled tire rubber (MB15-G), and
- Half-thickness (45 mm) MAC15-G gap-graded overlay with minimum 15 percent recycled tire rubber.

The conventional overlay was designed using the current (2003) Caltrans overlay design process. The various modified overlays were either full (90 mm) or half thickness (45 mm). Mixes were designed by Caltrans. The overlays were constructed in one day.

## Phase 2

Phase 2 includes high-temperature rutting and low-temperature reflective cracking testing with the HVS as well as laboratory shear and fatigue testing. The rutting tests will start in the fall of 2003. For these tests, the HVS will be placed above a section of the underlying pavement that was trafficked during Phase 1. Reflective cracking testing will start on completion of the rutting study. For these tests, the HVS will be positioned precisely on top of the sections of failed pavement from the Phase 1 HVS tests to investigate the extent and rate of crack propagation through the overlay.

In conjunction with Phase 2 HVS testing, a full suite of laboratory testing, including shear and fatigue testing will be carried out on field-mixed, field-compacted, field-mixed, laboratory-compacted, and laboratory-mixed, laboratory-compacted specimens.

### Phase 3

Phase 3 entails a second-level analysis and will be carried out on completion of HVS and laboratory testing (the focus of this report). This will include extensive analysis and characterization of the mix fatigue and mix shear data, backcalculation of the FWD data, performance modeling of each HVS test, and a detailed series of pavement simulations carried out using the combined data.

An overview of the project timeline is shown in Figure 1.1.

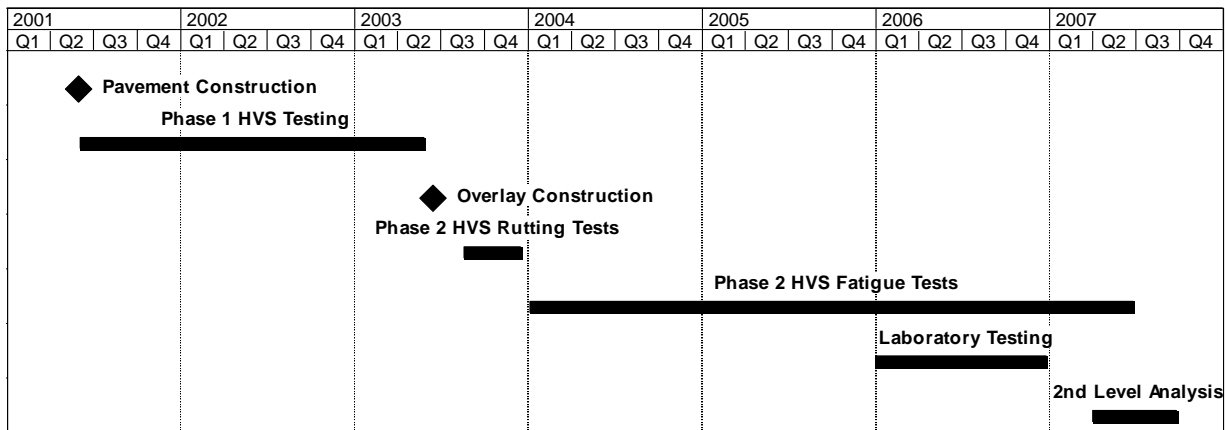


**Figure 1.1: Timeline for the Reflective Cracking Study.**

### Reports

The reports prepared during the reflective cracking study will document data from construction, HVS tests, laboratory tests, and subsequent analyses. These include a series of first- and second-level analysis reports and two summary reports. On completion of the study this suite of documents will include:

- One first-level report covering the initial pavement construction, the six initial HVS tests, and the overlay construction (Phase 1);
- One first-level report covering the six Phase 2 rutting tests (but offering no detailed explanations or conclusions on the performance of the pavements);
- Six first-level reports, each of which covers a single Phase 2 reflective cracking test (containing summaries and trends of the measured environmental conditions, pavement responses, and pavement performance but offering no detailed explanations or conclusions on the performance of the pavement);
- One first-level report covering laboratory shear testing;
- One first-level report covering laboratory fatigue testing;
- One report summarizing the HVS test section forensic investigation;
- One report summarizing the backcalculation analysis of deflection tests,

- One second-level analysis report detailing the characterization of shear and fatigue data, pavement modeling analysis, comparisons of the various overlays, and simulations using various scenarios (Phase 3), and
- One four-page summary report capturing the conclusions and one longer, more detailed summary report that covers the findings and conclusions from the research conducted by the UCPRC.

### **1.3. Structure and Content of this Report**

This report presents a summary of the test track construction, Phase 1 HVS testing, and a summary of the overlay construction. The report is organized as follows:

- Chapter 2 describes the test track layout and construction
- Chapter 3 summarizes the tests undertaken to characterize the materials
- Chapter 4 summarizes the HVS testing on six sections
- Chapter 5 summarizes the design and construction of the overlays
- Chapter 6 provides conclusions and recommendations.

### **1.4. Measurement Units**

Metric units have always been used in the design and layout of HVS test tracks, all the measurements and data storage, and all associated laboratory testing at the eight HVS facilities worldwide (as well as all other international accelerated pavement testing facilities). Use of the metric system facilitates consistency in analysis, reporting, and data sharing.

In this report, metric and English units are provided parentheses after the metric units in the Executive Summary, Chapters 1 and 2, and the Conclusion. In keeping with convention, only metric units are used in Chapters 3, 4 and 5. A conversion table is provided on Page iv at the beginning of this report.

## 2. TEST TRACK LAYOUT AND CONSTRUCTION

---

### 2.1. Test Track Location

The site for the project is located at the Pavement Research Center at the University of California Richmond Field Station (RFS). The site is located on Lark Drive between Avocet Way and Building 280. Figures 2.1 and 2.2 show the location of the project and Figure 2.3 shows the layout of the HVS test sections at the test site.

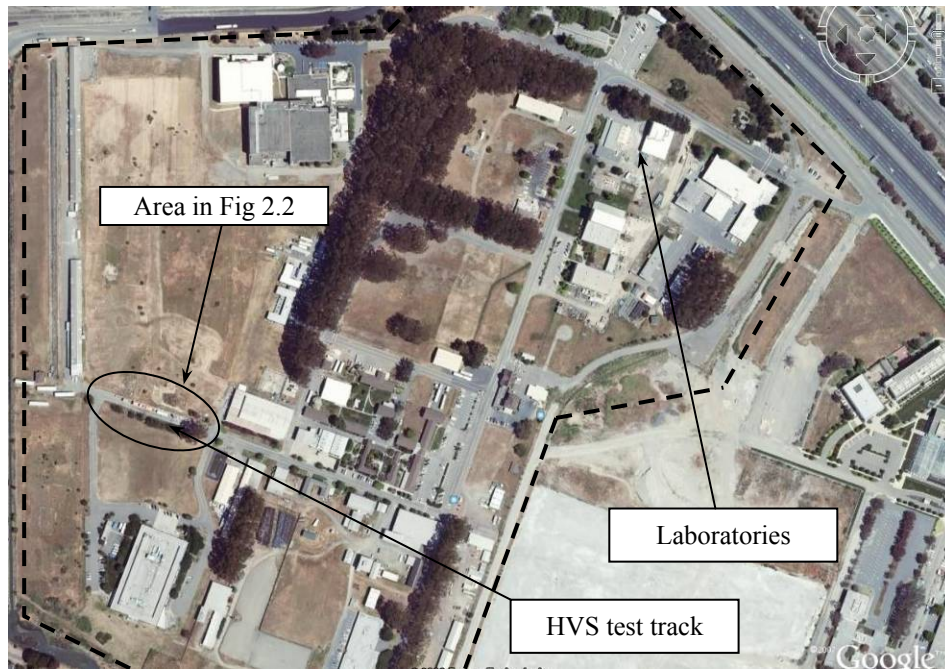


**Figure 2.1: Location of HVS test track at Richmond Field Station (1)**

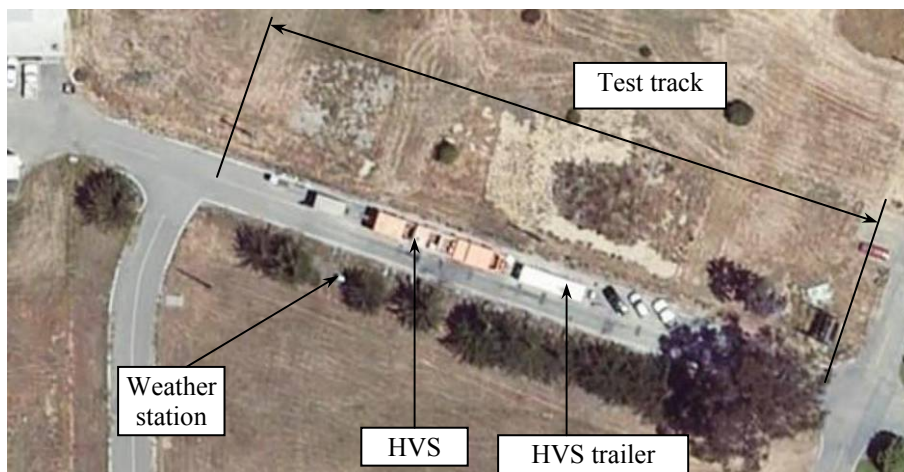


**Figure 2.2: Location of HVS test track at Richmond Field Station (2)**

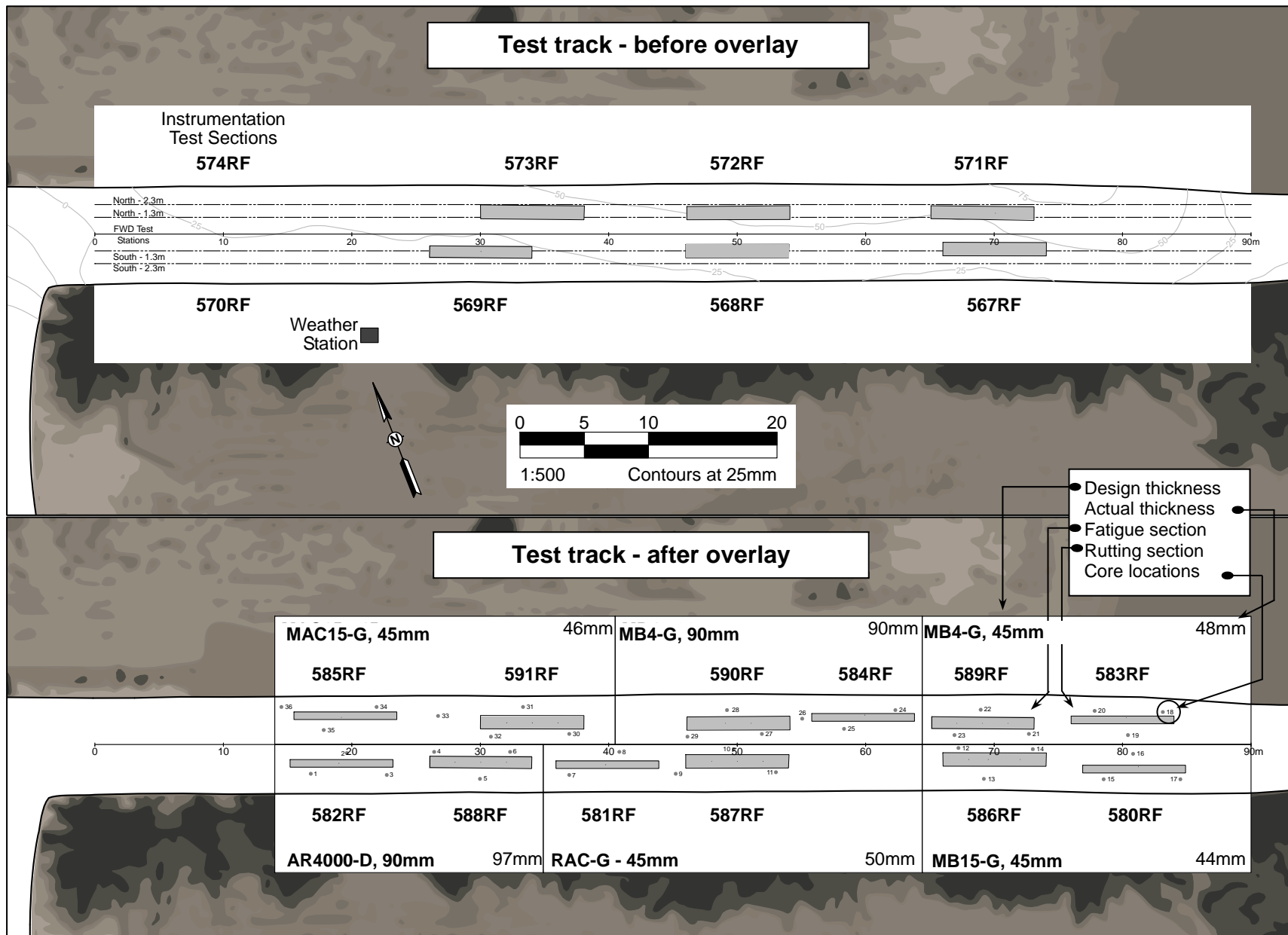
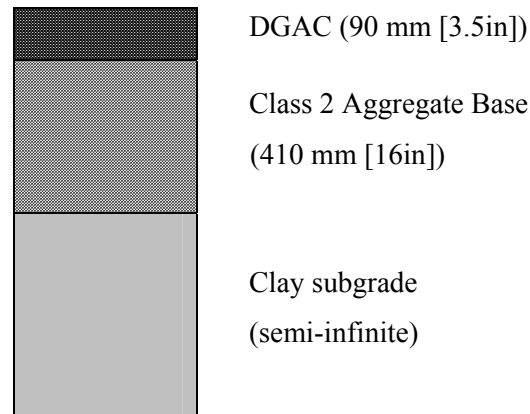


Figure 2.3: Layout of Reflective Cracking Study project.

## 2.2. Test Track Design

The pavement for the first phase of HVS trafficking was designed according to the Caltrans Highway Design Manual Chapter 600 using the computer program NEWCON90. Design thickness was based on a tested subgrade R-value of 5 and a Traffic Index of 7 (~121,000 ESALs) (3). The pavement design for the test road is illustrated in Figure 2.4.



**Figure 2.4: Test track pavement design**

A limited mechanistic analysis was conducted to ensure that subgrade rutting would be minimal under HVS trafficking. For the worst case conditions of soft subgrade and cracked asphalt concrete, subgrade deviator stress-to-strength ratios were estimated to be below 0.4 under the 40-kN (9,000 lb) load and below 0.5 under the 80-kN (18,000 lb) load. A subgrade deviator stress-to-strength ratio below 0.5 is considered to limit permanent deformation from the subgrade (4). Actual stress-to-strength values may be lower than those estimated under the worst case scenario.

Gallagher and Burke, a local paving contractor, was selected to construct the test pavement. The project was constructed during the period September 14–24, 2001. The bid document is provided in Appendix A.

## 2.3. Staking of the Test Pavement

Construction staking of the test pavement was performed by University of California Pavement Research Center (UCPRC) personnel. Stakes were located along the southern edge of the proposed test pavement at a distance of 3.0 m (10 ft) from the edge of the pavement at 15 m (49 ft) intervals. Elevation of subgrade, edge of pavement, final grade elevation, and cross-slope of the test pavement were recorded on each stake. Additional stakes were placed to define the two taper sections at the ends of the test pavement and the positions of instrumentation.



## 2.4. Milling of Existing Aggregate Base and Asphalt Concrete

The existing aggregate base and asphalt concrete layer were milled to a depth of 250 mm (10 in), which removed all material to the surface of the subgrade (Figures 2.5 and 2.6). The ends of the pavement (25 m [82 ft] in length) were tapered to a thickness of 100 mm (4 in) to remove the existing asphalt concrete, leaving the existing aggregate base and subgrade in place.



**Figure 2.5: Milling of existing roadway**



**Figure 2.6: Exposed subgrade**

## 2.5. Subgrade Compaction

Following the milling operation, the subgrade was scarified to a depth of 150 mm (6 in). The water content was then modified and remixed to improve workability (Figure 2.7). The subgrade was graded to uniform cross-slope of two percent, compacted with a sheepsfoot roller, and finished with a 20-ton steel-wheel roller to remove the surface irregularities formed by the sheepsfoot roller. Relative compaction of the subgrade was determined from field wet densities obtained using a nuclear gauge and the laboratory maximum wet density of the subgrade according to California Test Methods (CTM) 231 and 216, respectively (5).

The test results indicated that the relative compaction did not meet the Caltrans specification of 95 percent of laboratory determined maximum dry density (6). This was likely due to the water content being approximately 2.5 percent below the optimum according to CTM 216. To improve the degree of compaction, the subgrade moisture content was adjusted, and the material reworked to a depth of 200 mm (8 in) before being recompacted. This resulted in relative compaction of 97 percent. To limit hauling of in-situ material, the cross slope of the subgrade was increased to 2.25 percent.



**Figure 2.7: Subgrade preparation**

## **2.6. Drainage Construction**

Although the existing access road had drainage ditches, these were considered inadequate and poorly maintained. Accordingly, drainage ditches were constructed along each edge of the pavement. Realignment and widening of the road also required the construction of an additional drainage system. This was accomplished by replacing the existing drainage pipe under the road with a larger pipe on a new alignment of the drainage ditch.

## **2.7. Subgrade Instrumentation**

Following compaction of the subgrade soil, seven Time Domain Reflectometers (TDRs) and five pressure cells were installed in the subgrade (Figures 2.8 and 2.9). The description and locations of these instruments within the test pavement are provided in Appendix B.

Six TDRs were placed horizontally at a depth of 50 mm (2 in) below the subgrade surface while one TDR was positioned vertically at a depth of 200 mm (8 in) below the subgrade surface. The TDRs were compacted in-place using a hand tamper and the wires taken to the edge of the shoulder, and then buried in the subgrade layer to protect them from damage by the aggregate trucks and the larger aggregate particles of the compacted base material.

Soil pressure cells were installed in excavations approximately 75 mm (3 in) in diameter to limit disturbance of the surrounding material (Appendix B). The wires for the pressure cells were buried in the subgrade in the same manner as for the TDRs. After installation, the wires protruding from the edge of the shoulder were sealed in waterproof bags and buried in the shoulder material to protect the instrumentation

from moisture and to prevent accidental damage during construction of the aggregate base and asphalt concrete layer.



**Figure 2.8: Installation of Time Domain Reflectometer**



**Figure 2.9: Installation of pressure cell**

## **2.8. Aggregate Base Construction**

The aggregate base was constructed from material supplied by the Dutra Materials plant in San Rafael, California in a uniform thickness of 410 mm (16 in) along the 80-m (262 ft) length of the test sections. The base was placed in three lifts of 150 mm (6 in), 150 mm, and 110 mm (4.3 in) to achieve a relatively uniform material (Figure 2.10). Base thickness was varied in the taper sections in order to link the test pavement elevation with the existing pavement elevations.

The base material was compacted at the optimum water content for the maximum wet density according to CTM 216 using a steel drum vibratory roller. Nuclear density testing (CTM 231) was performed on the second and final lifts in order to ensure that Caltrans compaction requirements for Class 2 aggregate base were met. The resulting average relative compaction of the aggregate base was 97.0 percent in the second lift and 98.6 percent in the third lift.



**Figure 2.10: Base construction**

## **2.9. Aggregate Base Instrumentation**

Instrumentation in the aggregate base included seven TDRs and five pressure cells. Positions and locations are shown in Appendix B. In order to facilitate installation and to limit stand-by time of the contractor, these instruments were positioned at elevations corresponding to the lifts of the aggregate base. Six TDRs were installed after the first lift and one was installed after the second lift. Of the five pressure cells, only one, designated PC 7 (Appendix B), was installed during construction. Due to the time required these instruments, those located within 150 mm of the surface of the aggregate base layer were installed after construction of the base.

The wires of the pressure cells and TDRs were installed and protected in the same manner as those of the subgrade. After completion of the instrumentation installation, Heavy Weight Deflectometer (HWD) testing was performed on the aggregate base. These data were used to back-calculate the moduli of the pavement layers.

## **2.10. Priming of the Aggregate Base and Installation of Strain Gages**

The aggregate base was primed two days prior to paving using a CS-70 binder (Figure 2.11). The road was closed to traffic during this application and until the asphalt concrete was placed. After priming, asphalt concrete strain gages were installed in their respective positions using the method specified by the instrument manufacturers (Figure 2.12). A sand asphalt hot mix was used to secure the strain gages in position and the leads were run to the edge of the shoulder where they were bagged and buried in a similar method to that used in the installation of the pressure cells and TDRs.



**Figure 2.11: Base priming**



**Figure 2.12: Installation of strain gauges**

## **2.11. Asphalt Concrete Mix Design**

The mix design as specified in the bid documentation (Appendix A), was a 19 mm (0.75 in) maximum, medium coarse type A dense-graded asphalt concrete with an AR-4000 binder. The mix design, submitted by Dutra Materials, utilized an asphalt content of 5.0 percent (aggregate basis).

The Theoretical Maximum Specific Gravity of the asphalt concrete mix was 2.462. The aggregate was sourced from the Dutra San Rafael Quarry with a blend of sand from Tidewater.

## **2.12. Paving Operation**

The asphalt concrete was placed in two lifts of 45 mm (1.8 in) each with a paving width of 3.7 m (12 ft). Each lift was compacted using a steel drum roller. Density was controlled by means of nuclear density testing (Figures 2.13 and 2.14). As stated in the bid documentation, the degree of compaction was required to be in the range 92 to 95 percent (air-void content of 5 to 8 percent) of the theoretical maximum density (CT 309).

During the paving of the first lift, asphalt concrete was removed from the skip of the paver and spread evenly in a thickness of approximately 20 mm (0.8 in) over the strain gages and tamped in place using a hand tamper. The leads of the strain gages were also covered with asphalt concrete to prevent damage by the paver.



**Figure 2.13: Asphalt concrete placement**



**Figure 2.14: Nuclear density testing**

After the first lift was placed and compaction of the asphalt concrete was accepted, an asphalt emulsion was applied to the surface of the first asphalt concrete lift. The second lift was then placed and compacted. Some segregation was noted at certain locations (most notably at the end of the test pavement adjacent to Building 280), but was outside of the planned HVS testing area.

Average air-void contents in the asphalt concrete were 9.7 and 10.3 percent for the first and second lifts, respectively.

### **2.13. Full Depth Patching**

Two days after completion of the test pavement, failure was observed near the end of the pavement near the instrumented test section (Section 574RF). This area was not part of the overlay experiment (see Figure 2.3). The probable reason for this failure was high moisture content in the aggregate base.

Due to the large number of trucks making use of this entrance, the contractor was instructed to patch this section of road. The new 90-mm DGAC layer was removed and the aggregate base re-mixed and allowed to dry before compaction. A 150-mm thick DGAC patch was then paved and compacted to complete the repair.

### **2.14. Shoulder Backing and Completion of Instrumentation**

Once the asphalt concrete patch had been placed, the shoulder backing was completed by hand to avoid disturbing the instrumentation cables in the aggregate base shoulder. Following construction, the buried instrument leads were exposed in the shoulders of the test pavement, combined at each location of

instrumentation, bagged, and secured to stakes. This operation was performed to place the ends of the instrument leads above the water level to protect them from moisture damage during potentially heavy rains.

### 3. MATERIAL TESTING

---

A number of tests were conducted during and after construction of the pavement test section to characterize the pavement materials and the subgrade.

#### 3.1. Air-Void Content and Thickness of Asphalt Concrete Layer

Nuclear density measurements and extracted cores were obtained to determine the air-void content distribution in the asphalt content layer after construction. The data were also used to establish a relationship between the nuclear test and laboratory test air-void contents. Laboratory air-void contents were determined on extracted cores according to Caltrans CT308 and AASHTO T-166 test procedures at locations where nuclear readings were obtained. Acceptance was based on AASHTO T-166 test results. Figure 3.1 shows the relation between Caltrans CT308, the nuclear device air void data, and AASHTO T-166 air void data. As shown in the figure, the average measured air-void content difference between AASHTO T-166 and the nuclear device was 4.6 percent.

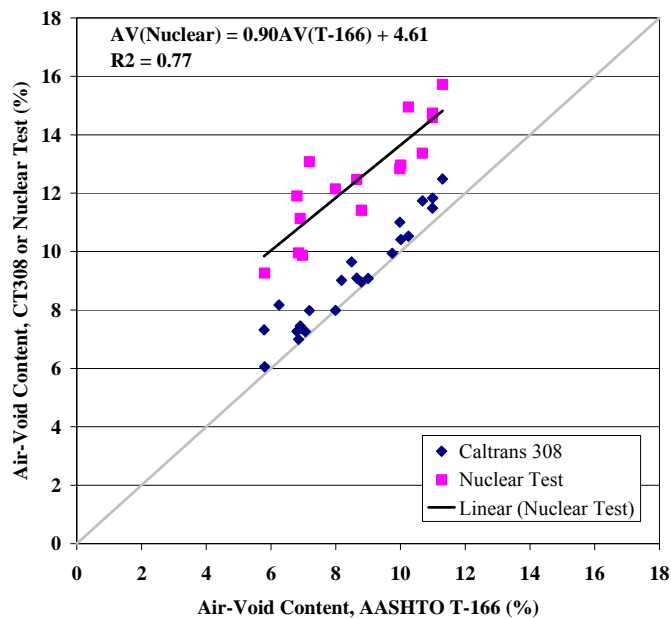


**Figure 3.1: Relationship between air-void content measurements.**

Figure 3.2 shows a relative frequency and cumulative histogram for the air-void content in the dense-graded asphalt concrete. A wide range of air voids with more than one peak value is evident. More than one data distribution can be found over the range of measured air voids. This may be due to the presence of segregated areas on the asphalt concrete mat observed during construction. These areas were primarily



caused by the asphalt mix in the hopper of the paver cooling while waiting for the next truck to deliver mix to the site. Because the cooled mix in the paver was not completely remixed with the new hot mix, proper compaction of the cooled mix was not possible. As a result, some areas had higher air voids. These segregated areas were excluded from consideration when selecting the sub-sections for accelerated pavement testing.

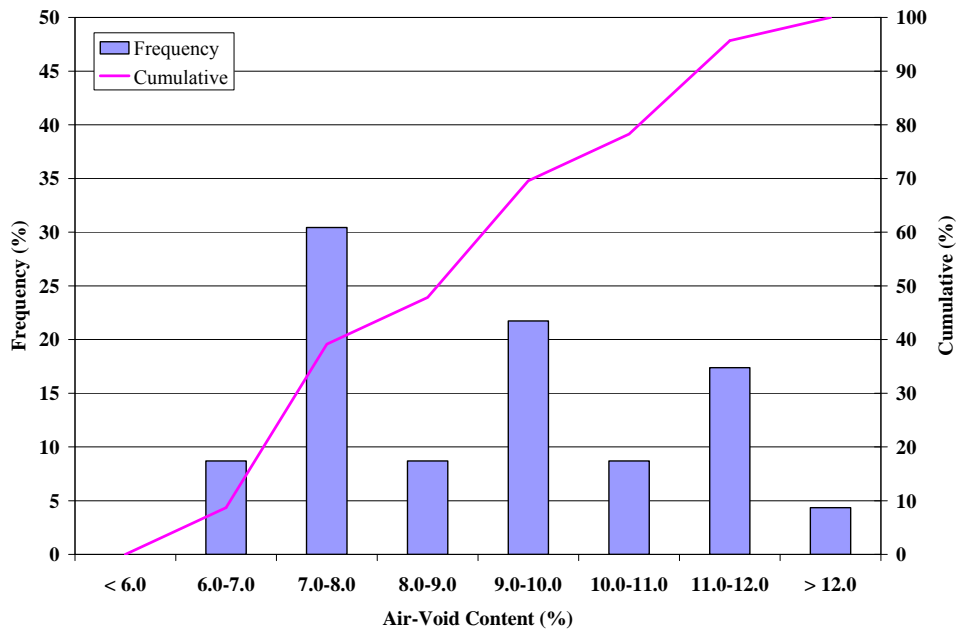


**Figure 3.2: Air-void content relative frequency and cumulative histogram.**

The distribution of air voids along the project is critical for the evaluation of the accelerated pavement tests since the air void contents of the mixes have a significant impact on the fatigue performance of asphalt concrete layers. The average air-void content in the compacted asphalt concrete layer was 9.1 percent with a standard deviation of 1.8 percent. This average excludes air-void contents in the segregated areas. Figure 3.3 shows the distribution of air voids in the pavement section based on AASHTO T-166. The distribution of air voids in the mix indicates that high air-void contents were usually recorded near the shoulder.

Extracted cores were also used to determine the distribution of asphalt concrete thickness along the test section. Figure 3.4 shows the relative frequency and cumulative histogram for the asphalt concrete thickness. The data show that about 76 percent of the asphalt concrete cores were between 70 and 90 mm thick. The average thickness along the pavement section was 79.0 mm with a standard deviation of 9.9 mm. The design thickness for this project was 90 mm.

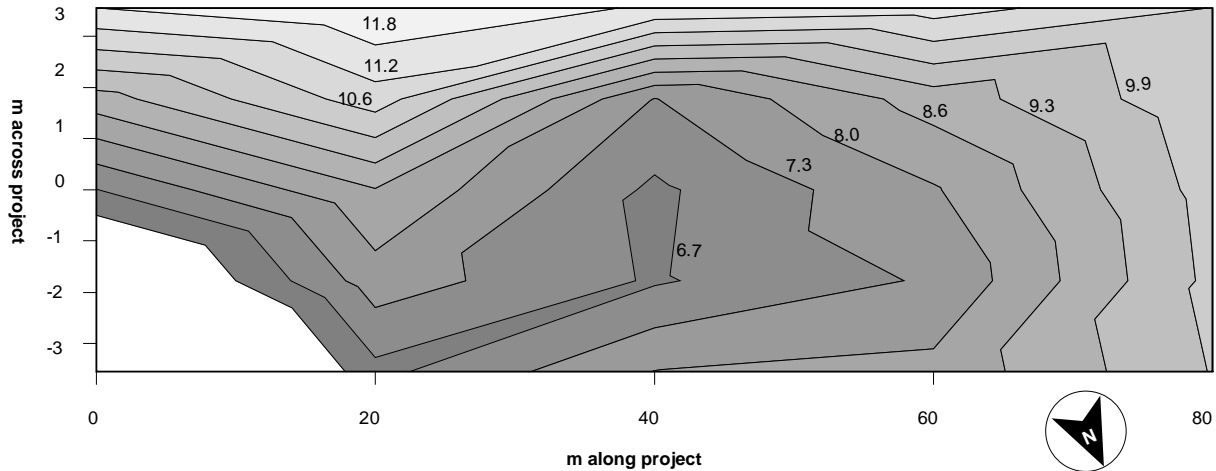


**Figure 3.3: Air-void distribution in asphalt concrete layer along the project.**

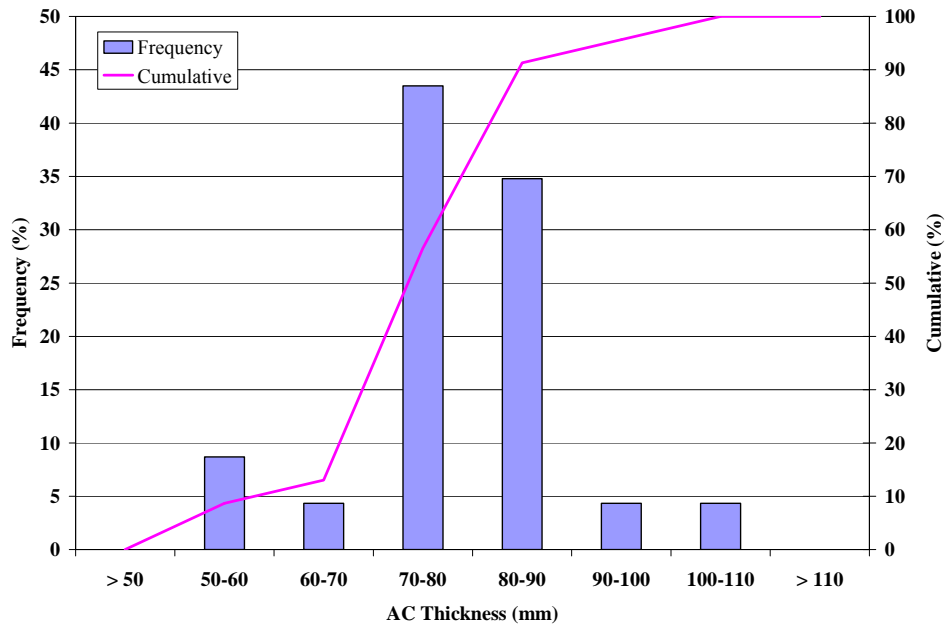


**Figure 3.4: Relative frequency and cumulative histogram for asphalt concrete thickness.**

Figure 3.5 shows the distribution of the pavement thicknesses across the entire section. Distribution of thickness along the project can also influence the fatigue and rutting performance of the test sections. An increase in pavement thickness increases the service life of the pavement by reducing the tensile strain at the bottom of the asphalt concrete, thereby increasing the fatigue performance of the asphalt concrete. Increased thickness also reduces the state of the stresses in the unbound layers, which improves the rutting performance of the granular base and subgrade.

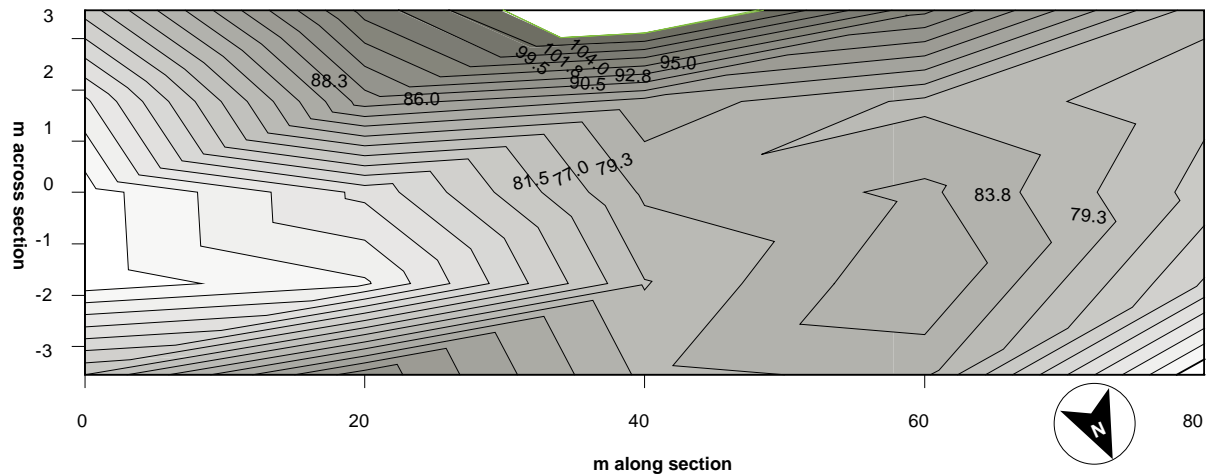


**Figure 3.5: Distribution of asphalt concrete thickness across pavement section.**

### **3.2. Asphalt Extraction and Gradations**

Asphalt binder extractions and aggregate gradations were obtained from two loose mix samples to check in-place mixtures. The binder contents of the samples were 4.34 and 5.69 percent (aggregate basis). Target binder content was 5.0 percent. Figure 3.6 summarizes aggregate gradations for the two samples and for the mix gradation used in the mix design. Sample 1 appeared to be within the specification but Sample 2 appeared to be slightly finer than the specification. There was insufficient information to perform a statistical evaluation of the impact of binder content and mix gradation on the performance of the pavement. However, these two parameters might have had an influence on the air-void contents of the compacted mix.

### **3.3. Dynamic Cone Penetrometer Testing of Unbound Materials**

Figure 3.7 summarizes Dynamic Cone Penetrometer (DCP) tests in terms of penetration rates in the aggregate base and subgrade along the pavement section. These were obtained after construction of the aggregate base and asphalt concrete layers. DCP tests were performed at the same 17 locations where asphalt concrete cores were extracted. Average penetration rates for the aggregate base and subgrade before placing the asphalt concrete were 6.4 mm/blow and 23.4 mm/blow, respectively with standard deviations of 1.0 mm/blow and 9.0 mm/blow, respectively. After placing the asphalt concrete layer, the average penetration rates in the aggregate base and subgrade were 2.4 mm/blow and 17.8 mm/blow, respectively with standard deviations of 0.4 mm/blow and 5.4 mm/blow, respectively.

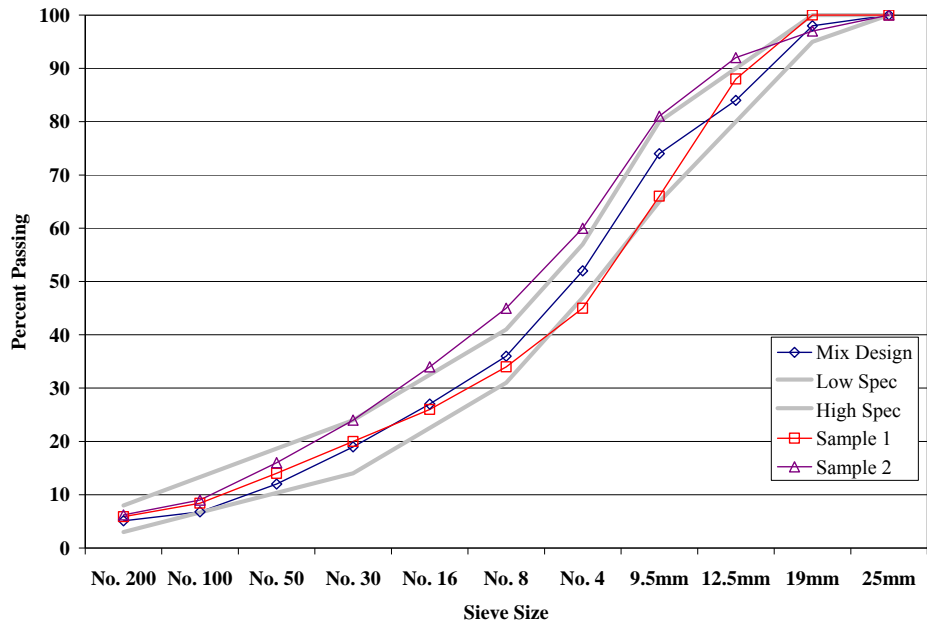


**Figure 3.6: Asphalt concrete mix gradations.**

The DCP tests obtained after the asphalt concrete layer was placed were conducted five months after completion of the project. The decrease in penetration rates over this period indicate a significant strengthening (drying out) of the aggregate base over time. Strengthening of the subgrade is observed at most test locations, with dramatic increases observed near stations 30 and 45. Increased strength of the subgrade probably resulted from compaction during construction of the covering layers, and drying back of the material.

Aggregate base thicknesses along the pavement section were estimated from DCP data at the point where the slopes of the penetration rates of the aggregate base and subgrade intersect. The average thickness of the aggregate base was 375 mm with a standard deviation of 47 mm (design thickness was 410 mm). Figure 3.8 shows aggregate base thickness along the pavement section. The data indicate a difference between the thickness obtained before and after placing the asphalt concrete. The results are not conclusive at this point because they were obtained at different locations.

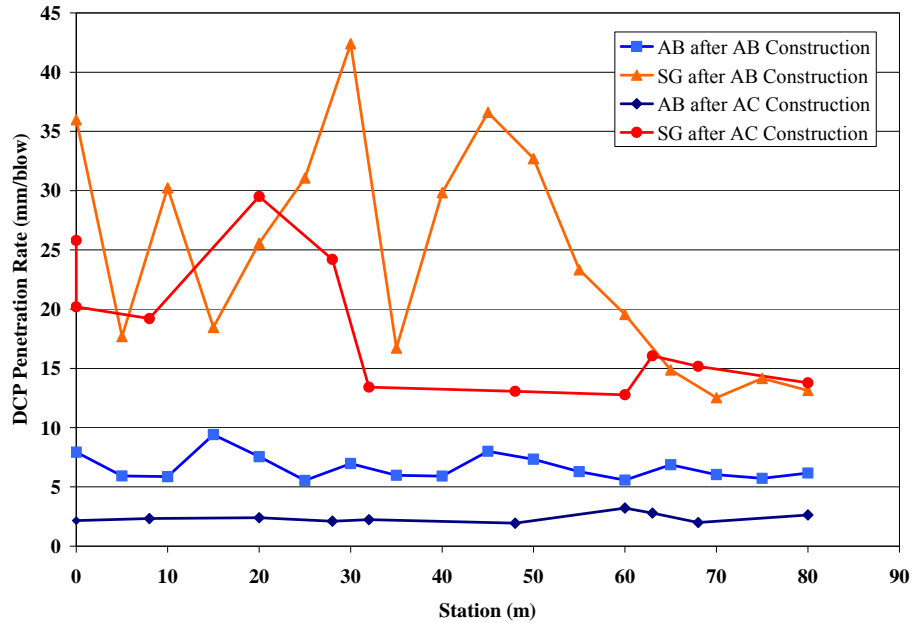


Figure 3.7: DCP data for unbound materials.

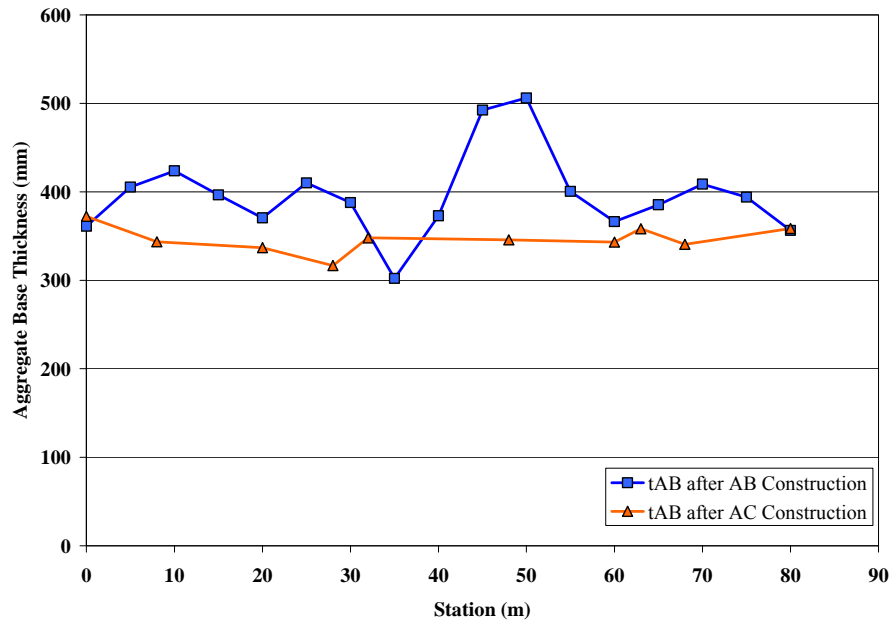


Figure 3.8: Thickness of aggregate base estimated from DCP measurements.

### 3.4. Unbound Materials Classification

The aggregate base material met gradation specifications for Class 2 aggregate. While visual evaluation of the material indicated that it contained more than 50 percent recycled material including brick, asphalt concrete, and portland cement concrete (upper limit of 50 percent for Class 2 material), subsequent laboratory testing showed that the material met or exceeded the requirements for Class 2 aggregate base. The dark brown clay subgrade was classified as a lean clay (CL) with Atterberg limits as follows:

- Liquid limit: 38 to 42 percent
- Plasticity index: 20 to 27.

### 3.5. Falling Weight Deflectometer Tests

FWD testing was conducted at various stages during construction to study the effect of the subsequent overlay on the behavior of the pavement. This included tests on the consolidated subgrade, aggregate base, and asphalt concrete layers. FWD tests were conducted along five lines of testing parallel to the roadway centerline (Table 3.1).

**Table 3.1: FWD Test Location**

Location	Description
1.3 S	Along a line 1.3 m south of centerline
2.3 S	Along a line 2.3 m south of centerline
CL	Along centerline
1.3 N	Along a line 1.3 m north of centerline
2.3 N	Along a line 2.3 m north of centerline

Moduli of the pavement layers were calculated from deflections using the back-calculation program ELMOD 5.0 (7), a program using Odemark’s transformation of a layered system and Boussinesq’s equations.

#### 3.5.1 FWD Testing on the Subgrade during Construction

Results of FWD tests on top of the cohesive subgrade are not included since shear failure occurred in the subgrade under the loading plate.

#### 3.5.2 FWD Testing on the Aggregate Base

FWD testing was conducted on top of the aggregate base using 22.2- and 40-kN loads. Back-calculated moduli under the 40-kN load for the aggregate base and subgrade are presented in Figures 3.9 and 3.10, respectively. Significant variability was observed in the moduli of both layers. The average modulus for the aggregate base was 125 MPa with a standard deviation of 48 MPa, while the average modulus for the subgrade was 38 MPa with a standard deviation of 25 MPa. Relative frequency and cumulative histograms for moduli of the aggregate base and subgrade are presented in Figures 3.11 and 3.12, respectively. At this stage, the calculated modulus of the aggregate base was lower than representative values for similar California aggregate base materials. The lower value was attributed to absence of confinement provided by the asphalt concrete wearing course.

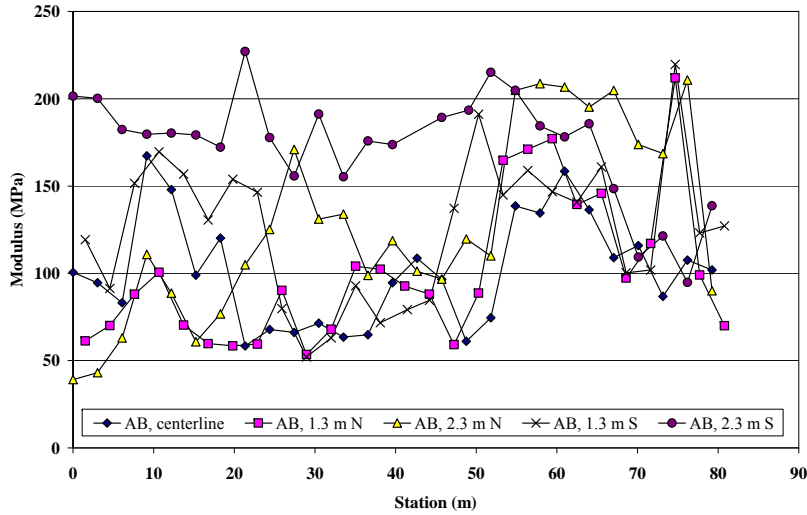


**Figure 3.9: FWD determined aggregate base modulus (tested on base).**

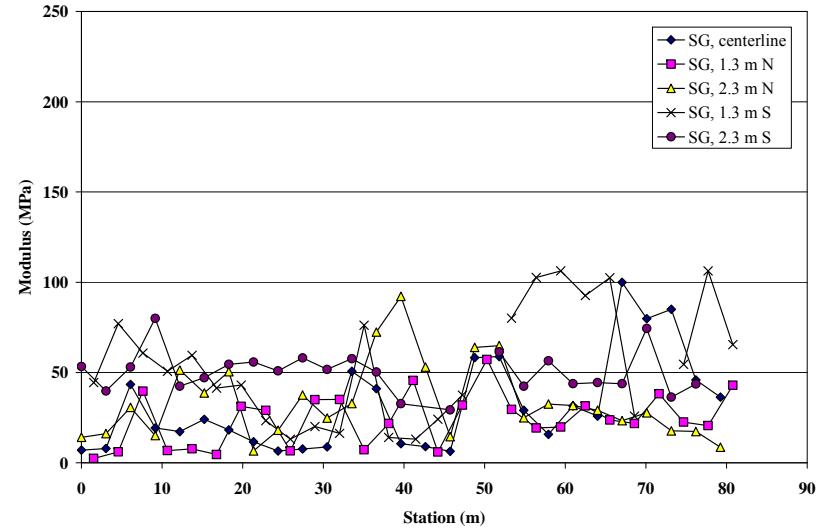


**Figure 3.10: FWD determined subgrade modulus (tested on base).**

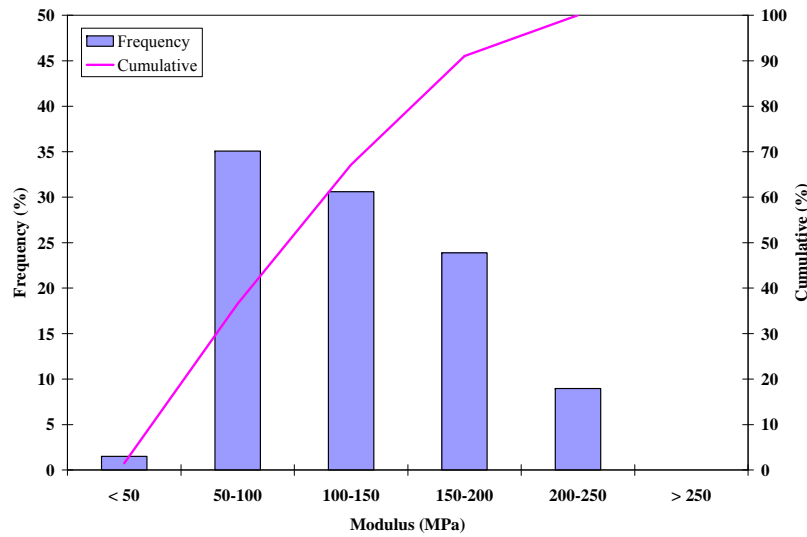


**Figure 3.11: Relative frequency and cumulative histogram for base modulus**

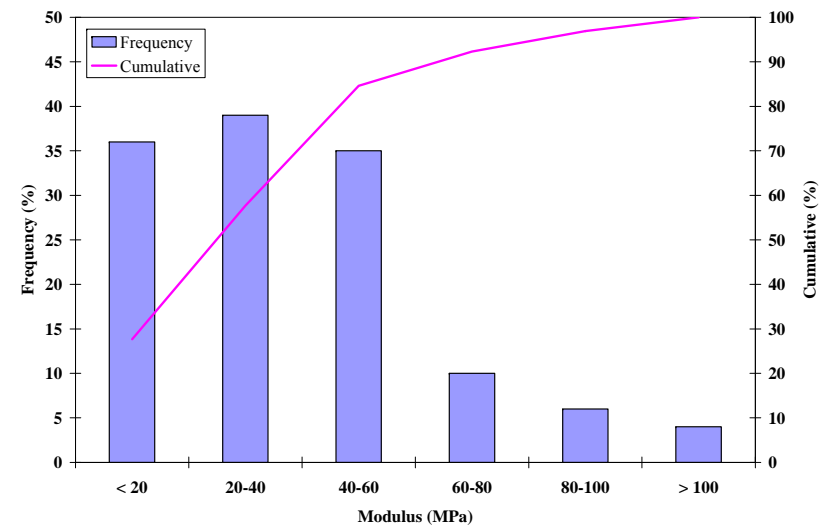


**Figure 3.12: Relative frequency and cumulative histogram for subgrade modulus**

### 3.5.3 FWD Testing on the Asphalt Concrete

FWD testing was conducted on the surface of the asphalt concrete layer after construction at loads of 22.2 kN, 40 kN, and 60 kN. Backcalculated moduli for the asphalt concrete, aggregate base, and subgrade for the 40-kN load are presented in Figures 3.13 through 3.15, respectively. Substantial variability in moduli was observed for the pavement layers and the subgrade. Table 3.2 summarizes the statistics for the moduli. Averages and standard deviations are based on data from all five testing lines.

**Table 3.2: Summary of Moduli of Pavement Layers and the Subgrade**

Layer	Average Modulus (MPa)	Standard Deviation (MPa)
Asphalt Concrete	2,035	602
Aggregate Base	284	104
Subgrade	99	37

#### Effect of Asphalt Concrete on Unbound Materials

Direct comparison of the moduli of the unbound materials before and after construction of the asphalt concrete layer indicated an increase in the unbound layer moduli (see Figures 3.9, 3.10, 3.14 and 3.15). The average moduli increased by 127 percent and 160 percent for the aggregate base and subgrade, respectively.

The observed trend of increased moduli is reasonable. The aggregate base modulus increase is likely due to the confinement provided by the asphalt concrete layer and to added densification resulting from the compactive effort applied to the asphalt concrete. Increase in the subgrade modulus is attributed to additional cover provided by the asphalt concrete layer and stiffening of the aggregate base, which combine to reduce the level of stresses on the subgrade. This in turn results in an increase in the modulus of fine-grained cohesive soils such as the CL material at this site.

#### Modulus of the Asphalt Concrete

Figures 3.16 and 3.17 show the relative frequency and cumulative histograms, respectively for the back-calculated moduli obtained along the centerline as well as the north and south lanes of the test pavement section. As seen in this figures, higher moduli were generally obtained along the south lane of the pavement section. A summary of modulus values is provided in Table 3.3.

**Table 3.3: Summary of Average Asphalt Concrete Modulus along the Pavement Section**

Parameter	FWD Measurements			
	North	South	Centerline	All
Average (MPa)	1,625	2,425	2,057	2,035
Standard Deviation (MPa)	394	527	566	602



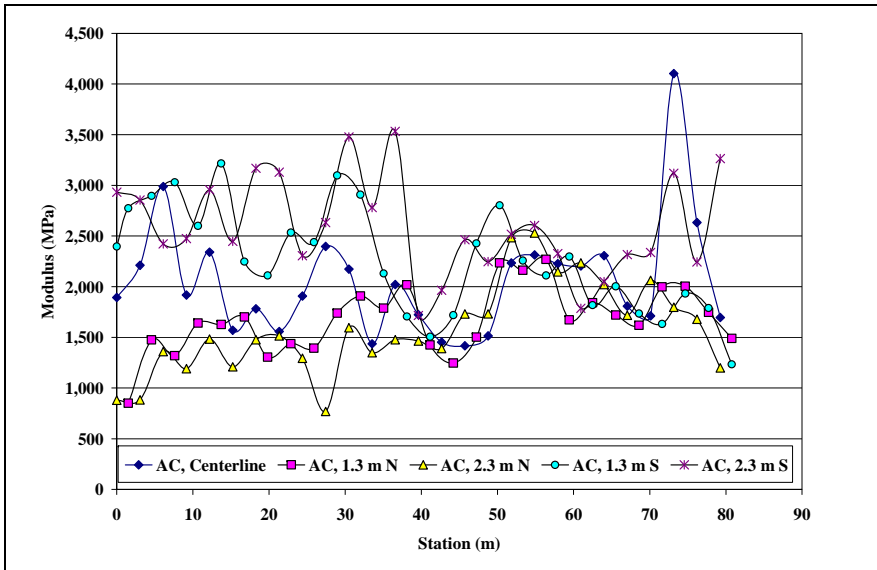


**Figure 3.13: Back-calculated modulus of asphalt concrete (tested on AC).**

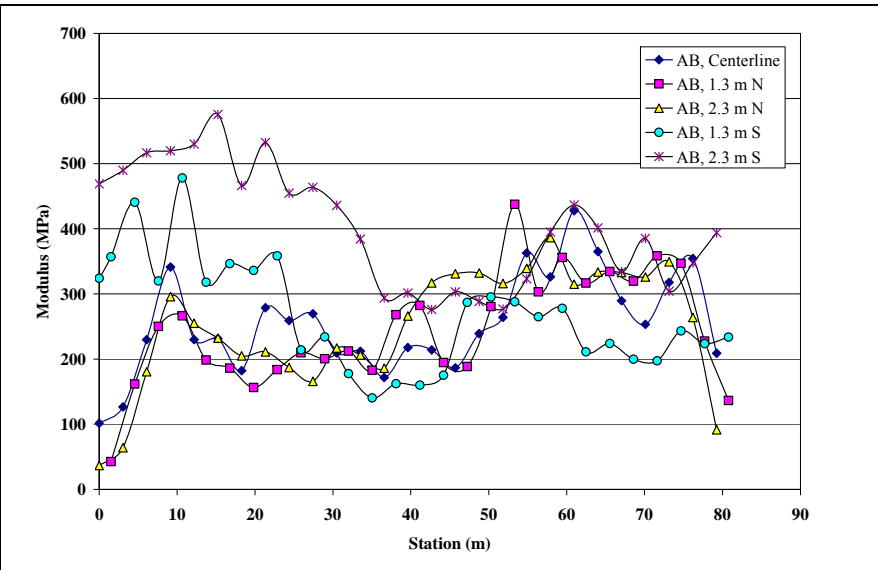


**Figure 3.14: Back-calculated modulus of aggregate base (tested on AC).**

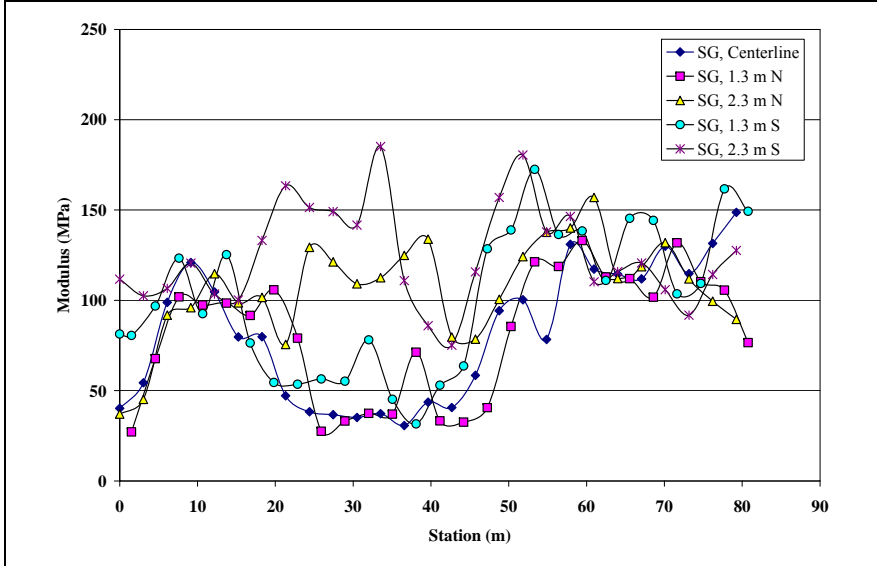


**Figure 3.15: Back-calculated modulus of subgrade (tested on AC).**

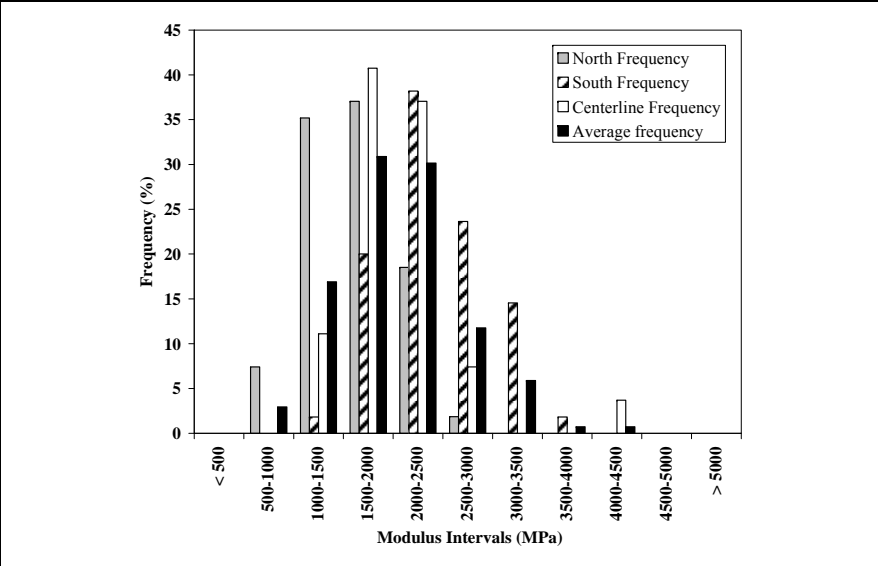


**Figure 3.16: Relative frequency of asphalt concrete modulus.**

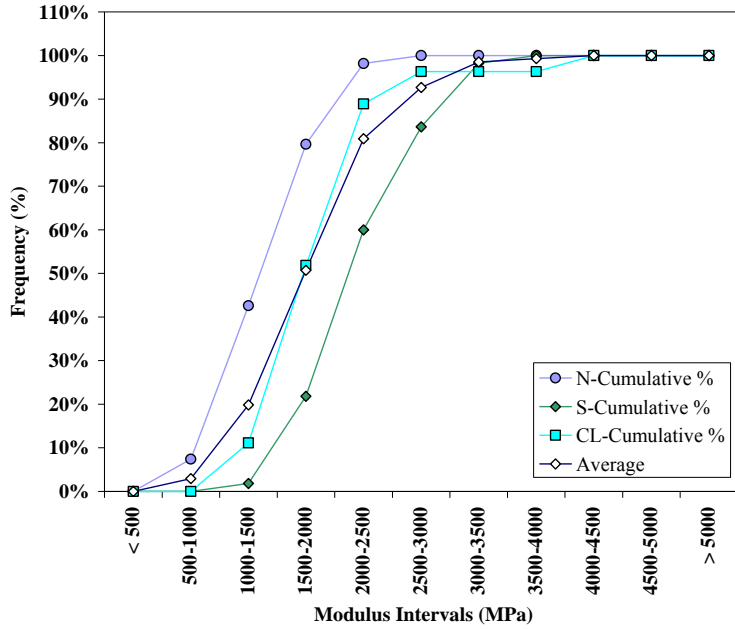


**Figure 3.17: Cumulative histogram of asphalt concrete modulus.**

Distribution of the asphalt concrete moduli along the pavement section is shown in Figure 3.18. Darker areas indicate higher modulus values. The distribution corresponds with the location of the segregated areas along the section and will be used when analyzing the performance of the six sub-sections subjected to HVS loading.

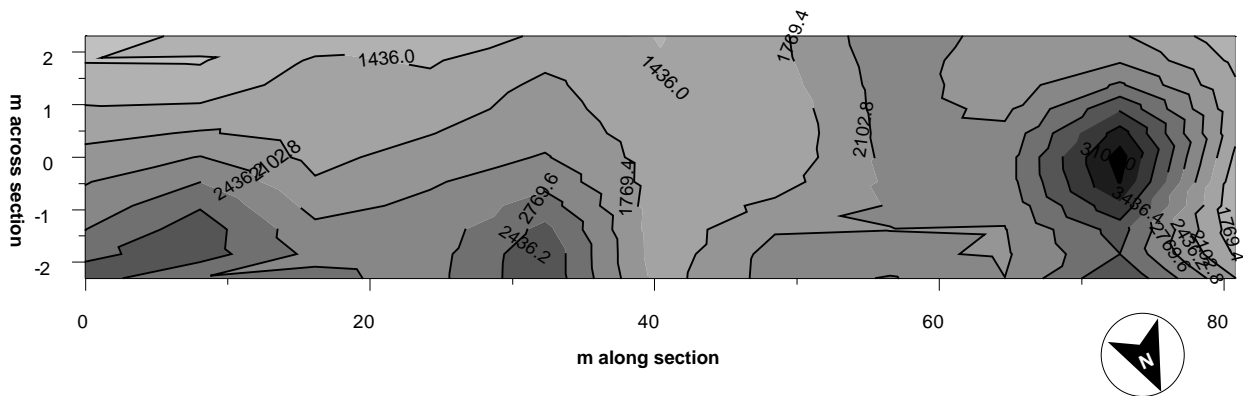


**Figure 3.18: Distribution of asphalt concrete moduli along the pavement section.**

### Modulus of the Aggregate Base

Figures 3.19 and 3.20 show the relative frequency and cumulative histogram, respectively of aggregate base moduli along the pavement section obtained from backcalculation of the FWD data. Results suggest that the first area may consist of two populations of moduli with values of approximately 250 MPa and 350 MPa, with the high modulus values on the northbound lane between stations 0.0 m and 30 m. Figure 3.21 shows the distribution of aggregate base modulus along the pavement section. In the figure, darker color indicates higher aggregate base modulus.

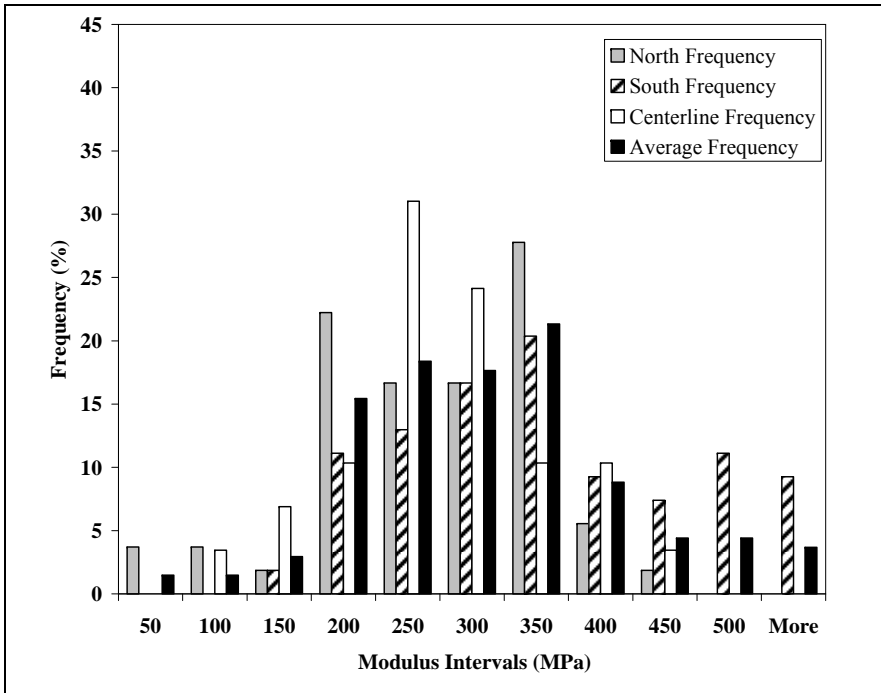


**Figure 3.19: Relative frequency of base layer modulus.**

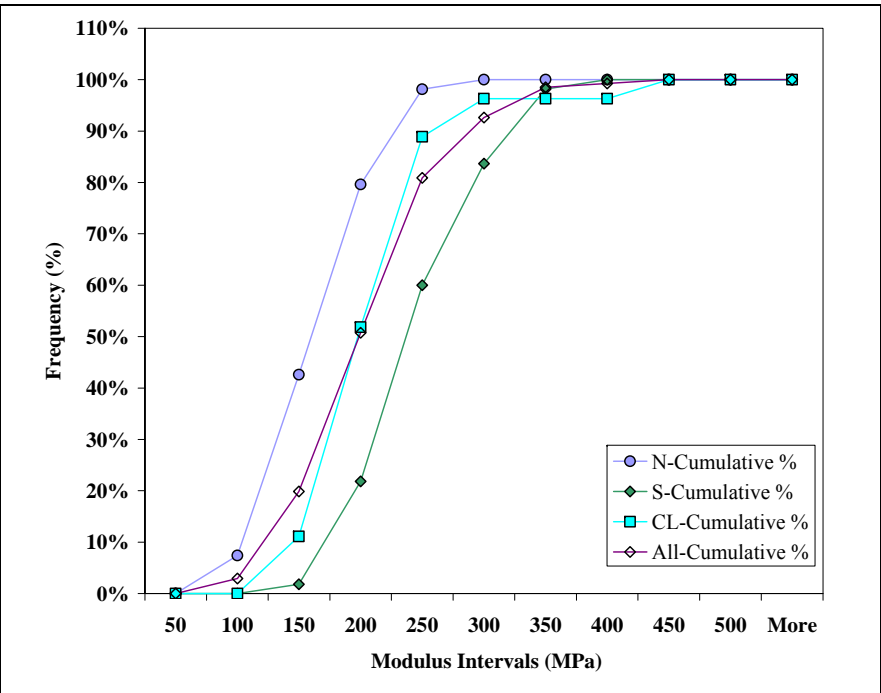


**Figure 3.20: Cumulative histogram of base layer modulus.**

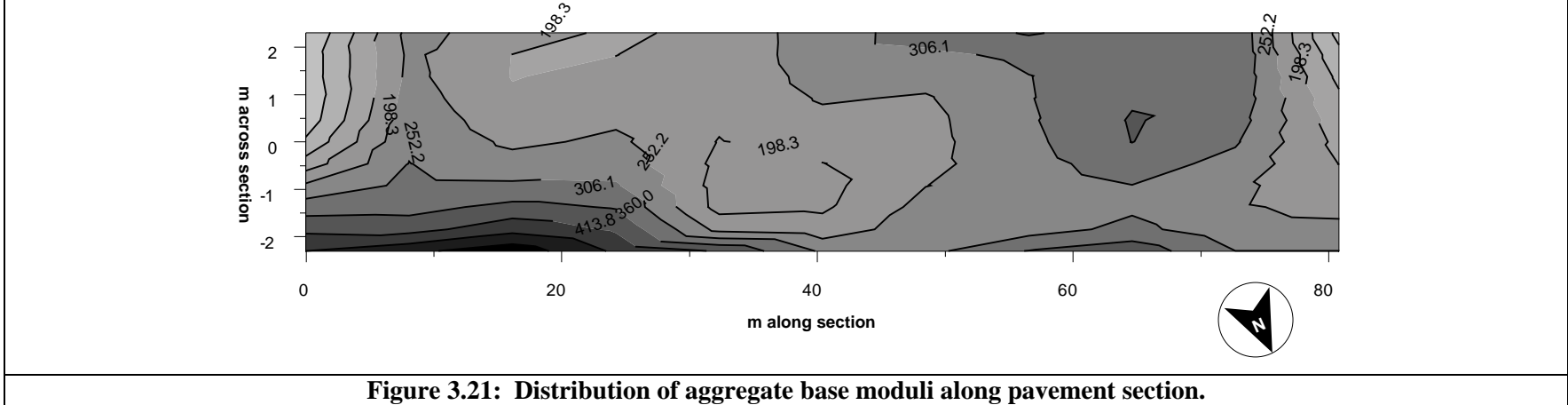


**Figure 3.21: Distribution of aggregate base moduli along pavement section.**

Table 3.4 provides a summary of aggregate base moduli at the different locations across the section.

**Table 3.4: Summary of Aggregate Base Moduli along Pavement Section**

Parameter	FWD Measurements			
	North	South	Centerline	All
Average (MPa)	247	334	254	283
Standard Deviation (MPa)	87	110	76	103

Modulus of the Subgrade

The average modulus of the subgrade was 98 MPa with a standard deviation of 37 MPa. Relative frequency and cumulative histogram are shown in Figure 3.22, while Figure 3.23 shows the distribution of subgrade modulus along the pavement section. In the figure, darker color indicates higher modulus. A weak subgrade (lower modulus) was observed between Stations 20 m and 50 m in the southbound lane (test lines 1.3 and 2.3 m). While the reason for the low subgrade modulus in this area is not clear, based on observations during construction the subgrade in this area was compacted at high moisture content (to the right of the line of optimum). Compaction in this moisture region induces dispersed particle orientation in this type of soil. This, in turn, results in higher resilient deformations (low resilient modulus) than if compaction occurs to the left of the line of optimum (lower moisture content).

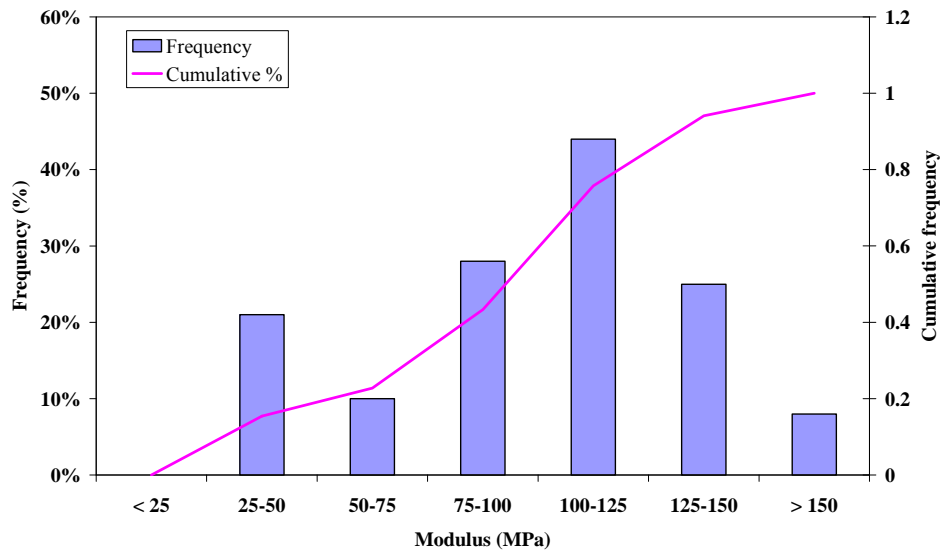


**Figure 3.22: Relative frequency and cumulative histogram of subgrade modulus.**

A comparison of Figures 3.21 and 3.23 indicates that low aggregate base moduli and low subgrade moduli were observed in the same locations. Direct comparison of these two parameters (Figure 3.24) indicates that, after construction, the modulus of the aggregate base was related to that of the subgrade. This observation is particularly important for aggregate base construction because a stiffer subgrade provides a compaction platform that promotes higher base densities.

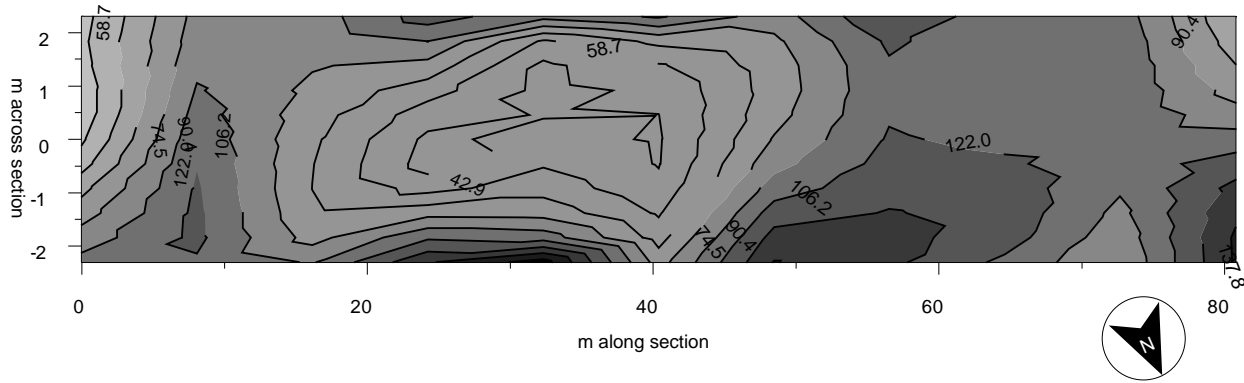


**Figure 3.23: Distribution of subgrade moduli along pavement section.**

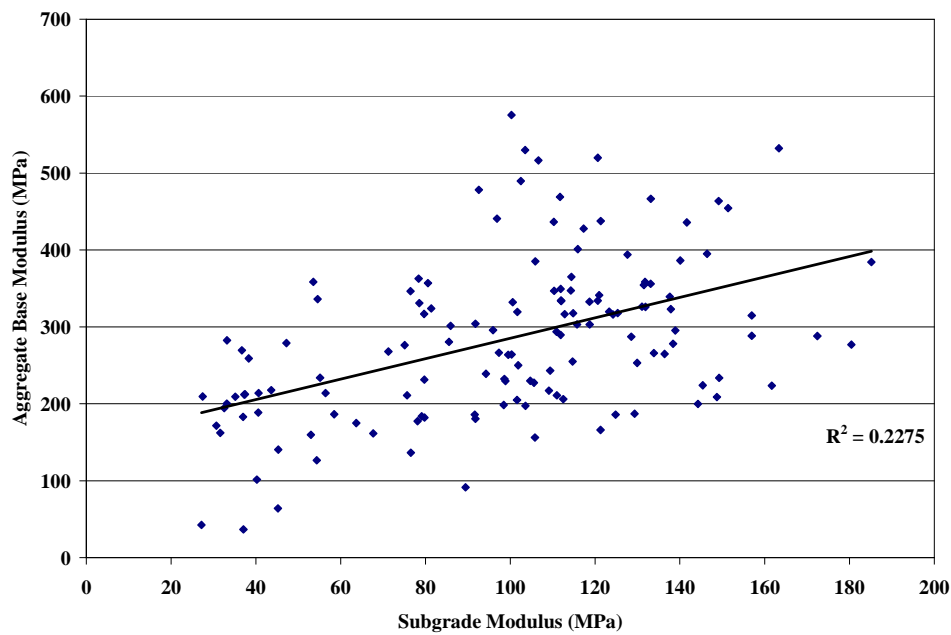


**Figure 3.24: Comparison of aggregate base and subgrade moduli.**

### 3.5.4 Phase 1 FWD Testing

FWD testing was conducted at various times during Phase 1 HVS testing to monitor changes in the modulus of the bound and unbound layers over time.

#### Deflections

Center plate deflection data ( $D_0$ ) collected from October 2001 through May 2003 along the five lines of FWD testing at a nominal load of 40 kN are presented in Table 3.5 and Figure 3.25. FWD testing was conducted every three meters (ten feet) along the five test lines with the purpose of studying the effect of climate on pavement stiffness. The data do not include the damage produced by accelerated pavement testing on the six HVS sections.

In addition, the data suggest that the subgrade between approximately Stations 17 m and 50 m may be somewhat less stiff than the sections of subgrade from Stations 0 m to 17 m and Stations 50 m to 70 m (on either side within the boundaries of the various test sections).

**Table 3.5: Average FWD Deflections by Date**

Date	Average Deflection ( $D_0$ )					
	Station					
	10-20	20-30	30-40	40-50	50-60	60-70
10/03/2001	263	276	282	285	204	224
10/11/2001	306	324	331	287	211	238
10/25/2001	397	415	424	411	306	322
11/07/2001	279	286	277	274	223	242
12/14/2001	313	346	277	339	231	271
01/08/2002	261	273	305	312	244	293
01/09/2002	274	274	230	251	214	236
02/13/2002	262	274	264	309	261	249
10/07/2002	240	258	284	263	236	277
01/02/2003	180	193	179	185	186	191
05/19/2003	280	290	381	322	333	305

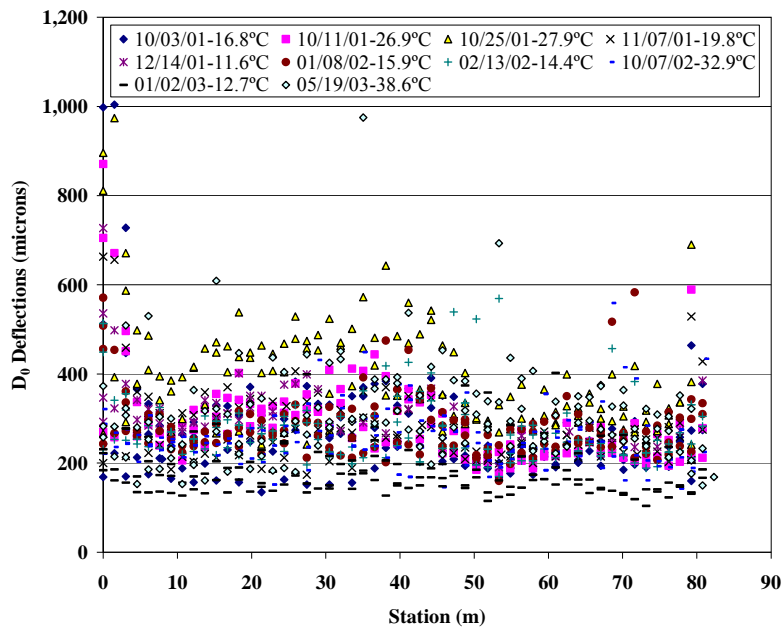


**Figure 3.25: FWD deflections at the load plate ( $D_0$ ) along the pavement section.**

### Back-Calculated Moduli

Moduli were calculated from FWD deflections using the computer program ELMOD 5.0 (7). A non-linear subgrade and no bedrock were assumed in the back-calculations. Results of the back-calculations are summarized in Figure 3.26 for average layer moduli along the north and south lanes. Y-bar errors indicate one standard deviation from the average value.

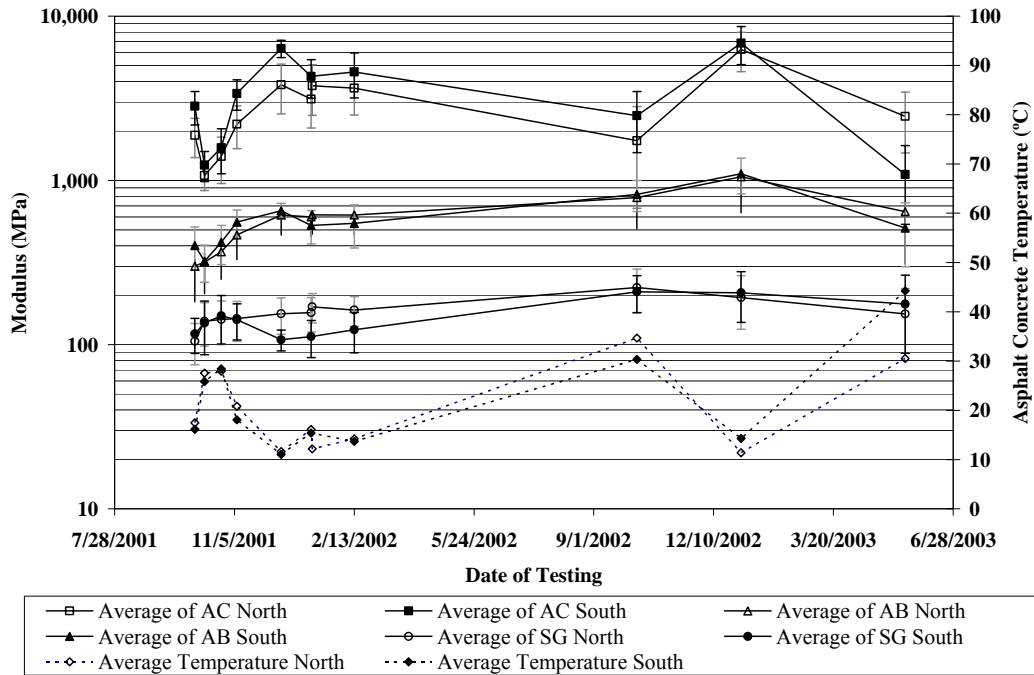


**Figure 3.26: Summary of back-calculated moduli for pavement section.**

Figure 3.26 shows a rapid increase in moduli of all the pavement layers and the subgrade from September 2001 to December 2001. The increase is particularly significant for the asphalt concrete and the aggregate base. The change in asphalt concrete modulus with time is typical and expected for asphalt concrete layers. However, the decrease in unbound layer moduli during the 2003 summer period does not coincide with expected results. It would be expected that the measured aggregate base stiffness moduli would increase because the asphalt concrete is less stiff and the stresses are higher. It is possible that the confining effect of the asphalt concrete was less significant due to its reduced stiffness, thereby resulting in the decrease in the aggregate base moduli. The lower moduli of the subgrade are likely a result of increased moisture content during the wet season.

Figure 3.27 shows the variation of asphalt concrete modulus with pavement temperature for the north and south lanes. Pavement temperatures were estimated from air temperatures using BELLS equation (8). The data show an increase in modulus with low temperatures, which is typical behavior for asphalt concrete layers. On average, the data indicate that for a given pavement temperature, moduli of the asphalt concrete in the south lane are higher than those in the north lane. This is more evident in Figure 3.28, which shows average asphalt concrete moduli along the two pavement section lanes. Differences in moduli between the sections occur mainly in the first 50 m of the section.

As noted earlier, the behavior of the aggregate base did not follow expected trends (i.e., an increase in stiffness with increase in stress [e.g., sum of principal stresses]). For example, Figure 3.29 shows aggregate base moduli versus asphalt concrete moduli. Laboratory repeated load triaxial compression tests indicated that the aggregate base materials increased in stiffness with increase in confining pressure. It is possible that increases in asphalt concrete moduli resulted in increased confining pressures in the aggregate base layer, resulting in increased aggregate base stiffness moduli.

Effects of subgrade stiffness moduli on aggregate base moduli are shown in Figure 3.30. These trends follow expected results and are relative to the inability of the untreated aggregate base to accommodate tensile stresses as reported by the Shell investigations (9). These investigations suggested modular ratios between base and subgrade materials in the range two and to three.

Average variations of the aggregate base and subgrade moduli presented in Figures 3.31 and 3.32 supports, at least to a reasonable degree, this observation by the Shell investigation.

Figure 3.33 shows precipitation and moisture content in the unbound materials as a function of time. Water content is presented as a relative number due to the errors in the absolute measurements. However, overall fluctuations and trends in the relative moisture content were correct. The precipitation and subgrade moisture content variation exhibited a significant offset; peak moisture contents were recorded seven months after peak monthly precipitation and one month after the last rainfall was recorded. This offset between precipitation and measured moisture content could be due to poor drainage of the subgrade. On the other hand, the precipitation and aggregate base display typical trends with the rate of moisture content decrease lower than the rate of moisture content increase.

Figures 3.34 and 35 indicate variations of base, subgrade modulus, and moisture content with time. The effect of moisture content on the aggregate base somewhat contradicts experience for the period of data collected. Figure 3.34 shows an increase in moisture content in the aggregate base and is associated with an increase in the aggregate base modulus; usually a decrease in stiffness with increase in water content is expected. As discussed earlier, factors such as asphalt concrete modulus variations could have a more significant effect on the aggregate base modulus than moisture content. Figure 3.35 shows a decrease in subgrade moisture content and modulus during the months of May and June 2003. This pattern is expected because fine grained soils are affected significantly by moisture content.



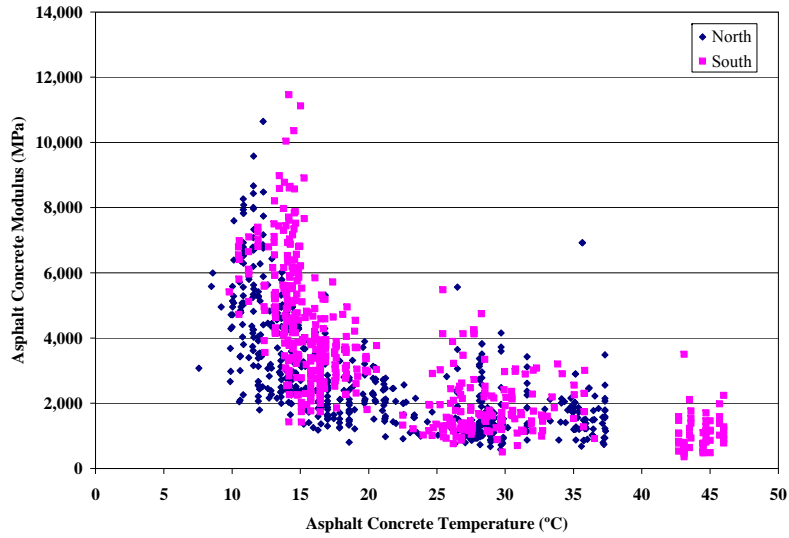


**Figure 3.27: Effect of temperature on modulus of the asphalt concrete layer.**

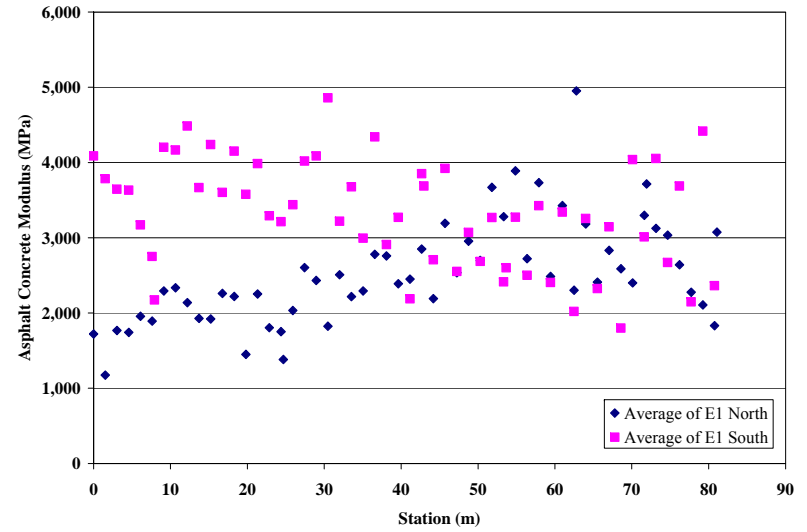


**Figure 3.28: Variation of asphalt concrete moduli along the pavement section.**

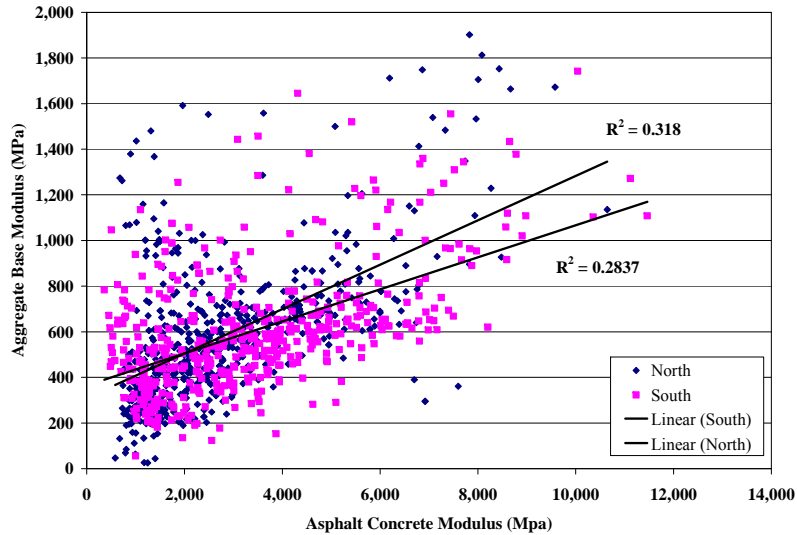


**Figure 3.29: Variation of aggregate base modulus with asphalt concrete modulus.**

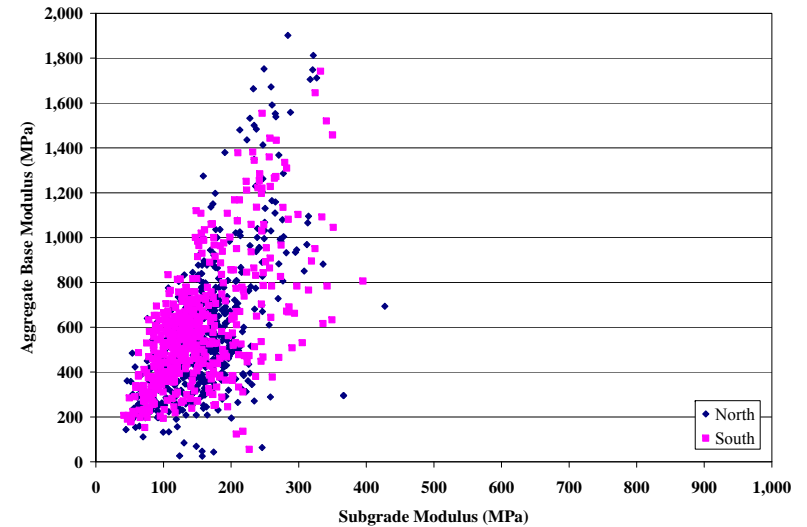


**Figure 3.30: Variation of aggregate base modulus with subgrade modulus.**

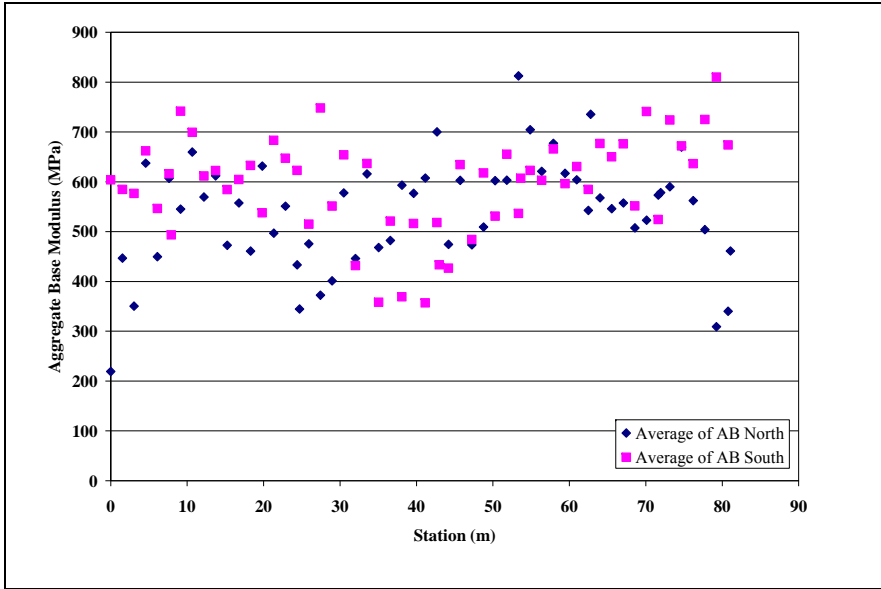


**Figure 3.31: Average aggregate base modulus along the pavement test section.**

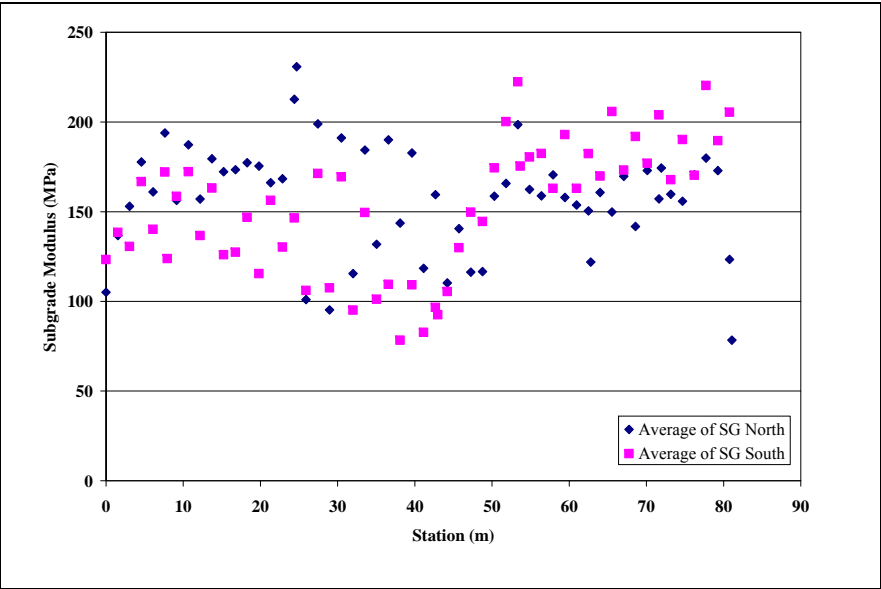


**Figure 3.32: Average subgrade modulus along the pavement test section.**

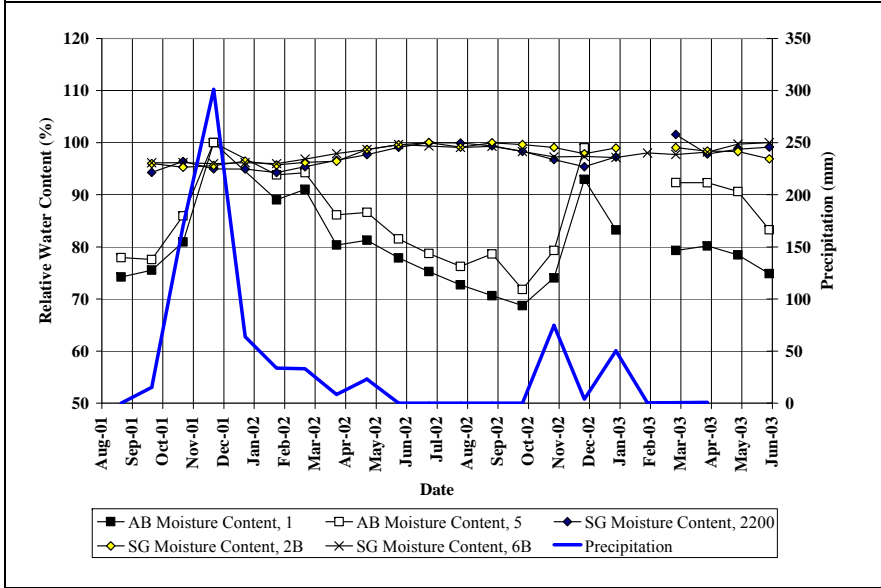


**Figure 3.33: Variation of moisture content with precipitation over time.**

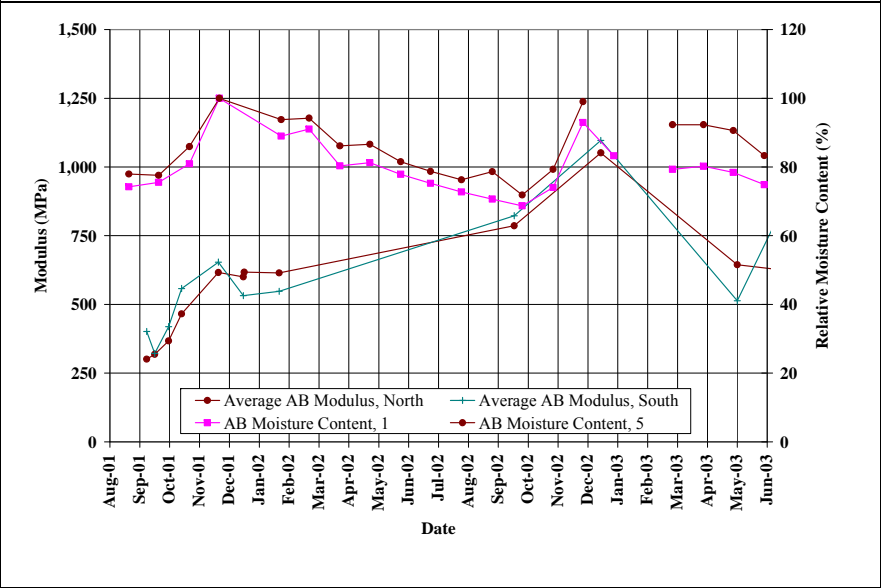


**Figure 3.34: Variation of modulus with time as a function of moisture content for aggregate base.**

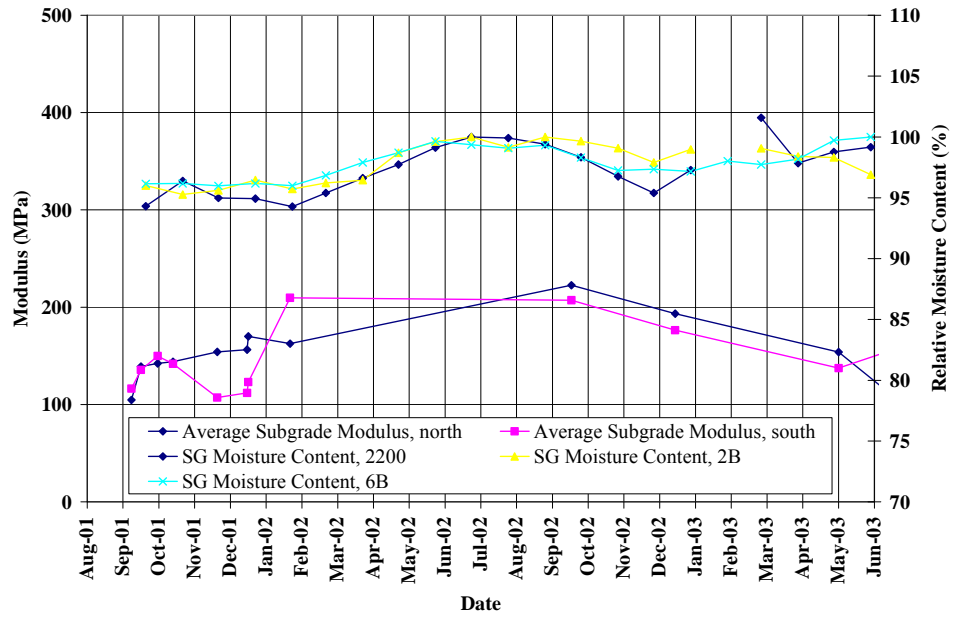


Figure 3.35: Variation of modulus with time as a function of moisture content for subgrade.

## **4. PHASE 1 HVS TESTING**

---

Phase 1 HVS testing was carried out on six demarcated sections on the test track to induce fatigue cracking. Locations of the test section are shown in Figure 2.3.

### **4.1. Test Section Layout**

The typical section layout for each HVS test is shown in Figure 4.1. Station numbers refer to fixed points on the test section and are used for measurements and as a reference for discussing performance.

### **4.2. Pavement Instrumentation and Monitoring Methods**

Measurements were taken with the following instruments:

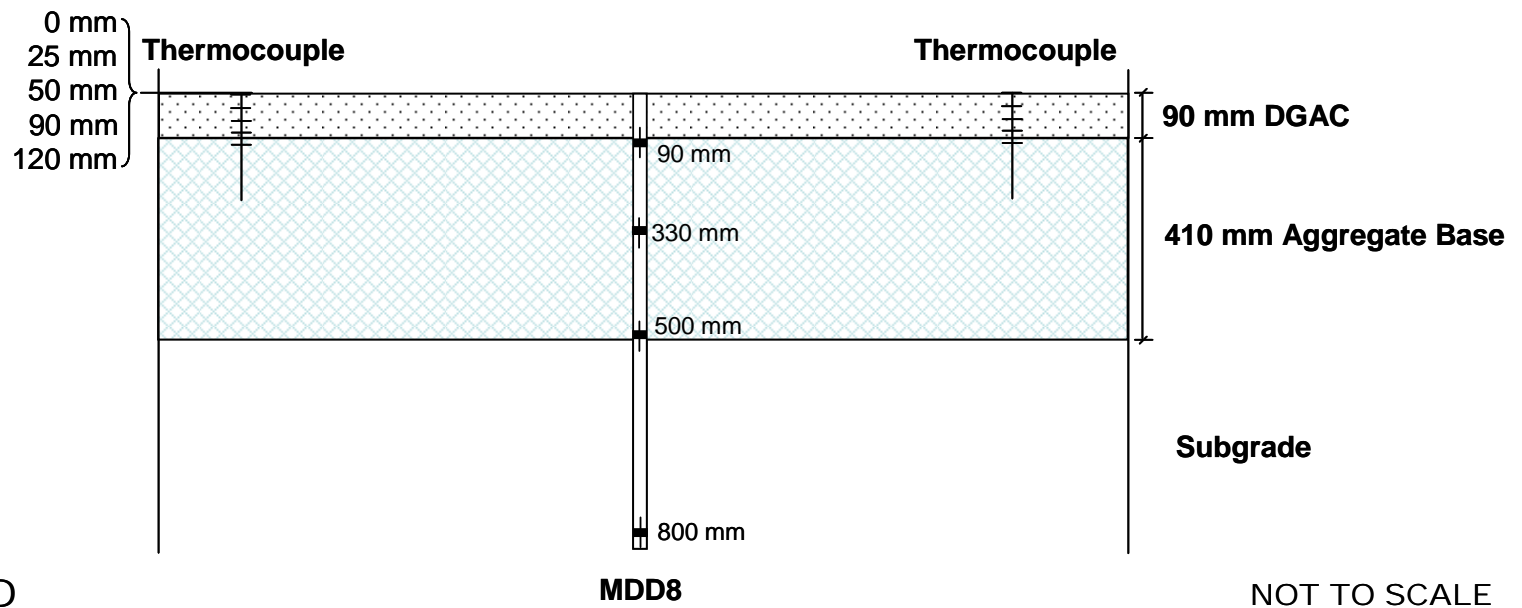
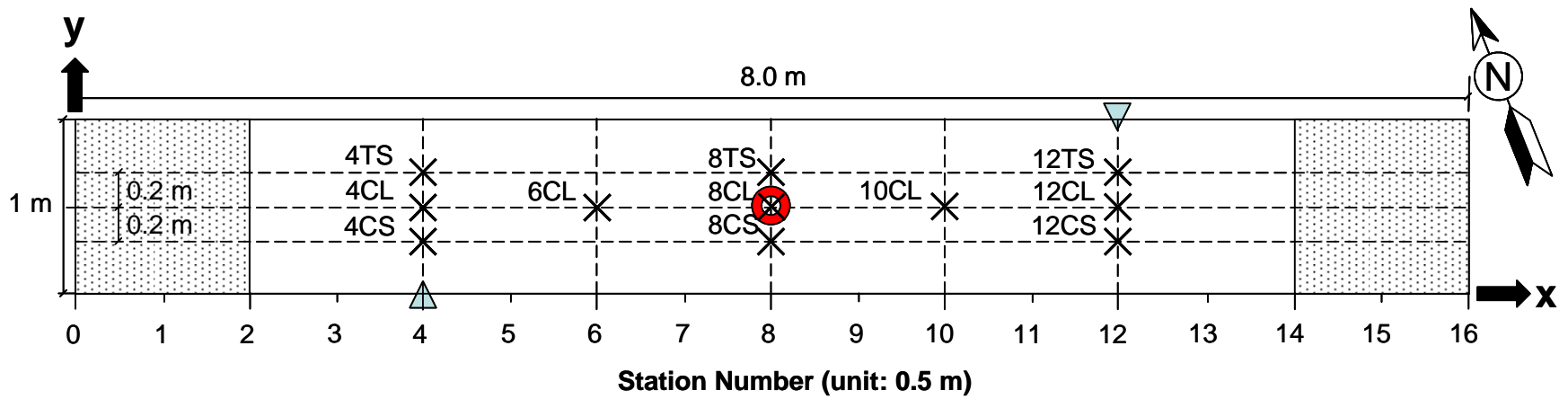
- Road Surface Deflectometer (RSD), measuring elastic vertical surface deflection;
- Multi-depth Deflectometer (MDD), measuring elastic deflection and permanent deformation at different depths in the pavement;
- Laser Profilometer, measuring surface profile (at each station);
- Falling Weight Deflectometer (FWD), measuring elastic deflection before and after testing, and
- Thermocouples, measuring pavement temperature and ambient temperature.

Visual assessments and digital photographs were used to monitor surface distress, including cracking.

Instrument positions are shown in Figure 4.1. Detailed descriptions of the instrumentation and measuring equipment are included in Reference 10. Intervals between measurements, in terms of load repetitions, were selected to enable adequate characterization of the pavement as damage developed.

### **4.3. Test Section Design**

The test section design is discussed in Chapter 3. A summary of the asphalt content layer thicknesses and air-void contents for each section is provided in Table 4.1. These were determined from cores removed from outside each HVS section. Layer thicknesses for each section, determined from these cores and from DCP measurements prior to placement of the DGAC, are provided in Figure 4.2.



**LEGEND**

	MDD		RSD		Thermocouple		MDD LVDT module	TS	Traffic Side	CL	Central Line	CS	Caravan Side
(MDD – Multi-depth Deflectometer, RSD – Road Surface Deflectometer, LVDT – Linear Variable Displacement Transducer)													

**Figure 4.1: Test section layout and location of instruments.**

Design	567RF	568RF	569RF	571RF	572RF	573RF
DGAC (90 mm)	DGAC (81 mm)	DGAC (80 mm)	DGAC (89 mm)	DGAC (78 mm)	DGAC (80 mm)	DGAC (80 mm)
Class 2 Aggregate Base (410 mm)	Class 2 Aggregate Base (398 mm)	Class 2 Aggregate Base (398 mm)	Class 2 Aggregate Base (369 mm)	Class 2 Aggregate Base (372 mm)	Class 2 Aggregate Base (352 mm)	Class 2 Aggregate Base (411 mm)
Clay subgrade (semi-infinite)	Clay subgrade (semi-infinite)	Clay subgrade (semi-infinite)	Clay subgrade (semi-infinite)	Clay subgrade (semi-infinite)	Clay subgrade (semi-infinite)	Clay subgrade (semi-infinite)

**Figure 4.2: Pavement layer thicknesses for Phase 1 HVS test sections (design and actual).**

**Table 4.1: Asphalt Concrete Thickness and Air-Void Content of HVS Test Sections**

Section	Thickness (mm)		Air-Void Content (%)	
	Average	Std Deviation	Average	Std Deviation
567RF	80.3	2.6	8.6	1.2
568RF	80.5	7.8	7.4	0.1
569RF	88.7	13.6	7.1	1.1
571RF	78.0	9.6	9.6	1.2
572RF	80.3	5.0	9.1	1.9
573RF	79.5	9.5	9.3	2.8

#### 4.4. Test Summary

##### 4.4.1 Test Section Failure Criteria

Failure criteria for analyses were set at:

- Cracking density of 2.5 m/m<sup>2</sup> or more, and/or
- Average maximum surface rut depth of 12.5 mm (0.5 in) or more.

##### 4.4.2 Environmental Conditions

The pavement surface temperature was maintained at 20°C±4°C to minimize rutting in the asphalt concrete and to promote fatigue damage. A temperature control chamber (10) was used to maintain the test temperatures.

The pavement surface received no direct rainfall as it was protected by the temperature control chamber. The sections were tested during both wet and dry seasons and hence water could have infiltrated the pavement from the side drains and through the raised groundwater table.

##### 4.4.3 Test Duration and Configuration

Phase 1 HVS trafficking took place between December 21, 2001, and March 25, 2003, and is summarized in Table 4.2. The loading program followed differs from the original test plan due to an incorrect hydraulic control system setup on loads less than 65 kN (14,600 lb). Testing was undertaken with a dual-wheel configuration, using radial truck tires (Goodyear G159 - 11R22.5 - steel belt radial) inflated to a pressure of 720 kPa (104 psi), in a bidirectional loading mode. Lateral wander over the one-meter width of the test section was programmed to simulate traffic wander on a typical highway lane.

**Table 4.2: Summary of Testing on the DGAC Layer**

Section	Start Date	End Date	Repetitions	Wheel Load (kN)	Wheel	Tire Pressure (kPa)	Direction
567RF	12/21/01	01/07/02	78,500	60 <sup>1</sup>	Dual	720 <sup>2</sup>	Bi
568RF	01/14/02	02/12/02	377,556	60	Dual	720	Bi
573RF	03/19/02	07/08/02	983,982	60	Dual	720	Bi
571RF	07/12/02	10/02/02	1,101,553	60	Dual	720	Bi
572RF	01/23/03	03/12/03	537,074	60	Dual	720	Bi
569RF	03/25/03	04/11/03	217,116	60	Dual	720	Bi

<sup>1</sup> 13,500 lb      <sup>2</sup> 104 psi

## 4.5. HVS Test Data Summary

### 4.5.1 Climate Conditions

The HVS test sections were tested in sequence at different periods during the year. The climate conditions under which each section was tested are critical for interpreting accelerated pavement test results. Figure 4.3 shows the sequence of HVS tests together with the average measured monthly air temperatures and precipitation amounts collected at a nearby weather station. The figure includes estimates of relative moisture content in the aggregate base and subgrade layers. Observations include:

- Sections 567RF, 568RF, 573RF, 572RF, and 569RF were tested during the rainy season.
- Sections 571RF and 573RF were tested when the air temperatures were the highest.
- In terms of moisture content, Sections 567RF, 568RF, 572RF and 569RF were tested when the aggregate base moisture content was relatively high ( $\geq 80$  percent relative moisture content), and Sections 571RF and 573RF when the aggregate base moisture content was comparatively lower ( $< 80$  percent).
- Subgrade moisture varied little throughout testing on all HVS test sections.

### 4.5.2 Elastic Deflection

#### Surface Elastic Deflection from RSD

Average surface deflections for each HVS test section measured with the RSD under a slow moving 60 kN wheel are presented in Figure 4.4. Surface deflection generally increased with increasing number of load repetitions, as expected. Change in deflection with load repetitions was reduced for some sections. For example, for Sections 571RF and 573RF, the deflections remain relatively constant in the range 200,000 to about 800,000 repetitions.



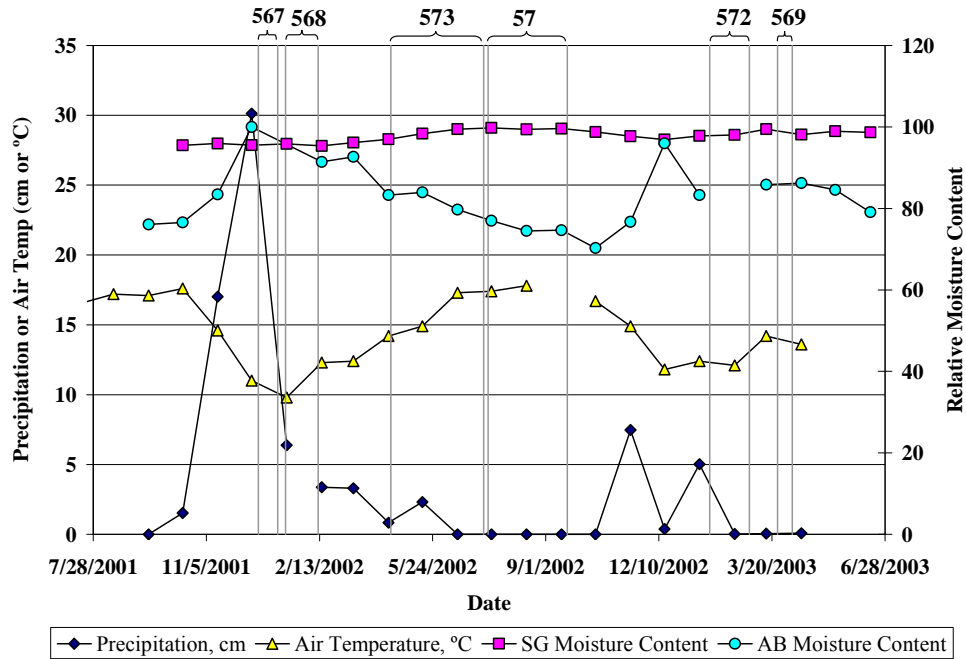


**Figure 4.3: Sequence climatic conditions during Phase 1 HVS testing.**

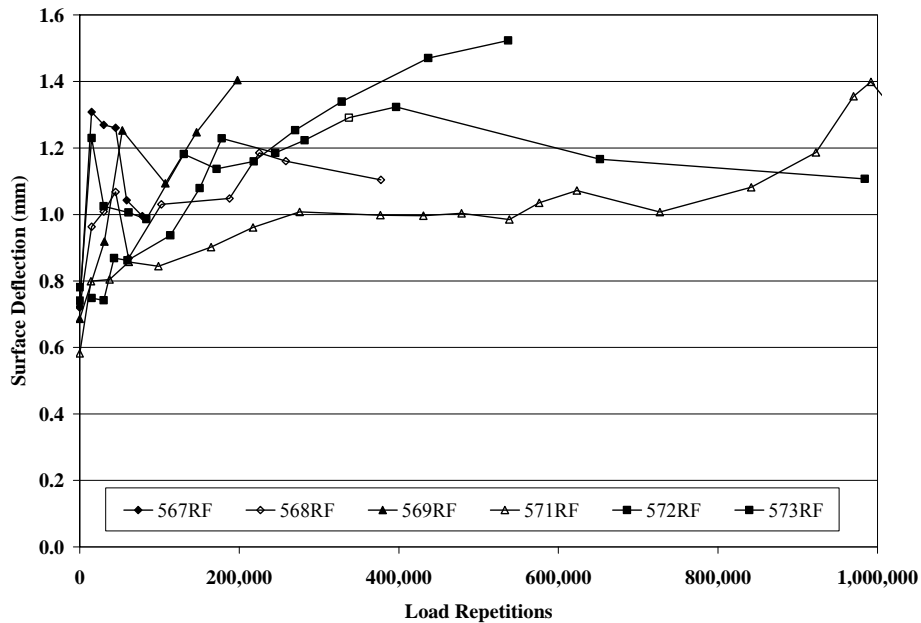


**Figure 4.4: RSD surface deflections.**

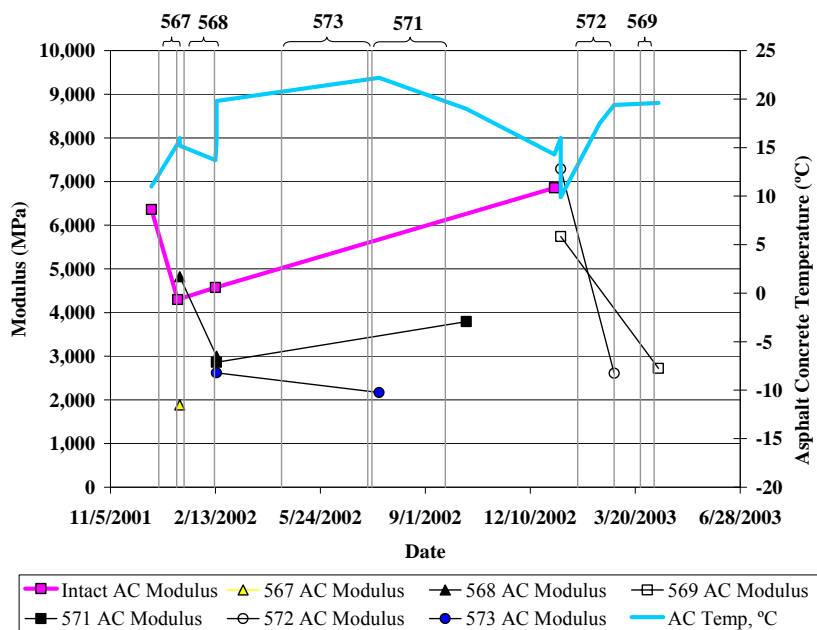
Surface Elastic Deflection from FWD

FWD testing was conducted on the sections before and after HVS testing to monitor changes in layer moduli. Modulus values for the asphalt concrete and the aggregate base are presented in Figures 4.5 and 4.6 respectively. Values were, backcalculated from:

- FWD deflection data obtained from the individual test sections, and
- The initial FWD deflection data presented in Section 3.5, shown as “Intact” in the figures.

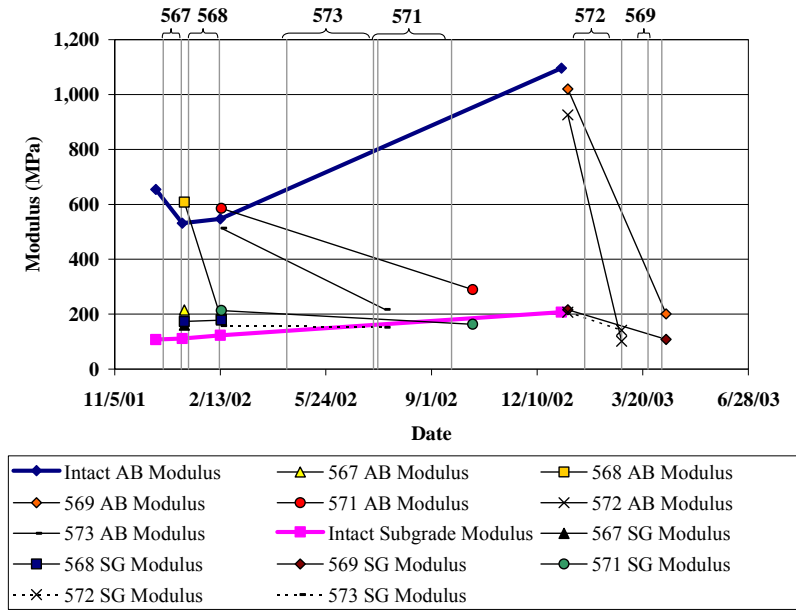
FWD testing was conducted several weeks before and after each HVS test. Modulus values for Section 567RF are from FWD tests after HVS testing.

Figure 4.5 shows a clear reduction in asphalt concrete modulus after HVS testing on Sections 567RF, 568RF, 569RF, and 572RF, while Section 573RF shows a slight reduction and Section 571RF a slight increase in modulus. The moduli change on the latter two sections is explained by the large temperature difference between the FWD tests conducted after HVS testing and those conducted before HVS testing. Data interpretation accounted for these variations. Asphalt concrete modulus values were in the range of 4,000 to 7,000 MPa before HVS testing, depending on temperature, and between 2,000 MPa and 4,000 MPa after HVS testing.



**Figure 4.5: Backcalculated asphalt concrete moduli for HVS sections.**

Modulus values for the aggregate base are shown in Figure 4.6. The data show a clear reduction in aggregate base modulus over time for all sections. Values were in the range of 500 MPa to 1,100 MPa before HVS testing and between 100 MPa and 300 MPa after HVS testing. The agreement between intact modulus and modulus before HVS testing for each of the sections appeared reasonable.



**Figure 4.6: Backcalculated aggregate base and subgrade moduli for HVS sections.**

Results for the aggregate base are less certain. FWD testing indicated higher modulus during the wet-cold periods, which could imply better resistance to deformation. However, the sections tested during wet-cold periods failed faster than those tested during the dry-warm periods. These results suggest that care must be exercised in using these values to estimate performance since base moisture content significantly affects asphalt concrete pavement behavior.

Modulus reductions for these subgrade were not as significant as those for the asphalt concrete and aggregate base layers.

#### In-Depth Elastic Deflection from MDD

Problems were experienced with the MDD linear variable displacement transducers (LVDT), which resulted in questionable data being collected. These problems were attributed to very wet conditions in the subgrade, which influenced the anchor points of the MDD stack. No in-depth deflection data will thus be discussed in this report.

#### **4.5.3 Permanent Deformation**

Permanent deformation at the pavement surface (rutting) was monitored with the Laser Profilometer. In-depth permanent deformation could not be analyzed due to problems with the MDDs discussed above.

Permanent Surface Deformation (Rutting)

A summary of surface rutting data collected on the six HVS test sections is presented in Table 4.3 and Figure 4.7. HVS testing was continued beyond the 12.5-mm rutting failure criterion in order to provide more complete data for performance model development and calibration. The data show significant variability between the HVS tests. Sections 571RF and 573RF show less permanent deformation and a lower rate of rutting than the other sections. Based on the climatic and moisture content data presented, Sections 571RF and 573RF developed less surface rutting because they were tested when the aggregate base had lower moisture content values. Sections 567RF, 568RF, 572RF, and 569RF experienced large rates of rutting believed to stem from plastic deformation in the aggregate base. Sections 572RF and 567RF had the largest rates of surface rutting. Although the average surface rutting for Section 569RF was less than 6.0 mm, half of the section exhibited surface rutting in the range of 12 mm.

**Table 4.3: Summary of Surface Rutting Performance**

Section	Average Maximum Rut (mm)
567RF	13.7
568RF	14.2
569RF	3.8
571RF	14.1
572RF	8.8
573RF	15.3

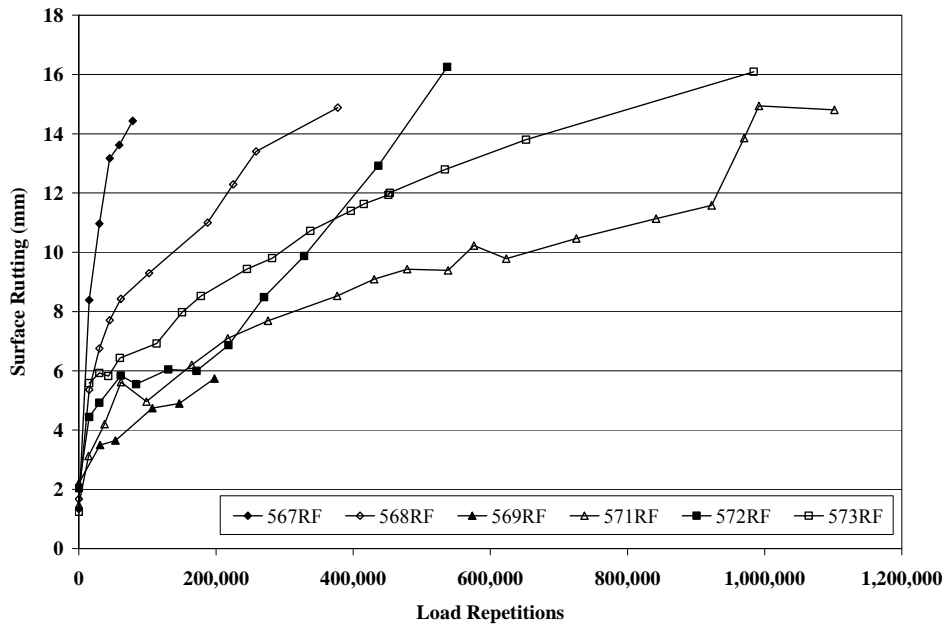


**Figure 4.7: Summary of surface rutting performance.**

#### 4.5.4 Visual Inspection

Fatigue distress in an asphalt concrete pavement manifests itself in the form of surface cracks. Since this study centered on fatigue cracking, crack monitoring was an essential component of the data collection program. This entailed:

- Visual inspections of the test section and marking of visible cracks;
- Photographic documentation of the marked cracks;
- Correction of the photos for camera angle;
- Digitization of the photos;
- Calculation of the crack length using *Optimas*<sup>TM</sup> software, and
- Presentation of the cracking in terms of crack length per area of pavement.

Regular crack inspections were made from the time that the first crack was detected through to the end of testing. Figure 4.8 illustrates the final surface cracking patterns observed at the end of HVS testing for each of the pavement sections. Final crack densities were:

- 567RF: 8.1 m/m<sup>2</sup>
- 568RF: 5.5 m/m<sup>2</sup>
- 569RF: 5.9 m/m<sup>2</sup>
- 571RF: 6.2 m/m<sup>2</sup>
- 572RF: 8.1 m/m<sup>2</sup>
- 573RF: 4.1 m/m<sup>2</sup>

Surface crack patterns were different for each section:

- Alligator cracks appeared on Sections 567RF and 572RF;
- Transverse cracks developed on Sections 568RF, 571RF, and 573RF, and
- A combination of alligator cracking, transverse cracking, and no cracking was observed on Section 569RF.

The type of crack pattern observed could be associated with the condition of the aggregate base and subgrade layers and was similar to patterns in surface rutting and surface deflection data. Sections 571RF and 573RF were tested during a dry summer season. A weaker foundation typically produces more alligator cracking as seen in the remaining test sections except for Section 568RF.

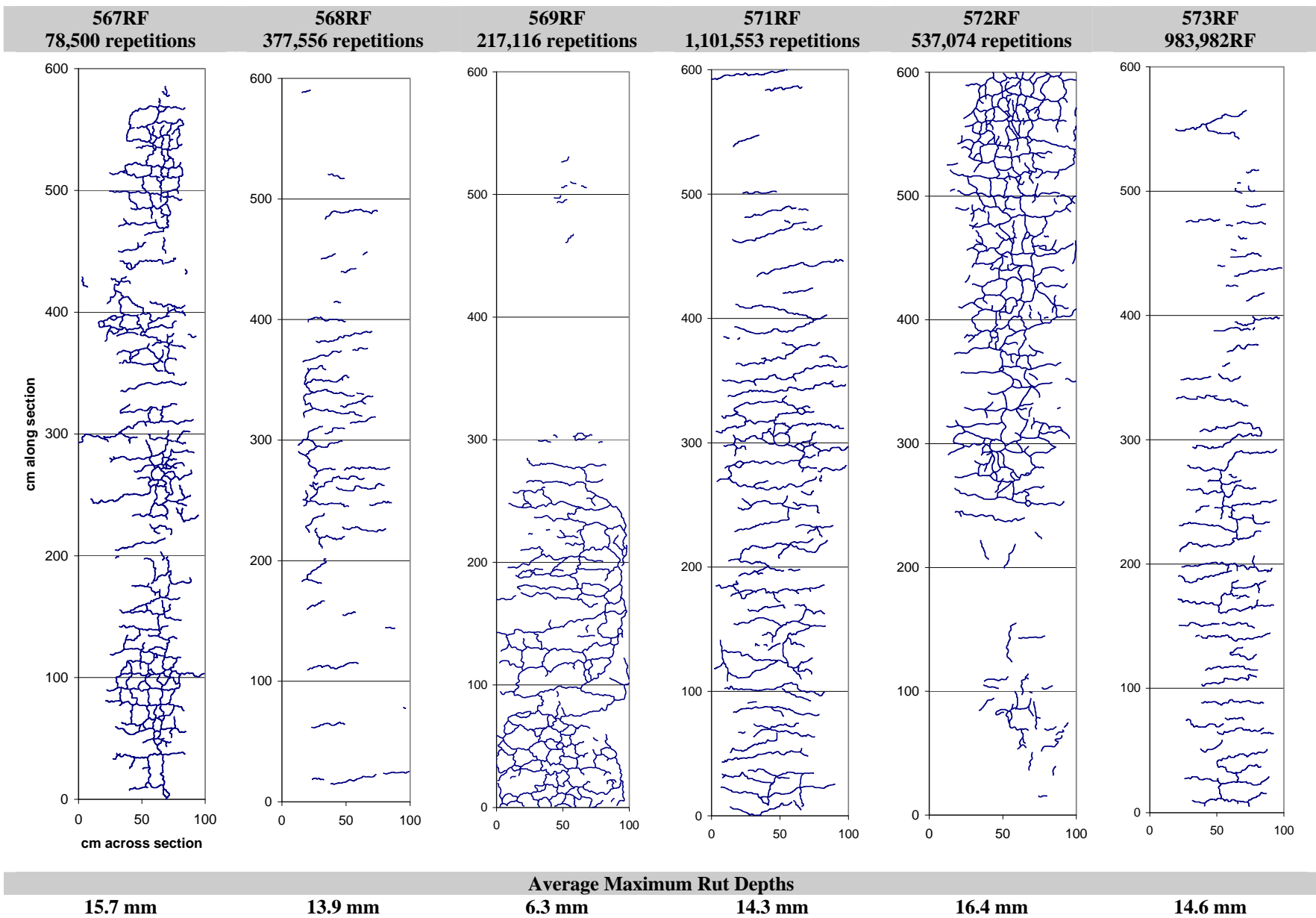


**Figure 4.8: Cracking patterns and rut depths on Sections 567RF through 573RF after HVS testing.**

Figure 4.9 summarizes surface cracking measurements with number of load applications for each HVS test. Testing was continued beyond the 2.5 m/m<sup>2</sup> crack density failure criterion because the rut limit had not been reached and additional data were desired for developing and calibrating performance models. Only one crack density point is shown for Sections 567RF, 569RF, and 573RF. The data show much lower crack density on Sections 571RF and 573RF than on the other sections. This observation is consistent with the drier aggregate base and subgrade when Sections 571RF and 573RF were tested. The effects of aggregate base and subgrade moisture conditions on the performance of the test sections conform to accepted pavement theory and practice.

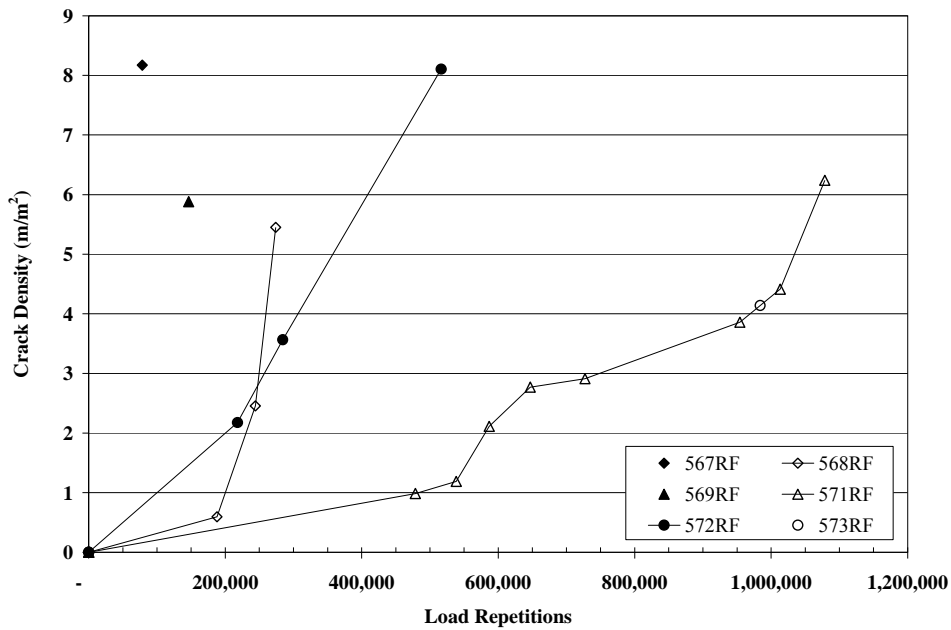


**Figure 4.9: Summary of surface cracking performance.**

#### 4.5.5 Test Summary

The ranking of HVS sections from best to worst performance was:

1. 573RF
2. 571RF
3. 568RF
4. 572RF
5. 569RF
6. 567RF

The performance of the sections appears significantly influenced by the behavior of the aggregate base under conditions of high and low moisture content. Sections 571RF and 573RF were tested when the aggregate base was at lower moisture content than the other pavement sections and showed less permanent deformation and less surface cracking than the other test sections.

## 5. OVERLAY DESIGN AND CONSTRUCTION

### 5.1. Overlay Design

The overlay thickness was determined according to Caltrans Test Method CTM 356 using Falling Weight Deflectometer and Road Surface Deflectometer data collected on completion of HVS testing. The input data for this design is provided in Table 5.1.

**Table 5.1: Summary of Surface Rutting Performance**

Parameter	Section					
	567RF	568RF	569RF	571RF	572RF	573RF
Average Deflection (mm)	1.12	1.18	1.40	1.10	1.37	1.24
80 <sup>th</sup> Percentile (mm)	1.16	1.22	1.89	1.21	1.42	1.28
Tolerable Deflection (mm)	0.71	0.71	0.64	0.70	0.71	0.71
Overlay thickness (mm)	65	74	156	74	102	83
Average thickness (mm)	92					
Standard deviation (mm)	34					
Selected full-thickness (mm)	90					
Selected half-thickness (mm)	45					

A full-thickness design of 90 mm was selected for the AR4000-D control section and one of the modified binder mixes (MB-G). The remaining sections would be constructed to half-thickness (45 mm). The experiment layout is summarized in Table 5.2 and illustrated in Figure 2.3.

**Table 5.2: Overlay Descriptions**

Phase 1 Section	Overlay Type	Description	Phase 2 Rutting	Phase 2 Cracking
567RF	45 mm MB15-G	MB4 gap-graded overlay with minimum 15% recycled tire rubber	580RF	586RF
568RF	45 mm RAC-G	Rubberized asphalt concrete gap-graded overlay, included as a control	581RF	587RF
569RF	90 mm AR4000-D	Dense-graded asphalt concrete overlay included as a control	582RF	588RF
571RF	45 mm MB4-G	MB4 gap-graded overlay	583RF	589RF
572RF	90 mm MB4-G	MB4 gap-graded overlay	584RF	590RF
573RF	45 mm MAC15-G	MAC15TR gap-graded overlay with minimum 15% recycled tire rubber	585RF	591RF

### 5.2. Overlay Construction

The overlays were constructed on June 14, 2003. The work was undertaken by O.C. Jones. The asphalt mixes were produced at the Syar Industries Lake Herman asphalt plant in Benecia. The information and specification sheet provided to the bidding contractors prior to construction is provided in Appendix C.



### 5.2.1 Surface Preparation

The test track was broomed prior to application of the tack coat. No repairs were undertaken on areas of distressed pavement.

### 5.2.2 Overlay Placement

The overlays were placed on the same day, within a few hours of each other. A tack coat (rapid-setting emulsion) was applied prior to placement at a rate of  $0.3 \text{ l/m}^2$ . The 90 mm layers were placed in two lifts of 45 mm and a tack coat was applied between lifts at a rate of  $0.3 \text{ l/m}^2$ . The overlays were compacted with steel drum roller (Figures 5.1 through 5.3).



Figure 5.1: Overlay placement (RAC-G).



Figure 5.2: Overlay compaction (AR4000-D).



Figure 5.3: Overlay placement (MB4-G).

### 5.2.3 Density Measurements

Nuclear gauge measurements were recorded on the overlays, however, the measurements were considered unreliable due to overlay thickness constraints. Instead, densities were determined from cores removed along the edge of the test track. Results are provided in Section 5.3.

### 5.3. Materials Testing

Laboratory testing was carried out by Caltrans and UCPRC on samples collected during construction to determine actual binder properties, binder content, aggregate gradation, and air-void content. The binders met requirements, based on testing performed by Caltrans.

The average ignition-extracted binder contents of the various layers, corrected for aggregate ignition and compared to the design binder content, are listed in Table 5.3. For each section, actual binder contents were higher than design contents. It is not clear whether this is a function of the test or contractor error.

**Table 5.3: Design versus Actual Binder Contents**

Section	Mix	Binder Content (%)	
		Design	Actual
580RF and 586RF	MB15-G	7.1	7.52
581RF and 587RF	RAC-G	8.0	8.49
582RF and 588RF	AR4000-D	5.0	6.13
583RF and 589RF	MB4-G (45 mm)	7.2	7.77
584RF and 590RF	MB4-G (90 mm)	7.2	7.77
585RF and 591RF	MAC15-G	7.4	7.55

The aggregate gradations for the DGAC and modified binders generally met Caltrans specifications for 19.0 mm (3/4 in) maximum size coarse and gap gradations respectively, with specifics for each mix detailed below. Gradations are illustrated in Figure 5.4 (AR4000-D) and Figure 5.5 (modified binders).

- AR4000-D: Material passing the 0.6 mm (#30), 2.36 mm (#8), and 4.75 mm (#4) sieves was on the upper envelope limit (Figure 5.4).
- RAC-G: Material passing the 0.3 mm (#50), 0.6 mm (#30), and 2.36 mm (#8) sieves was on the upper envelope limit (Figure 5.5).
- MB4-G: Material passing the 6.35 mm (1/4 in) and 9.5 mm (3/8 in) sieves was on the lower envelope limit (Figure 5.5).
- MB15-G: Material passing the 6.35 mm (1/4 in), 9.5 mm (3/8 mm), 12.5 mm (1/2 in), and 19.0 mm (3/4 in) sieves was on the lower envelope limit (Figure 5.5).
- MAC15-G: Material passing the 0.6 mm (#30), 9.5 mm (3/8 in), 12.5 mm (1/2 in), and 19.0 mm (3/4 in) sieves was on the upper envelope limit, while material passing the 2.36 mm (#8), 4.75 mm (#4), and 6.35 mm (1/4 in) sieves was outside the upper limit (Figure 5.5).

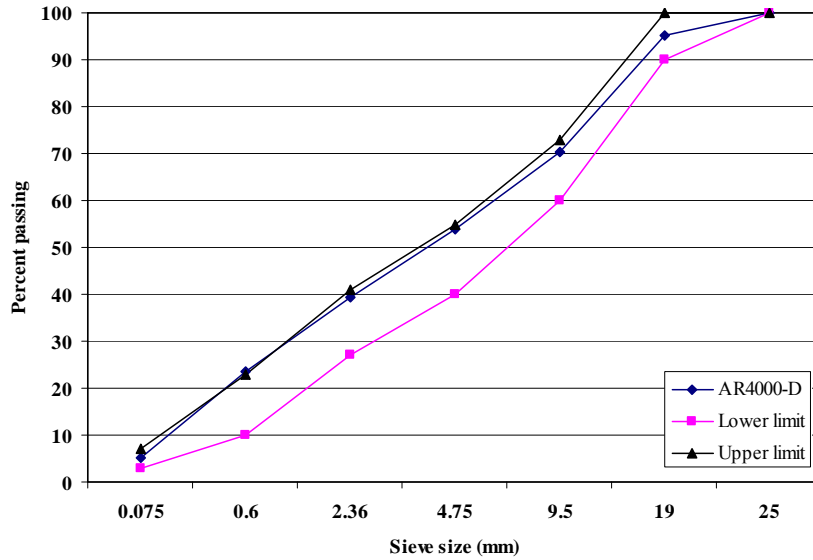


Figure 5.4: Gradation for AR4000-D overlay.

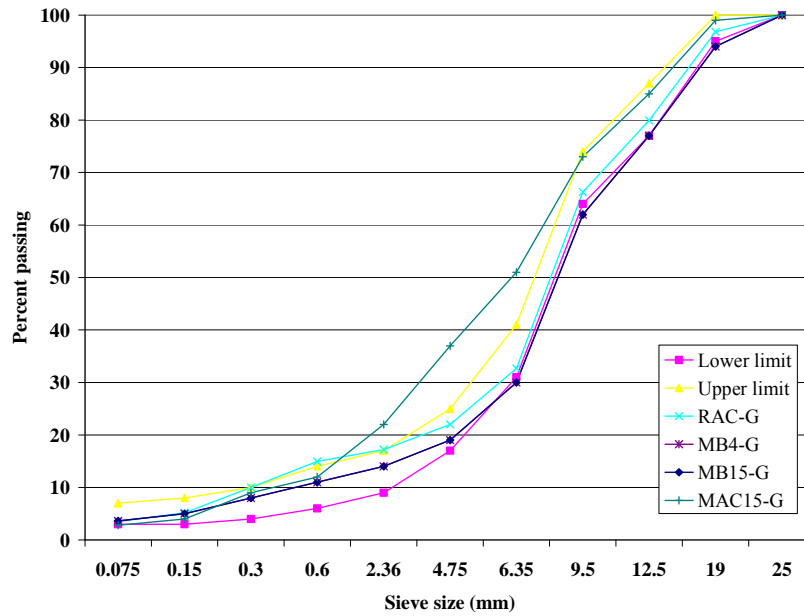


Figure 5.5: Gradation for modified binder overlays.

The preliminary as-built air-void contents for each section, based on cores taken outside of the HVS sections prior to HVS testing are listed in Table 5.4.

Table 5.4: Air-Void Contents

Section	Mix	Air-Void Content (%)	
		Average for Section	Standard Deviation
580RF and 586RF	MB15-G	5.1	1.7
581RF and 587RF	RAC-G	8.8	1.3
582RF and 588RF	AR4000-D	7.1	1.5
583RF and 589RF	MB4-G (45 mm)	6.5	0.6
584RF and 590RF	MB4-G (90 mm)	6.5	0.6
585RF and 591RF	MAC15-G	4.9	1.0

## 6. CONCLUSIONS

---

This first-level report describes the design and construction of a Heavy Vehicle Simulator (HVS) test track that will be used to validate Caltrans overlay strategies for the rehabilitation of cracked asphalt concrete. The report also summarizes the first phase of HVS testing, carried out on six separate sections to crack the pavement, as well as design and construction of the overlays for the reflective cracking HVS experiments. The construction, preliminary field and laboratory data, and accelerated pavement tests reveal several issues regarding the performance of the asphalt concrete pavement cross section tested under the Heavy Vehicle Simulator.

The pavement was designed according to the Caltrans Highway Design Manual Chapter 600 using the computer program *NEWCON90*. Design thickness was based on a subgrade R-value of 5 and a Traffic Index of 7 (~121,000 ESALs). The test track was constructed in September 2001 according to Caltrans practice. The existing aggregate base and asphalt concrete layer were first milled, followed by scarification, watering, shaping, and compaction of the subgrade. The aggregate base was placed and compacted and primed two days later. The asphalt concrete was placed in two lifts, with a tack coat applied between lifts. Although construction was carefully monitored throughout, the average thickness of the asphalt concrete was thinner than the design (79 mm versus 90 mm).

A full suite of laboratory tests, together with Falling Weight Deflectometer tests on the test track, were carried out to characterize the materials. The findings of these tests are summarized as follows:

- Proper compaction of the subgrade and aggregate base layers was primarily affected by the water content in these layers. Current Caltrans specifications for subgrade and aggregate base compaction do not explicitly address this issue, and water content during compaction is left for the field engineer to decide. Water content based on optimum moisture content to reach the maximum wet density according to Caltrans specifications would produce a base/soil too wet to compact. Performance of unbound layers could be negatively affected if this issue is not addressed.
- The compaction of the aggregate base layer was significantly affected by the support provided by the subgrade. Data indicated that low aggregate base moduli were obtained in locations where low subgrade moduli were observed.
- The asphalt concrete layer had a significant effect on the behavior of the aggregate base and subgrade. In general, the asphalt concrete provided a confining pressure that increased the modulus of the aggregate base. In addition, it provided additional cover to the subgrade by reducing the subgrade vertical stresses, which in turn increased the subgrade modulus.

Six sections were demarcated onto the test track for HVS testing, which took place between December 21, 2001, and March 25, 2003. Each section was trafficked with a 60 kN (13,500 lb) load using a bi-directional loading pattern with wander. Pavement temperature at 50 mm depth was maintained at 20°C (68°F) using a temperature control chamber. A summary of the repetitions applied, and the average maximum rut depth and crack density measured on each section on completion of testing is provided in Table 6.1.

**Table 6.1: Summary of HVS Testing on the DGAC Layer**

Section	Repetitions	Rut Depth (mm [in])	Crack Density (m/m <sup>2</sup> [ft/ft <sup>2</sup> ])
567RF	78,500	13.7 (0.54)	8.1 (2.5)
568RF	377,556	14.2 (0.56)	5.5 (1.7)
573RF	983,982	3.8 (0.15)	5.9 (1.8)
571RF	1,101,553	14.1 (0.56)	6.2 (1.9)
572RF	537,074	8.8 (0.35)	8.1 (2.5)
569RF	217,116	15.3 (0.60)	4.1 (1.3)

Findings from the HVS testing include:

- Analysis of FWD measurements during the course of the study revealed that the modulus of the asphalt concrete was significantly affected by the asphalt concrete temperature. In general lower moduli were obtained during the hot summer months, and higher moduli during the cold winter months, as expected.
- The performance of the HVS test sections appeared to be significantly influenced by the behavior of the aggregate base. Sections that were tested during the dry months lasted longer both in fatigue and surface rutting than the sections tested during the wet months.
- Air-void contents and thicknesses were similar for the test sections; therefore, the effect of these variables could not be addressed.
- Analysis of FWD and Road Surface Deflectometer test results indicated that the modulus of the aggregate base can not be used as an indicator of aggregate base performance. Aggregate base moduli were higher during the cold/wet months but decreased rapidly when tested under the HVS. The aggregate base moduli of the sections during the dry/warm months were lower than those during the cold/wet months, but the sections tested during the dry period had longer pavement lives.

Deflections determined with the RSD during HVS testing and an FWD after testing were used to determine overlay thicknesses. A full-thickness design of 90 mm (3.5 in) was selected for the AR4000-D control section and one of the modified binder mixes (MB-G). The remaining sections were designed as half-thickness (45 mm) (1.7 in). The six different overlay treatments on the test track included:

- Full-thickness (90 mm) AR4000-D included for control purposes.
- Half-thickness (45 mm) RAC-G included for control purposes.
- Full-thickness (90 mm) MB4-G.
- Half-thickness (45 mm) MB4-G.
- Half-thickness (45 mm) MB4-G with 15 percent tire rubber.
- Half-thickness (45 mm) MAC15TR.

The overlays were placed on June 14, 2003. The test track was first broomed, after which a tack coat was applied. The half-thickness overlays were placed in a single lift and compacted with a steel drum roller. The full-thickness overlays were placed in two lifts, with a tack coat applied between lifts.



## 7. REFERENCES

---

1. **Generic experimental design for product/strategy evaluation** — crumb rubber modified materials. 2005. Sacramento, CA: California Department of Transportation.
2. **Reflective Cracking Study: Workplan for the Comparison of MB, RAC-G, and DGAC Mixes Under HVS and Laboratory Testing**. 2003. Davis and Berkeley, CA: University of California Pavement Research Center. (UCPRC-WP-2003-01).
3. **Highway Design Manual**. 1991. Sacramento, CA: California Department of Transportation. (Section 600).
4. BEJARANO, M.O. 1999. **Subgrade Soil Evaluation for the Design of Airport Flexible Pavements**. Ph.D. Thesis, University of Illinois, Urbana, IL.
5. **California Test Methods**. Sacramento, CA: California Department of Transportation. Division of Engineering Services. (<https://www.dot.ca.gov/hq/esc/ctms/>).
6. **Construction Manual**. 2001. Sacramento, CA: California Department of Transportation. Division of Construction. (<http://www.dot.ca.gov/hq/construc/manual2001/>).
7. **ELMOD 5.0. Software program**. Copenhagen, Denmark: Dynatest International.
8. LUKANEN, E.O., Stubstad, R. and Briggs, R. 2000. **Temperature Predictions and Adjustment Factors for Asphalt Pavement**. Washington, DC: Federal Highway Administration. (Report FHWA-RD-98-085).
9. HARVEY, J.T. et al. 1996. **Initial Cal/Apt Program: Site Information, Test Pavements Construction, Pavement Materials Characterizations, Initial CAL/HVS Test Results, and Performance Estimates**. Davis and Berkeley, CA: University of California Pavement Research Center.
10. HARVEY, J., Du Plessis, L., Long, F., Deacon, J., Guada, I., Hung, D. and Scheffy, C. 1997. **CAL/APT Program: Test Results from Accelerated Pavement Test on Pavement Structure Containing Untreated Base – Section 501RF**. Davis and Berkeley, CA: University of California Pavement Research Center. (Report Numbers UCPRC-RR-1997-03 and RTA-65W4845-3).



## **APPENDIX A: INITIAL CONSTRUCTION BID DOCUMENTATION**

---

### **INVITATION TO BID**

#### 1. Introduction

Attached are plans and specifications for the construction of a research pavement test section and associated work at the University of California Berkeley Richmond Field Station, CA. The test section is 125 m (410 ft) in length with a width of 8.8 m (28.9 ft). You are invited to submit a price proposal to perform this work. The site will be available for construction activities between 1 September and 1 October 2001.

#### 2. Site Inspection

The owner's site representative is Mr. Ed Diaz (510) 231-5750, who can be contacted with regards to the site inspection. The site inspection will be held at 10:00 am on Thursday 16 August 2001. Clean copies of plans and specifications will be available at this time. Refer to attached map for directions to the Richmond Field Station.

#### 3. Bid Due Date

All bids are due at 12:00 noon on Monday 27 August 2001. Bids submitted after this time will not be considered.

#### 4. Submission of Bids

Submit bids to:

**N.F. Coetzee Ph. D., P.E.**  
**Dynatest Consulting, Inc.**  
**165 South Chestnut Street**  
**Ventura, California 93001**  
**Fax +1 805 648-2231**

## **Subject: Site Work for HVS Study Test Job (Goal 9)**

### Intent of Project:

The intent of the test section is to simulate actual freeway paving. This is crucial to ensure that the tests performed on the pavement duplicate as closely as possible the effects of trafficking on in-service pavements.

### Site Conditions:

The site is located at the University of California Berkeley Richmond Field Station, at 1353 South 46<sup>th</sup> Street, Richmond, California. The site is located at the end of Lark Drive East of Building 280. The test section will extend along the existing Lark Drive from the intersection of Lark Drive and Avocet Way to the intersection of Lark Drive and the entrance road to Building 201 (EPA).

A line of trees is situated along the southern edge of the test section with amenities accommodated along the northern edge. Drainage is supplied in the form of drainage ditches along each shoulder, draining towards Building 280. A protected grassland extends the entire length of the test section and is situated approximately 15 m from the northern shoulder of Lark Drive.

Access to the Field Station is through the gate on Regatta Boulevard at the northwest corner of the Field Station. Access to the Field Station as well as the location of the construction site is illustrated in the attached figures.

### Test Section Provisions

1. The test section will be constructed according to the description provided below. All work shall conform to the 1999 edition of the standard plans and specifications of the State of California Department of Transportation (Caltrans), except as modified or supplemented by the provisions included within this document.
2. Contractor shall remove existing AC and AB from the existing road. The AC and AB will be off-hauled.
3. Contractor shall rip and recompact the existing subgrade to the design elevation and grade. The subgrade will be graded with a uniform cross slope of 2% across the entire width of the road. The elevation graded shall be as given in the attached figures. Compaction shall be to standard Caltrans Specifications. Cut and fill may be required to maintain elevation and cross slope. Excess material shall be off-hauled. Full compensation shall be considered as included in various items of work and no additional payment allowed.

4. Unsuitable material encountered below the designated subgrade grade-line shall be excavated and off-hauled as directed by the owner. Unsuitable material is defined as per section 19-2.02 of the standard specifications, and includes any existing AB encountered in the existing pavement structure. Excavated areas shall be replaced with excess subgrade, graded and compacted to standard specifications. Full compensation for furnishing all labor, equipment, materials, tools, and other costs and items necessary shall be considered included in the unit cost paid for excavation and replacement of all unsuitable material below the designated subgrade grade-line.
5. Contractor shall construct drainage ditches along the edge of the southern and northern shoulders. The drainage ditches will be constructed using existing in-situ material. The existing 150 mm Ø drainage pipe of length 12 m will be replaced with a 300 mm Ø drainage pipe with a length of 12 m. Compaction in the vicinity of the new 300 mm Ø drainage pipe shall be to Caltrans specifications
6. The contractor shall furnish and place Class 2AB. The compacted AB shall have a uniform thickness per standard specifications and shall maintain a 2% cross slope across the full width of the section and a longitudinal slope of 0.15 % as given in the attached figures.

Compacted lift thicknesses for AB shall be as follows:

*Lift 1: 150 mm*

*Lift 2: 150 mm*

*Lift 3: 110 mm*

7. Compaction requirements are as specified in the Caltrans standard specifications.
8. All grading shall be completed with electronic control (i.e. laser/ cross slope stringline/ cross slope).
9. Contractor shall apply a prime coating to the AB at least 24 hours prior to paving. Application rate of the prime coat shall be 1.15 L per square meter.
10. Contractor shall pave dense graded asphalt concrete (DGAC) in two passes maintaining the 2% cross slope of the AB and the longitudinal grading of the AB across the full width and length of the test section. The asphalt mat width for any pass shall not be less than 3.53 m and not more than 3.67 m
11. The DGAC shall be compacted in two layers, each of 45 mm compacted thickness.
12. An asphaltic emulsion tack coat will be applied to the DGAC between lifts. The application rate of the tack coat is specified as 0.3 L (residual asphalt) per square meter of surface covered. The second DGAC lift shall not be applied until the asphaltic emulsion has broken. AR-4000 asphalt cement can be substituted for emulsion and, if substituted, shall be applied at 0.3 L per square meter of surface covered.
13. Contractor shall furnish dense graded asphalt concrete (DGAC) meeting Caltrans specifications for 19 mm maximum, medium grading, Type A dense graded asphalt concrete, with AR-4000 binder.

- The contractor must provide a copy of the Caltrans certified mix design (less than one year old) and have it approved by owner at least 3 days prior to paving.
14. Compaction of the DGAC shall not be as specified in the standard specifications. Compaction is specified in terms of Maximum Theoretical Relative Density (MTRD), AASHTO Method T209. The MTRD of the compacted DGAC shall be between 92% and 95% MTRD. The MTRD of the DGAC to be used shall be tested by the UC-Berkeley Pavement Research Center if the MTRD test results are not available for the chosen mix. If the MTRD results are not available a DGAC sample of 10 kg of loose mix shall be made available to UC Berkeley by the accepted bid party 3 days prior to construction of the DGAC layer. In all other circumstances, the cost of testing the MTRD of the DGAC will be borne by the contractor.
  15. Contractor shall furnish samples of subgrade, AB and DGAC for lab testing at the time of construction. Contractor shall provide subgrade (100 kg), AB (150 kg) and DGAC (150 kg) to UC-Berkeley for research testing. Sampling shall be performed during construction as arranged between owner and contractor. Containers for the samples will be supplied by the owner.
  16. Contractor shall make the necessary arrangements to ensure that all paving and rolling equipment is clean of dirt and mud and will not contaminate the DGAC paving.
  17. Full compensation for furnishing all labor, equipment, materials, tools and other costs and items necessary for the complete placement of the aggregate base and dense graded asphalt concrete shall be considered included in the unit cost paid for the AB and DGAC.
  18. Full compensation for costs of labor, equipment, material, tools, and other costs and items incurred due to delays caused by the owner performing sampling, testing and instrumentation other than inspection testing after the completion of the AB layer, shall be considered included in the unit cost of standby time and no additional payment shall be considered. Standby time will be calculated in minimum increments of 0.25 hours. Standby time shall not be paid except between the hours of 7:00 AM and 5:00 PM, Monday through Friday, and a maximum of 4 hours standby time shall be paid for any day.
  19. A penalty shall be applied for each day after 1 October needed for completion of the project. This penalty will be based on the total bid amount and will constitute 1% of the total bid amount for every day late.
  20. Inspection will be performed by owners representatives, which may include UCB, Caltrans, Contra Costa County, or other staff.
  21. The contractor shall have in his possession at time of construction and during the construction period general liability insurance of in excess of \$1 million for each occurrence and auto insurance of in excess of \$1 million for each occurrence. This insurance shall include all operations, related to the

construction, that occur on the premises of the Richmond Field Station. The contractor shall need to present proof of such insurance prior to the initiation of construction. The contractor shall furthermore possess Workman’s Compensation insurance for all persons he employs in completion of the construction project.

Schedule of Quantities

Description of Activity	Estimated Quantity (unit)	Cost per Unit	Total Cost
Excavate existing AB and AC	210 m <sup>3</sup>	/m <sup>3</sup>	
Rip, grade and recompact subgrade	1056 m <sup>2</sup>	/m <sup>2</sup>	
Install drainage ditch (drainage pipe included)	250 m	/m	
Furnish and place AB	820 tons (SG = 2)	/ton	
Tack coat	900 m <sup>2</sup>	/m <sup>2</sup>	
Priming coat	900 m <sup>2</sup>	/m <sup>2</sup>	
Furnish and place DGAC	210 tons (SG = 2.5)	/ton	
		TOTAL \$	

Description of Activity	Cost/ (unit)
Clearing & Grubbing	/m <sup>2</sup>
Excavate unsuitable material	/m <sup>3</sup>
Standby Time	/hour

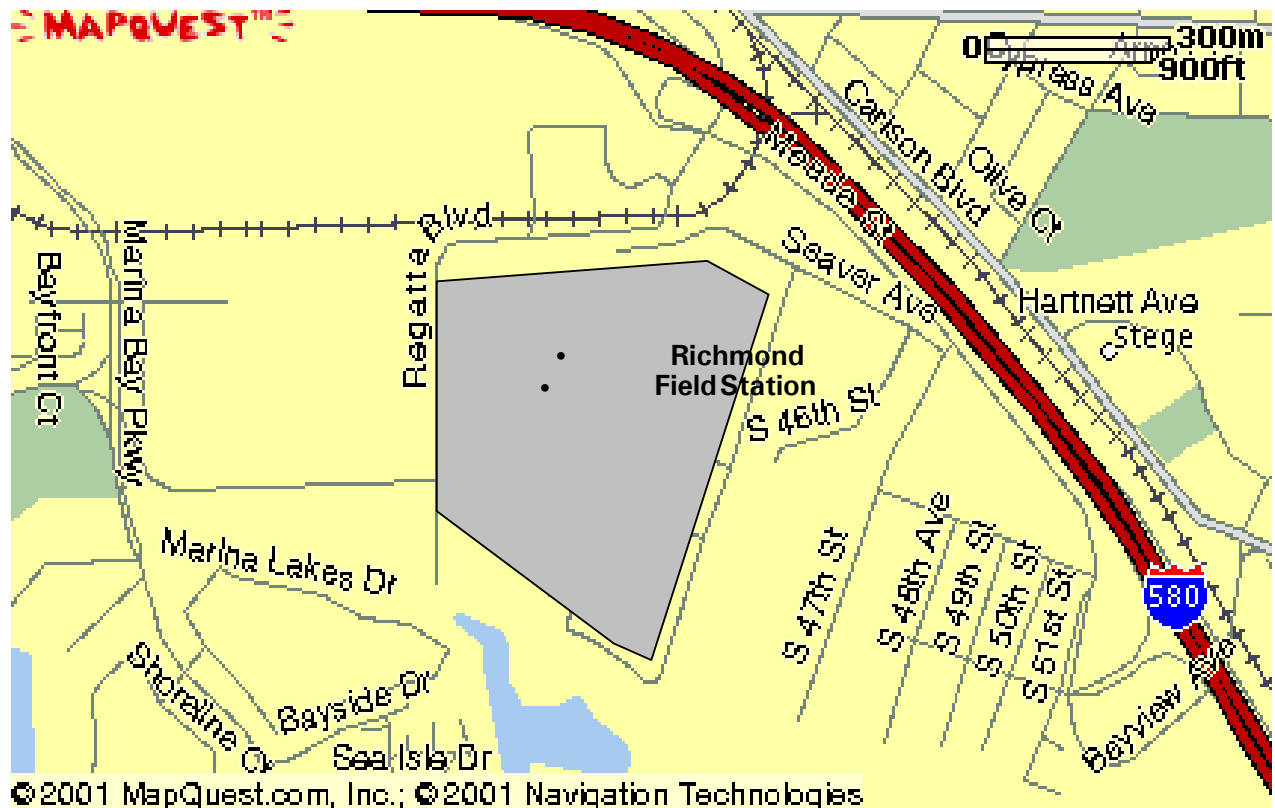
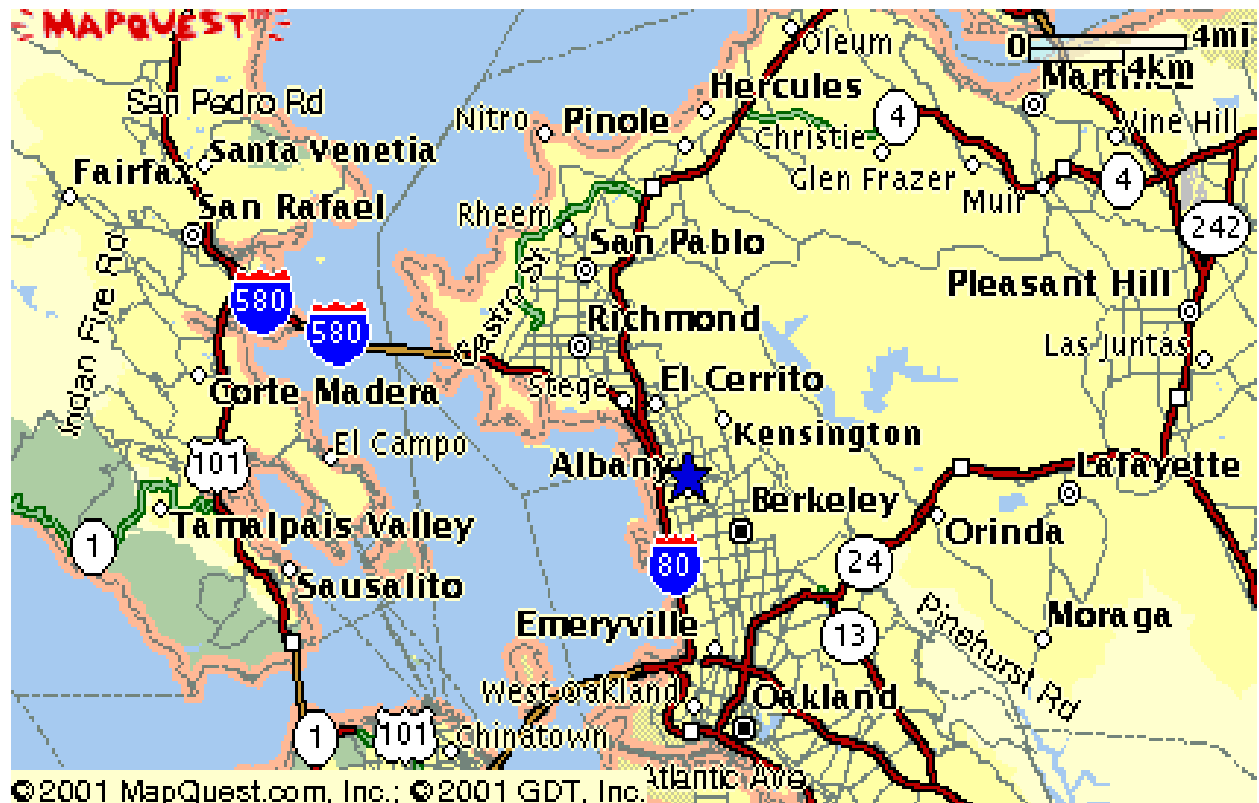
**Amendments to Bid**

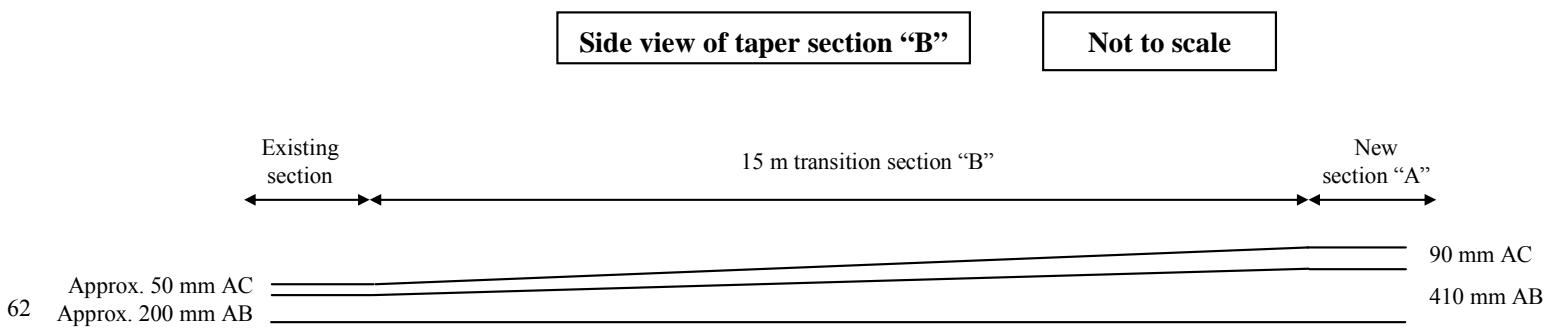
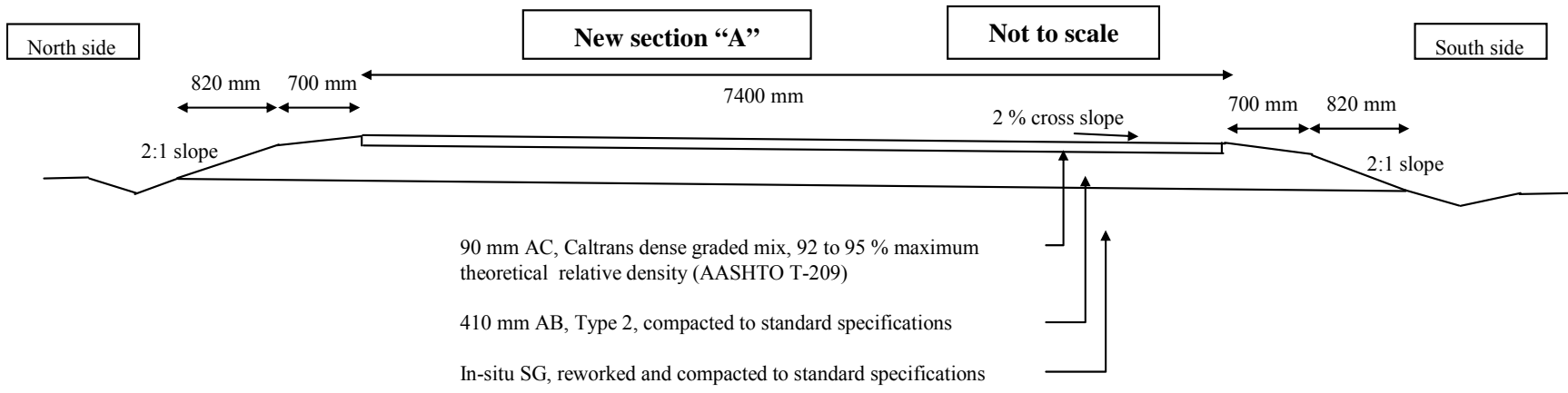
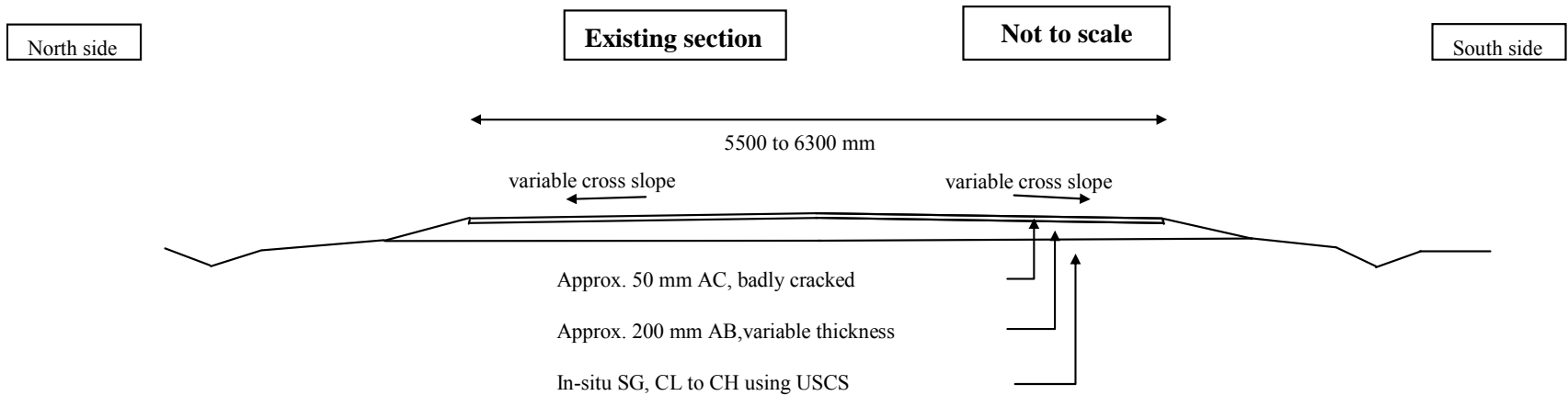
Amendment to Provision 10

Contractor shall pave dense graded asphalt concrete (DGAC) in two passes maintaining the 2% cross slope of the AB and the longitudinal grading of the AB across the full width and length of the test section. *An asphalt paver, possessing a solid extendable screed and electronic slope control, shall be used to pave the DGAC.* The asphalt mat width for any pass shall not be less than 3.53 m and not more than 3.67 m. *The contractor shall ensure that the paving of the DGAC is continuous, and simulates paving operations for highway construction.*

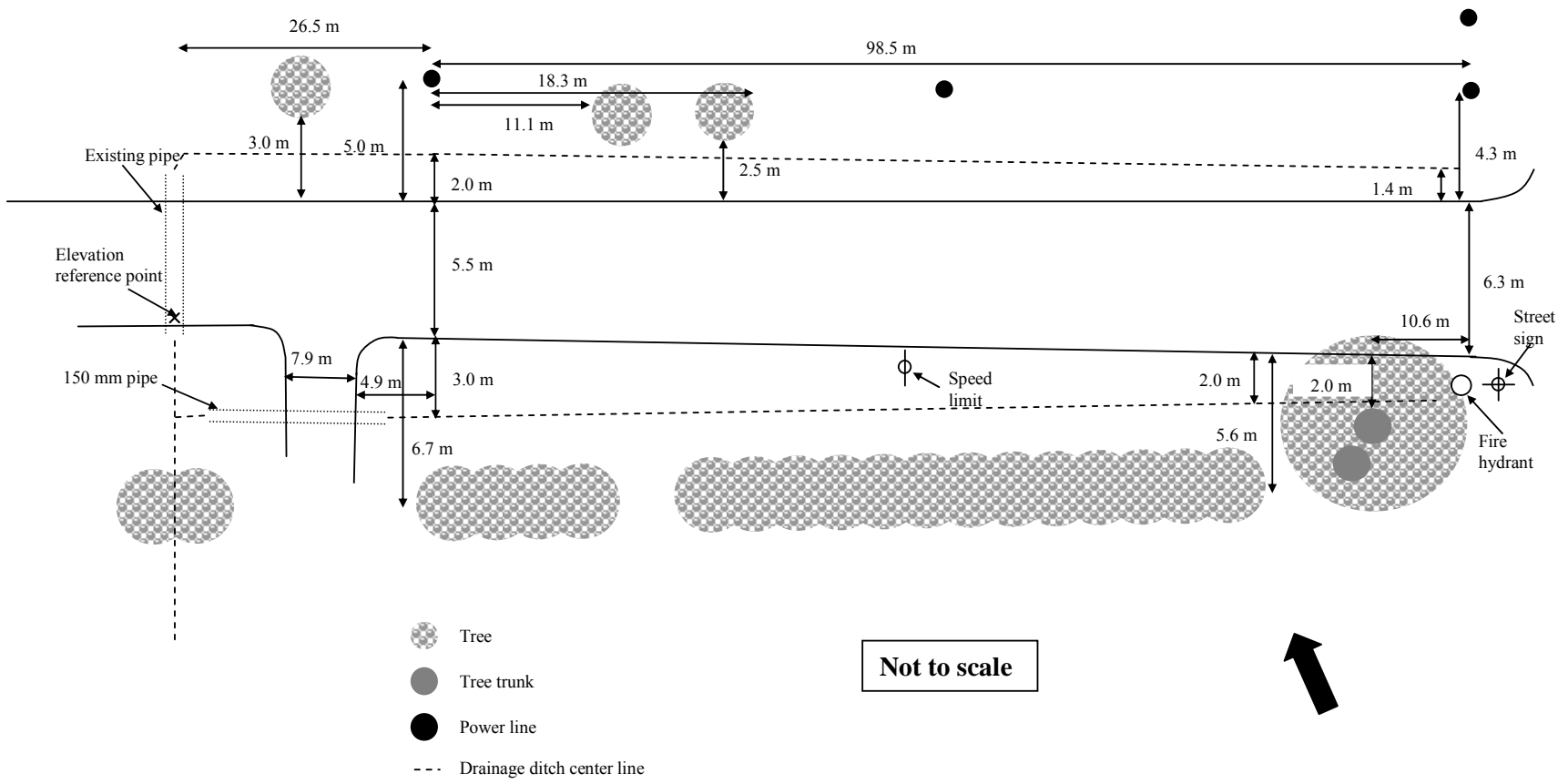
Additional Provision (Provision 22)

The contractor shall furnish the owner with a complete list of all equipment and machinery that shall be used during the completion of the project. This list shall be submitted by the contractor as part of the bid.





**Plan view of existing conditions**

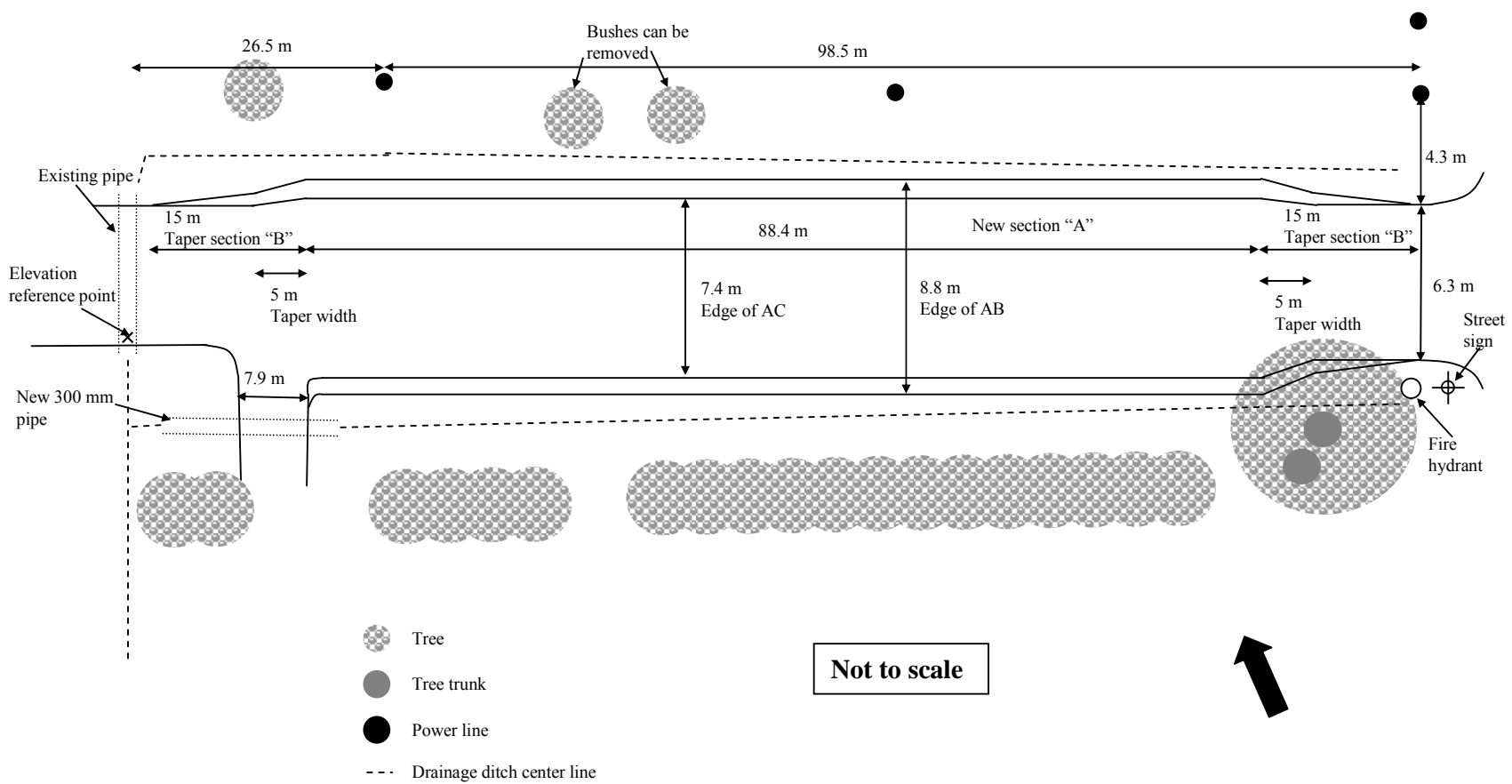


**Not to scale**

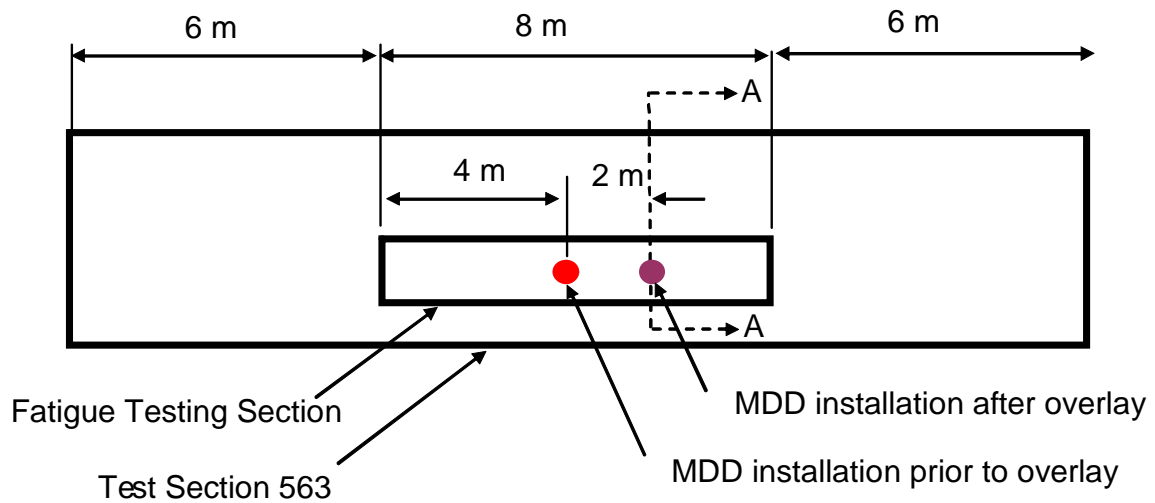




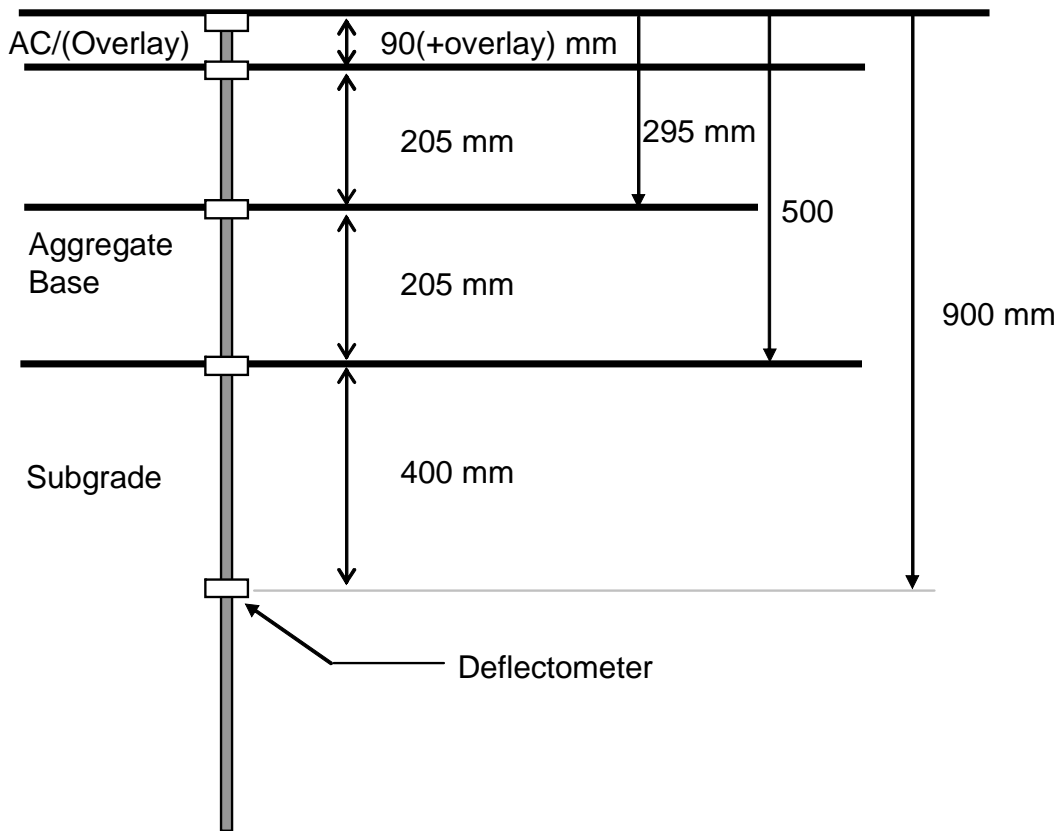
**Design plan view**



## APPENDIX B: INSTRUMENTATION TYPES AND LOCATIONS ON TEST SECTIONS

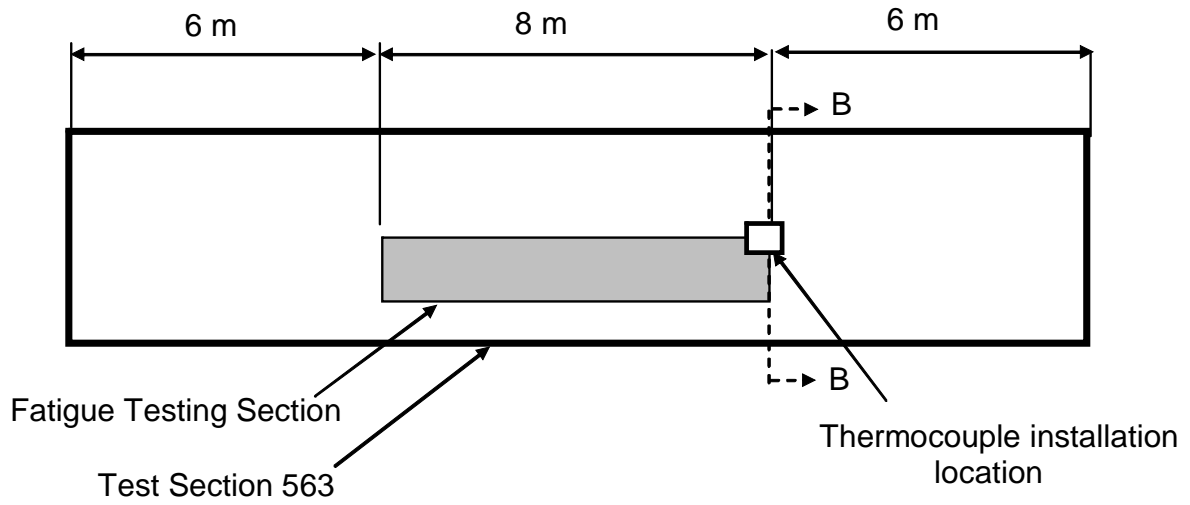


**Plan View.**

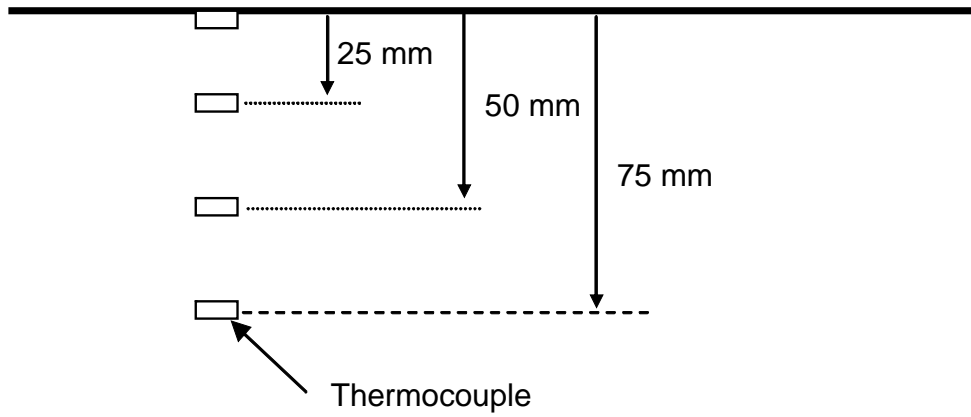


**Section A-A.**

**Figure B1. Multi-Depth Deflectometer (MDD) placement.**



**Plan View**



**Section B-B.**

**Figure B2. Thermocouple placement.**

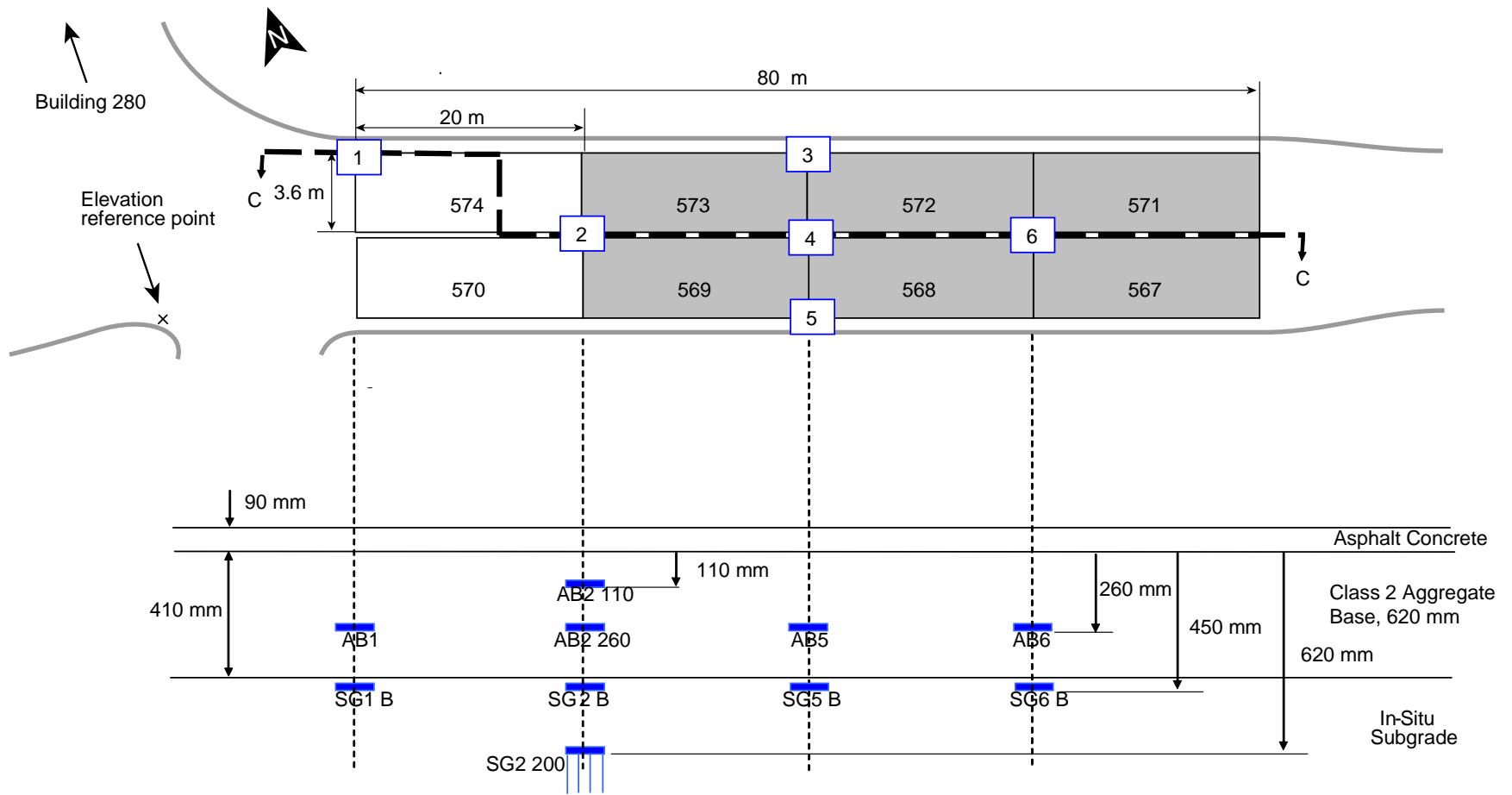


**Figure B3. Time Domain Reflectometer (TDR) placement.**

## **APPENDIX C: INFORMATION FOR OVERLAY CONSTRUCTION**

---

**Caltrans/University of California**

**Partnered Pavement Research Center**

**9 October, 2002 DRAFT (XX In text indicates items to be determined)**

**Information and Specifications for Construction of Overlays**

**“Comparison of MB, RAC-G and DGAC Mixes Under HVS and Laboratory Testing”**

### **Introduction**

This document shows plans and specifications for the construction of a research pavement test section and associated work at the University of California Berkeley Richmond Field Station, CA. The test section is 125 m (410 ft) in length with a width of 8.8 m (28.9 ft). The site will be available for construction activities as determined by arrangement between the contractor and the Owner’s Site Representative.

### **Site Inspection**

The owner’s site representative is Mr. Ed Diaz (510) 231-5750, who can be contacted with regards to the site inspection. Clean copies of plans and specifications are available from him. Refer to attached map for directions to the Richmond Field Station.

### **Payment**

Payment for reimbursable work will be made by:

**Dynatest Consulting, Inc.**

**165 South Chestnut Street**

**Ventura, California 93001**

**Fax +1 805 648-2231**

## **Intent of Project**

The intent of the test section is to simulate actual freeway paving. This is crucial to ensure that the tests performed on the pavement duplicate as closely as possible the effects of trafficking on in-service pavements.

## **Site Conditions**

The site is located at the University of California, Berkeley Richmond Field Station, at 1353 South 46th Street, Richmond, California. The site is located at the end of Lark Drive East of Building 280. The test section will extend along the existing Lark Drive from the intersection of Lark Drive and Avocet Way to the intersection of Lark Drive and the entrance road to Building 201 (EPA).

A line of trees is situated along the southern edge of the test section with amenities accommodated along the northern edge. Drainage is supplied in the form of drainage ditches along each shoulder, draining towards Building 280. A protected grassland extends the entire length of the test section and is situated approximately 15 m from the northern shoulder of Lark Drive.

Access to the Field Station is through the gate on Regatta Boulevard at the northwest corner of the Field Station. Access to the Field Station as well as the location of the construction site is illustrated in the attached figures.

## **Test Section Provisions**

1. The test section will be constructed according to the description provided below. All work shall conform to the 1999 edition of the standard plans and specifications of the State of California Department of Transportation (Caltrans), except as modified or supplemented by the provisions included within this document.
2. Six sections shall be overlaid using the following materials (see Figure 1 and Table 1 for Section locations, and required dimensions and thicknesses):
  - a. Dense Graded Asphalt Concrete (DGAC) on Section 567;
  - b. Rubber Asphalt Concrete – Type G (RAC-G) on Section 571;
  - c. Modified Binder Asphalt Concrete with 15 percent rubber – Type G (MB15R-G) on Sections 5XX and 5XX;
  - d. Modified Binder Asphalt Concrete – Type G (MB-G) on Sections 568 and 573;

3. An asphaltic emulsion tack coat will be applied to the existing asphalt concrete prior to paving. An asphaltic emulsion tack coat will also be applied between lifts for any sections requiring more than one lift of paving. The application rate of the tack coat is specified as 0.3 L (residual asphalt) per square meter of surface covered. Overlay material shall not be applied until the asphaltic emulsion has broken. AR-4000 asphalt cement can be substituted for emulsion and, if substituted, shall be applied at 0.3 L per square meter of surface covered.
4. Dense graded asphalt concrete (DGAC) shall meet Caltrans specifications for 19 mm maximum, medium grading, Type A dense graded asphalt concrete, with AR-4000 binder. The contractor shall provide a copy of the Caltrans approved mix design (less than one year old) and have it approved by owner at least 3 days prior to paving.
5. The contractor shall have a Caltrans approved mix design meeting the Special Provisions attached to this document for the following materials:
  - A. Rubber Asphalt Concrete – Type G (RAC-G) shall meet Caltrans specifications with 12.5 mm maximum.
  - B. Modified Binder Asphalt Concrete with 15 percent rubber – Type G (MB15R-G) shall meet Caltrans specifications with 12.5 mm maximum.
  - C. Modified Binder Asphalt Concrete – Type G (MB-G) shall meet Caltrans specifications with 12.5 mm maximum.

If an approved mix design is not available, the contractor shall supply a proposed aggregate gradation and binder, and shall supply XX kg of each bin size in the proposed gradation and 20 L of binder to the owner for the determination of binder content.

6. An asphalt paver, possessing a solid extendable screed and electronic slope control, shall be used to pave the overlay materials. The contractor shall ensure that the paving of the overlay materials on each section is continuous, and simulates paving operations for highway construction.
7. Compaction of the DGAC, RAC-G, MB15R-G and MB-G shall not be as specified in the standard specifications. Compaction is specified in terms of Maximum Theoretical Relative Density (MTRD) as determined by California Test Method 309. The density of the compacted DGAC shall be between 91% and 94% of MTRD. The density of the compacted RAC-G, MB15R-G and MB-G shall be between 89% and 93% of MTRD. Compaction will be monitored by UC PRC staff during rolling operations and they will provide the contractor with density information.
8. The MTRDs shall be provided by a commercial laboratory. The contractor shall supply sufficient materials for the determination of MTRD when materials are supplied for mix design, or if a Caltrans mix design is available for an overlay material the contractor shall supply sufficient materials to make 20 kg of mix for MTRD determination at least two weeks prior to paving. The cost of testing the MTRD of all overlay materials will be borne by the UC PRC.

9. Contractor shall furnish samples of each overlay material for lab testing at the time of construction. Contractor shall provide 150 kg of each material. Sampling shall be performed during construction as arranged between owner's site representative and contractor. The owner's site representative will supply containers for the samples.
10. Contractor shall make the necessary arrangements to ensure that all paving and rolling equipment is clean of dirt and mud and will not contaminate the paving.
11. Aggregate base meeting Caltrans standard specifications for Class 2 aggregate base shall be provided, placed, graded and compacted on the shoulders so that the shoulder elevations conforms to the overlay elevation.
12. Contractor shall provide the owner's site representative with notice of intention to begin work at least 48 hours prior to any operations on the site.
13. The contractor shall furnish the owner's site representative with a complete list of all equipment and machinery that shall be used during the completion of the project.
14. Inspection will be performed by owner's representatives, which may include UC PRC, Caltrans, Contra Costa County, or other staff.
15. The contractor shall have in his possession at time of construction and during the construction period general liability insurance of in excess of \$1 million for each occurrence and auto insurance of in excess of \$1 million for each occurrence. This insurance shall include all operations, related to the construction, that occur on the premises of the Richmond Field Station. The contractor shall need to present proof of such insurance prior to the initiation of construction. The contractor shall furthermore possess Workman's Compensation insurance for all persons he employs in completion of the construction project.



**Table 1: Schedule of estimated quantities.**

(XX approximate tonnage, actual values to be changed based on revised overlay thickness design.)

<b>Description of Activity</b>	<b>Estimated Quantity (unit)</b>
Tack Coat	X L
Dense Graded Asphalt Concrete (DGAC)	16 tonnes (XX)
Rubber Asphalt Concrete – Type G (RAC-G)	7 tonnes (XX)
Modified Binder Asphalt Concrete with 15 percent rubber – Type G (MB15R-G)	XX tonnes (to be paved in spring)
Modified Binder Asphalt Concrete – Type G (MB-G)	22 tonnes (XX)
Aggregate Base Class 2	XX tonnes (XX)

